Investigations into the Hyporheic Zone: Assessing the Influence of Groundwater-Surface Water Interactions on Metal Exposure and Effects to Aquatic Ecosystems

by

Anna Michelle Harrison

A dissertation submitted in partial fulfillment
of the requirements for the degree of
Doctor of Philosophy
(Resource Ecology and Management)
in the University of Michigan
2018

Doctoral Committee:

Professor G. Allen Burton, Chair
Emeritus Professor J. David Allan
Professor Joel D. Blum
Assistant Professor David M. Costello, Kent State University
Dr. Paul Drevnick, Alberta Environment and Parks

Anna M. Harrison

annaha@umich.edu

ORCID iD: 0000-0002-4752-5635

Dedication

This dissertation is dedicated to my family, specifically my parents, Dayle and Constance, who have been a constant source of support and encouragement throughout my educational endeavors.

Acknowledgements

Table of Contents

List of Tables

List of Figures

List of Appendices

List of Abbreviations and Acronyms

AVS – Acid Volatile Sulfides

CES – Chemical Exposure Substrate

Chl a – Chlorophyll a

EB – East Bay (Traverse City, MI)

EPA – Environmental Protection Agency

FC – Fleming Creek (at the UM Matthaei Botanical Gardens)

fOC – fraction of Organic Carbon

HZ – Hyporheic Zone

LBC – Little Black Creek (Muskegon, MI)

LOI – Loss-On-Ignition

MBG – Matthaei Botanical Garden

NPP – Net Primary Productivity

PEC – Probable Effects Concentration

QC – Quanicassee Wildlife Refuge (Big Bay, MI)

TEC – Threshold Effects Concentration

SEM – Simultaneously Extracted Metals

VHG – Vertical Hydraulic Gradient

Abstract

Metal contaminated sediments are a common stressor of biological communities in freshwater ecosystems. Sediments have the capacity to store metals (via various chemical binding ligands in sediments), rendering them unavailable for uptake by biological communities. Physical processes in streams, however, can influence the chemistry of sediments and ultimately control how sediments store metals. Groundwater-surface water interactions (hyporheic flows) are an example of a natural physical process that influences sediment chemistry and potentially the exposure of metals to aquatic biota. Hyporheic flows are generally characterized as either 'downwelling' (surface water entering streambed sediments) or 'upwelling' (from sediments into surface water). Flow direction can be related to the location in a stream riffle, as downwelling typically occurs at the head (upstream end) of a riffle and upwelling occurs on the tail (downstream end) of a riffle. Using multiple lines of evidence (field, mesocosm, and laboratory studies), this dissertation investigated the role of hyporheic flows on metal exposure and effects to aquatic organisms. Depending on the experiment, biological assessments included: test organism (*Hyalella azteca*) survival, benthic macroinvertebrate community composition, and biofilm structure and function. In the *in situ* experiments in Chapter 2, the heads of riffles were more oxidized and had greater benthic macroinvertebrate diversity and more sensitive species than the tails of riffles. Flow-through experiments in Chapter 2 also observed more oxidized sediments in downwelling conditions, compared to mesocosms without downwelling. In Chapter 3, oxygenated (oxic) hyporheic flows (downwelling) increased the bioavailability of metals, and

subsequent declines in *H. azteca* survival were observed. In Chapter 4, the *in situ* experiments at field sites with upwelling hyporheic flows showed that sediments exposed to upwelling zones had less oxygen (were more reduced) and metals were less bioavailable than sediments not exposed to hyporheic upwelling. This research demonstrates the importance of hyporheic flows on redox-sensitive binding ligands and the subsequent effects on aquatic biological communities. It also suggests that inclusion of hyporheic flows in ecological risk assessments could more accurately characterize metal exposure pathways to aquatic biota.

Chapter 1

Introduction

The primary objective of this dissertation is to understand how groundwater-surface water interactions (hyporheic flows) influence the effects of environmental stressors to biotic communities in aquatic ecosystems. The hyporheic zone (Figure 1.1), located at the interface of groundwater and surface water, is a dynamic zone where surface water and groundwater can intermix in the sediments. The hyporheic zone is important ecologically, as it can have distinct biogeochemistry related to surface and/or groundwater influences, which can affect habitat suitability for biota. Hyporheic water flowing into streams can also serve as a potential refuge for macroinvertebrates during hydrologic stress events (e.g., flooding or drought) (Wood et al. 2010). Despite its importance for habitat, we have limited understanding about potential interactive effects of groundwater flows and contaminants (particularly metals) on benthic and hyporheic biota. This research investigated how groundwater and hyporheic flows affected aquatic macroinvertebrate communities and biofilms exposed to both physical stressors and metal contaminant stressors.

Ecology of the hyporheic zone

The hyporheic zone defines the interface between surface waters and groundwaters in sediments (Figure 1.1), and is home to a biotic community referred to as the "hyporheos"

1

(Boulton et al. 1998, Findlay and Sobczak 2000). The hyporheos consists of microbial communities, meiofaunal invertebrates and macroinvertebrates. Biota that regularly utilize the hyporheic zone are adapted to conditions in the sediment, such as reduced light availability, limited food resources, and the ability to burrow and move within the sediment (Gilbert et al. 1994). Some organisms, such as amphipods and isopods, permanently reside within the shallow sediments (epibenthic), whereas other benthic macroinvertebrates regularly utilize hyporheic habitat, either as obligate species during a portion of their lifespan or as opportunistic and occasional residents (Boulton et al. 2010). In addition to macroinvertebrates, some fish rely on the stable temperature and dissolved oxygen conditions in the hyporheic zone for embryo development (Malcolm et al. 2005).

The primary food sources for many grazing invertebrates are the biofilms that grow on the sediment surface and in the shallow hyporheic zone (Barlocher and Murdoch 1989, Brunke and Gonser 1997). Downwelling zones may be important habitat for heterotrophic biofilms, as their growth can be stimulated by deposition of organic matter in fine sediments (Navel et al. 2011). If hyporheic flows are impacting biofilms, it is likely that the effects can directly alter consumer invertebrates (Gilbert et al. 1994, Gibert et al. 1995). In this dissertation, the term 'biofilm' will be used to represent the mixed heterotrophic and autotrophic communities residing on and within the sediment surface, in preference to 'periphyton'.

Hydrologic processes in the hyporheic zone can influence the distribution of benthic and epibenthic organisms across several scales (Boulton et al. 1998). On a reach-scale, the presence of organisms is related to dynamic cycling of nutrients and dissolved oxygen in the hyporheic zone, which can alter habitat suitability for organisms (Hendricks et al. 1993). Upwelling zones can supply nutrients to streams, while downwelling zones provide dissolved oxygen and organic

matter to biofilms and benthos residing in shallow sediments (Boulton et al. 1998). Mesoscale

processes occur over larger areas of the watershed and include larger catchment-scale properties

(i.e., regional groundwater potential). Hyporheic flows may also be influenced by microscale

processes, such as creation of interstitial spaces and pathways created by invertebrate burrowing

(Gilbert et al. 2003, Sarriquet et al. 2007).

The aquatic communities described above are often at risk from both chemical and

hydrologic stressors, especially as climate change progresses and anthropogenic land use

increases. Aquatic communities in systems with water level fluctuations showed increased risks

from the effects of contaminated surface waters and sediments (Stampfli et al. 2013) and drought

conditions can decrease density and richness of hyporheic and benthic invertebrates (Datry 2012)

as well as reduce growth in benthic invertebrates (Nedrich and Burton 2017a). In these unstable

hydrologic conditions, interactions with the groundwater and hyporheic flows can affect how

stressors from surface waters and sediments ultimately influence aquatic biotic communities

(Brunke and Gonser 1997, Lawrence et al. 2013).

Hyporheic zone and stressor effects

Within the hyporheic zone, upwelling and downwelling zones can produce different

routes of exposures from different sources, and to different ecological populations and

communities. Exposure routes often depend on the direction of hyporheic flow. For example,

streams with high groundwater baseflows can more easily tolerate drought periods and altered

surface hydrologic conditions. Streams with groundwater inputs are also more resilient to high

stream temperatures caused by warming air temperatures. Both of these characteristics of

streams with groundwater inflows can offer stable hydrologic and temperature conditions for

stream organisms (Dole-Olivier et al. 1997), including macroinvertebrates and fish, especially

3

when faced with climate change-related impacts (Wood et al. 2010, Stubbington 2012). However, upwelling zones in areas with contaminated groundwater often have higher contaminant release and increased bioavailability and exposure (Greenberg et al. 2002, Gandy et al. 2007, Crouch et al. 2013), thus organisms seeking refuge from physical/hydrologic stressors may inadvertently expose themselves to contaminant stressors.

Downwelling zones, conversely, can negate benthic and hyporheic exposure to stressors from sediment or groundwater, due to constant dilution of clean surface water. These zones also generally have greater dissolved oxygen, due to surface water input. However, biota in downwelling zones may be more at risk for impacts of sedimentation and surface water contaminants (Vadher et al. 2015), as surface water is forced into the benthic and hyporheic habitat. Downwelling zones may also be at higher risk of metal toxicity, as oxidized environments can increase bioavailable forms of metals in sediments (Calmano et al. 1993). Therefore, the hydrologic conditions in the hyporheic zone that are desirable to some organisms, under certain conditions, may be associated with unfavorable processes, particularly in human dominated landscapes (e.g., urban, agricultural). In addition to hyporheic flows, stressor effects on biota will depend upon the site itself, including: contaminant type, contaminant source (ground or surface water), sediment composition, physical stressors present (sedimentation and flow alteration) and ecological context of the site (Clements et al. 2012).

Aquatic organisms can be exposed to contaminants, like metals, through multiple sources, including their food, surface water and sediments. Metals are more bioavailable to aquatic organisms when they are dissolved (i.e., in their +2 oxidation state). The release of Zn from sediments can result in effects to aquatic organisms that reside at the sediment-water interface. When Zn concentrations in sediment and porewater exceed threshold concentrations,

4

toxicity may occur in aquatic organisms (U.S. EPA 2005). As sediment Zn increases, so does the concentration of Zn in the tissues of *Hyaella azteca* (Borgmann and Norwood 1997). Zinc is an essential micronutrient for organisms, but in excess can be toxic as it inhibits Ca^{2+} uptake (Borgmann and Norwood 1995), and can limit growth and reproduction, and ultimately result in mortality. The dietary uptake of metals by macroinvertebrates can increase metal accumulation in organisms (Brinkman and Johnston 2008). Metal contamination can also alter benthic community composition and functional feeding groups, which are important for ecosystem processes (Farag et al. 1998). In this experiment, sediment and porewater were the primary exposure pathways assessed.

To manage effects of contaminants on stream biota, sediment quality guidelines establish concentrations that contaminants should not exceed (Buchman 2008). Most sediment toxicity guidelines are based on effects to biotic organisms under laboratory test conditions in static water. While hyporheic flows have been manipulated in laboratory settings (Packman and Bencala 2000), few experiments both manipulate hyporheic flows and assess effects of contaminants on biota. It is well established that environmental risk may change due to site-specific conditions and ecological context (Clements et al. 2012, Burton 2013), thus a characterization of hyporheic flows is important to understand stressor effects. Research on stressor dynamics associated with the hyporheic zone, and effects on stream biota, can help focus the goals of future stream management and restoration (Boulton et al. 2010), as restoration of hyporheic flows could result in increased stream habitat quality and processing of contaminants.

Research plan & objectives

The ultimate goal of this research was to better understand how groundwater and hyporheic flows interact with metals in sediments to influence aquatic biota. The interactions

between physical stressors, metals and the hyporheic zone were analyzed in field experiments and small artificial stream (flume) mesocosm experiments. These experiments provided complementary information to one another. The *in situ* experimental exposures were more realistic than mesocosms as they took place in a natural stream ecosystem; however, they often had more confounding results and potentially unexplained variation. Mesocosm experiments reduced confounding variables and provided more control over experimental conditions. They were essential for teasing out fine scale relationships and determining which environmental factors controlled exposure and effects of multiple stressors. When conclusions varied between *in situ* and mesocosm exposures, the *in situ* results carried more weight as they represent real-world conditions. However, understanding why conclusions differed between the systems is both critically important and possible, given the experimental designs were comprised of multiple lines-of-evidence and intensive monitoring.

Each of the chapters in this dissertation addresses a different question regarding the influences of the hyporheic zone on the exposure and effects of metal-contaminated sediments (particularly zinc) in aquatic ecosystems. Chapter specific questions and hypotheses are outlined below.

Chapter 2. Question: What are the effects of stream bedform (head riffle vs. tail riffle) and hyporheic flows (downwelling) on sediment geochemistry and biological communities in *in situ* field experiments and streamside mesocosm experiments? **Hypothesis:** Head riffles and experiments with downwelling exposures will have better habitat for benthic and epibenthic biota (due to influence of surface water), but may also have higher risk for toxicity from metals (due to more oxidized sediments than tail riffles or upwelling zones).

Chapter 3. Question: How do oxic hyporheic flows influence zinc bioavailability to the epibenthic amphipod, *Hyalella azteca,* in contaminated sediments during laboratory flow-through flume experiments? **Hypothesis:** Exposures with oxic hyporheic flow (downwelling simulation) will have greater metal exposure and effects to *H. azteca*, compared to exposures without hyporheic flows. This effect will lessen over time as the sediments age and the system equilibrates.

Chapter 4. Question: How does hyporheic connectivity (and the influence of upwelling) alter the release of metals from sediments under oxidative drying conditions, and what are the effects to aquatic communities (benthic macroinvertebrates and biofilms) in field mesocosm experiments? **Hypothesis:** In upwelling zones, sediment mesocosms that are connected to the hyporheic zone will have lower metal bioavailability than mesocosms that are disconnected from hyporheic flows, because the reduced hyporheic flows will interact with sediments in the mesocosm, creating conditions in the sediments for metals to bind to anoxic binding ligands, like sulfide.

Together, these several experiments support the principal position of this thesis, that hyporheic flows (including both upwelling and downwelling) can influence the exposure and effects of metal contaminants to aquatic communities.

Figures

Figure 1.1. The hyporheic zone is located at the interface of groundwater and surface water. Local variability in stream gradient and bedform (e.g., pools, riffles) can cause surface water to move in and out of the hyporheic zone via shallow hyporheic flow paths (solid blue lines). Downwelling zones on the head (upstream end) of the riffle have high dissolved oxygen, like the stream, whereas upwelling zones on the tail (downstream end) of the riffle are less oxygenated. Depending on the hydraulic pressure of the system, groundwater can flow up into the hyporheic zone ultimately into surface water via long flow paths (dashed blue lines). Adapted from Boulton 1998.
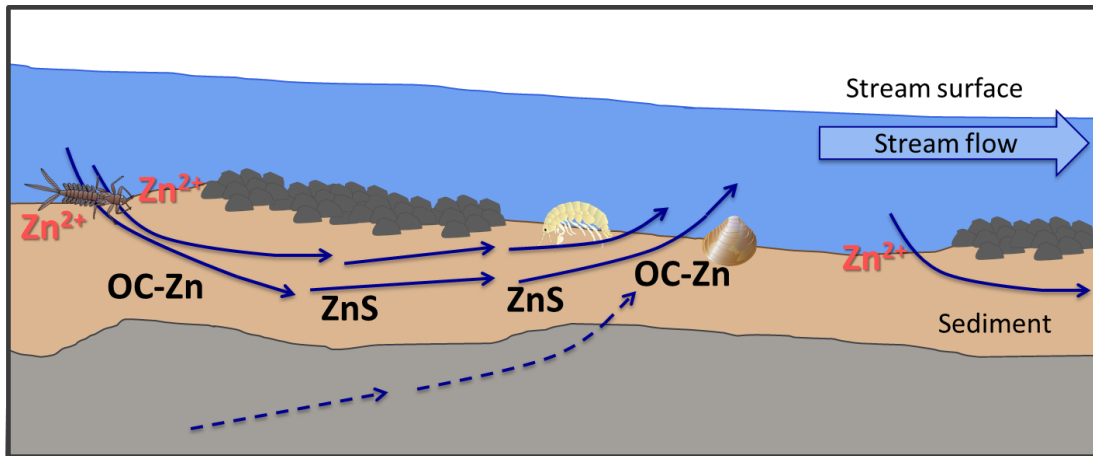
Chapter 2

Title: Stream bedform and hyporheic flows: effects on sediment biogeochemistry and biological communities

Abstract

The interface of groundwater and surface water in stream sediments (hyporheic zone) can have important implications for aquatic biota. In metal contaminated streams, the direction of hyporheic flow (upwelling or downwelling) may influence redox conditions and metal speciation, resulting in a range of effects for aquatic organisms. This research investigates the potential for metal toxicity in the head (upstream) and tail (downstream) ends of riffles, which generally represent downwelling and upwelling conditions, respectively, in a Southeastern Michigan stream. *In situ* experiments were paired with artificial stream mesocosms located on the streambank, which simulated downwelling exposures. Sediments from a stream with known zinc contamination were deployed for 30 days and effects to sediment geochemistry, metal chemistry, biofilms and benthic macroinvertebrates were assessed. Sediment redox and pH varied between the heads and tails of riffles. The riffle head was more oxidized and had higher pH, this correlated with greater bioavailable metals (i.e., (SEM-AVS)/fOC) in the riffle head than in the tail. Similar results from pH and redox were found in the mesocosm experiments. No differences in metal chemistry were observed between hyporheic treatments in either treatment. In the *in situ* experiment, macroinvertebrate community diversity and sensitivity were higher in the riffle head, where risk to metal contamination was higher. Biofilm communities responded

negatively to increases in (SEM-AVS)/fOC in the riffle head. No effects of metals or hyporheic flows were observed on test organisms in the mesocosm experiments. This research suggests that stream bedform location can alter processes in the hyporheic zone by affecting the extent of downwelling, and if metal concentrations are high enough, could increase exposure of metals to aquatic biota.

Introduction

Groundwater and surface water interactions within the hyporheic zone can alter sediment chemistry, resulting in habitat quality variability for benthic biota. Changes to sediment redox chemistry caused by hyporheic flows (Hendricks et al. 1993, Lawrence et al. 2013) may play an important role in the concentrations and bioavailability of metal contaminants in sediments (Gandy et al. 2007). Sediments in the hyporheic zone are often an important sink for metal contaminants, depending on the contaminant origin and physical characteristics of the system (Burton 2010). There is little research to explain under which conditions the hyporheic zone can act as a source or sink for metal contaminants. The effects of the hyporheic zone on metal contamination are likely due to flow path direction which can alter redox conditions that facilitate binding of metals by sediments (Gandy et al. 2007). This paper seeks to better understand how processes in the hyporheic zone (e.g., converging flow paths, microbial processing, etc…) influence sediment geochemistry and metal binding ligands, and how changes to geochemistry affect the benthic communities in hyporheic influenced aquatic habitats.

Hyporheic flow paths are commonly defined by their movement from the sediments into the stream (upwelling) or from the stream into the sediments (downwelling). This movement of water is driven by physical location in the streambed and hydraulic pressure differences between surface water and groundwater. Upstream end of riffles (heads), are considered "downwelling zones", whereas downstream riffles (tails) are "upwelling zones", which is a product of streambed topography (Boulton 1993). The redox conditions in downwelling zones reflect surface water conditions, typically characterized by higher dissolved oxygen and a higher pH more similar to surface water (Hendricks et al. 1993, Olsen and Townsend 2003). Upwelling zones are more reduced and have lower pH, likely a product of microbial respiration in sediments (Brunke and Gonser 1997).

11

Differences in sediment pH and redox can, in turn, create habitats with differing potential

metal toxicity, due to the presence or absence of important redox sensitive binding ligands.

Metals can bind to organic carbon (OC) compounds and sulfide (S^{2-}) in anoxic sediments, and to

iron/manganese oxyhydroxides under oxic conditions. Thus the redox conditions and

concentrations of different binding ligands in the sediments determine the bioavailability of

metals and toxicity to biota (Calmano et al. 1993, Chapman et al. 1998). By assessing the effects

of hyporheic flows on redox, pH, sediment chemistry and available binding ligands, this research

can better understand the potential for effects of hyporheic flows on metal contaminant

bioavailability.

Researchers have examined relationships between groundwater sourced metals and

sediment geochemistry, particularly in mining impacted streams (Benner et al. 1995, Brunke and

Gonser 1997, Gandy et al. 2007), but little work has been done in streams where metals are

primarily stored in sediments and not in groundwater or surface water. It is suggested that the

hyporheic zone acts as a zone of metal filtering of contaminated groundwater, due to the capacity

of sediments to store metals (Fuller and Harvey 2000). Metal contamination is also sourced from

surface waters, ultimately accumulating in sediments, as a product of runoff and legacy

contamination from industrial processes. Despite this important source of metals to aquatic

systems, research on sediment-sourced metals and relatively clean hyporheic flows (surface and

groundwater inputs) is limited, particularly *in situ*.

The interactions between hyporheic flows and sediment chemistry can affect the aquatic

communities that reside at the sediment surface and within the hyporheic zone, including

macroinvertebrates and biofilms. The hyporheic zone is critical habitat for benthic and

epibenthic invertebrates, as it provides food sources and refuge from predation (Gandy et al.

2007). The biological communities present are related to the cycling of nutrients and dissolved oxygen in the hyporheic zone (Hendricks et al. 1993), and these chemical processes are affected by physical processes in the hyporheic zone. Riffles heads were shown to have greater abundances of benthic macroinvertebrate communities (Pepin and Hauer 2002, Davy-Bowker et al. 2006) and greater protein content and biofilm biomass than riffles tails (Franken et al. 2001).

Biota may also face a trade-off between suitable habitat for physical conditions versus chemical conditions, depending on the source of contaminant and the direction and degree of hydrologic flow. In streams with contaminated groundwater, invertebrate community abundance declined in response to higher metal concentrations in upwelling zones (Gibert et al. 1995), compared to sites with active pumping and downwelling of surface waters into the hyporheic zone.

To test the effects of hyporheic flows on sediment chemistry and biota, this research paired *in situ* field experiments with controlled mesocosm experiments. Differences in site and scale are important when assessing hyporheic flows, because hyporheic exchange can vary a great deal across spatial scales (Boulton et al. 1998). Most hyporheic research takes place *in situ,* as it allows for inclusion of natural hyporheic flows. A smaller body of literature has focused on artificial stream or mesocosm experiments, which allow for more control of experimental conditions. Mesocosm experiments involving passive transport and transient storage have examined metal dynamics (Ren and Packman 2005, Zaramella et al. 2006), but without assessing biological effects. Other mesocosm experiments involving hyporheic flows have shown effects of sedimentation on biota (Mathers et al. 2014, Vadher et al. 2015), but did not consider redox or sediment chemistry.

The primary research objective is to assess effects of hyporheic flows on sediment porewater and metal chemistry, at relatively low Zn concentrations. Additionally, both direct effects of the experimental treatments (riffle location and sediment type) and their subsequent effects on sediment redox chemistry were assessed on benthic macroinvertebrate community structure and biofilm structure and function. Based on previous research, riffle heads were expected to have more oxidized conditions and better habitat quality for benthic organisms than riffle tails. Though better habitat, riffle heads were expected be more vulnerable to effects of metal contamination than riffle tails, due to oxidation from surface waters inputs which decrease metal binding capacity with anoxic binding ligands. The implications of this research could be particularly useful for assessments of streams impacted by mining operations (Nimick et al. 2005, Crouch et al. 2013) and in urban and agricultural streams receiving stormwater runoff, which is often high in dissolved Zn (Kayhanian et al. 2008). Zn added to aquatic ecosystems through surface and groundwater inputs can be bound by ligands and stored in the sediments.

Methods

Site selection

The field site was Fleming Creek at the University of Michigan's Matthaei Botanical Gardens (MBG), Ypsilanti Township, Michigan, during October and November 2016 (Figure 2.1). Two experiments assessed the role of hyporheic flows on sediment chemistry: (1) *in situ* experiments assessing hyporheic effects at the heads and tails of riffles, and (2) artificial stream mesocosms alongside the creek.

Initially this project intended to assess interactions between hyporheic flows and sediment zinc (Zn) on biological endpoints. However, despite documentation of high sediment Zn concentrations (Cooper et al. 2001, Wuycheck 2003) and high Zn concentrations collected

during November 2015 (~600 mg/kg), the sediments used in this study (collected August 2016) had much lower sediment Zn concentrations (maximum 161 mg/kg). Though two of the sediment types were near the Threshold Effects Concentrations (TEC) for Zn (121 mg/kg), no sediments approached the more toxic Probable Effect Concentrations (PEC) for Zn (459 mg/kg) (MacDonald et al. 2000, U.S. EPA 2005, Buchman 2008).

For the *in situ* experiment, hyporheic sampling equipment and sediments were deployed at head and tail ends of five riffle areas in Fleming Creek (Figure 2.1). For the artificial stream experiment, 12 artificial streams were set on the bank of Fleming Creek (Figure 2.1 – Flume Experiments). Sediments from Little Black Creek (LBC), Muskegon, MI were deployed as the sediments had slightly elevated Zn (Cooper et al. 2001). The sandy grain size of LBC sediments also allowed for hyporheic flow movement through the sediments.

In situ stream study design

Five riffles were selected in Fleming Creek, based on an obvious upstream start (head) and downstream end (tail) to each riffle. At each riffle location (i.e., head or tail), hyporheic sampling equipment and sediments were deployed to assess effects of hyporheic flow on sediment geochemistry and biological communities. Riffles heads were selected due to their potential for hyporheic downwelling and riffle tails were selected for their upwelling potential. At each location, minipiezometers were placed and sampled for vertical hydraulic gradient (VHG) via a manometer (Winter et al. 1988) at depths 5, 10 and 20 cm.

Five different sediments were deployed to assess effects of riffle location on sediment chemistry. These sediments included: reference site sediment from Fleming Creek (FC) and four sediments collected along a land-use gradient from LBC-1 (headwaters) to LBC-4 (mouth). Sediment Zn concentrations were low overall, but Zn increased from upstream to downstream

sites on LBC (ranging from 12.3 at LBC-1 to 161.8 mg/kg at LBC-4) (Table 2.1). Initial

sediment Zn concentrations at FC were 18.7 mg/kg. All five sediments were deployed into two

types of exposure containers at the head and tail ends of each riffle: (1) sediment colonization

trays and (2) chemical exposure substrate (CES) cups (Figure 2.2).

Colonization tray sediments were used measure sediment chemistry, porewater chemistry

and macroinvertebrate community colonization (Burton et al. 2005, Nguyen et al. 2011). The

open plastic colonization trays (200 cm^2 surface area, 8.3 cm deep) were lined with window

screen mesh, filled with sediment, covered with a coarse nylon mesh to prevent erosion, and

placed in the stream flush with the sediment surface. A porous stone attached to clamped tubing

was buried within the sediment basket (~7 cm depth) before deployment and used for porewater

sampling. On day 30 of the experiment, a 12-ml porewater sample was extracted from each

colonization basket using the porous stone. Porewater pH was measured with a handheld meter,

and the sample was filtered with a 0.45-μm polycarbonate syringe filter. A 1-ml sample was

reserved for the Ferrozine method, which determines reduced iron (Fe^{2+}) (Stookey 1970, Kostka

and Luther 1994). Reagents for Fe^{2+} were added to samples and standards in the field and the

absorbance measured on a spectrometer the same day. A 10-ml porewater sample was preserved

in 2% HNO$_3$ and stored for metal analyses (Zn, Fe, Mn). Sediments were collected from the top

2-cm of 1/3 of the colonization basket, stored in a 50-ml centrifuge and frozen.

For benthic macroinvertebrate characterizations, the remaining colonization basket

sediment was sieved using a #30 sieve bucket (595 micron), collected and preserved in a

Nalgene bottle with 70% ethanol. In the laboratory, samples were sorted, and identified to family

(non-insects) and genus (all insects with the exception of the family Diptera). Community

structure was assessed by calculating: abundance, abundance of dominant taxa, Chironomid

16

abundance, Richness, Gini-Simpson diversity index, Shannon's H Index, Evenness, EPT (Ephemeroptera, Plecoptera, Trichoptera) abundance, and Sensitive taxa abundance (Barbour et al. 1999).

The CES cups (30-mL polyethylene hinge-topped cup) were used to assess variation in biofilm net primary productivity (NPP) and chlorophyll a (Chl *a*) across sediments and hyporheic conditions (Costello et al. 2016). Cups were filled with sediment and a fritted glass disc was placed atop the sediment for biofilm (i.e., periphyton) colonization. Discs were held in place with an open top cap on the CES cup. At the end of the 30-day exposure, the CES discs were removed from the cups, gently rinsed with site water and processed for NPP. Discs were placed in 120-ml specimen cups filled with stream water, and incubated for four hours in direct sunlight. Dissolved oxygen (DO) was measured at the beginning and end of incubation and the difference in DO (adjusted for background NPP with 5 site water only replicates) was used to estimate NPP (Costello and Burton 2014). DO was measured using a YSI Professional Plus ODO meter. DO concentrations (mg/L) were measured in stream water prior to disc addition (DO_{stream}) and after 4-hour incubation ($DO_{biofilm}$). Disc NPP was corrected for site water only ($DO_{control}$) and adjusted for volume of water (L) and area of disc (m^2) (Equation 1). After the NPP measurements, glass discs were placed in 50-ml centrifuge tube and frozen for Chl *a* analysis. Chl *a* was measured by extracting biofilm discs in 90% ethanol and measuring absorbance on a spectrometer at 775nm, adjusted for turbidity at 665nm (Steinman et al. 2007).

Equation 1: $$NPP = \left(\frac{DO_{biofilm} - DO_{stream}}{time_{biofilm}} - \frac{DO_{control} - DO_{stream}}{time_{control}} \right) \times \frac{Volume}{Area}$$

Artificial stream study design

Artificial stream mesocosms (flumes) were constructed from 0.5-inch thick clear acrylic (Figure 2.3). A holding tank on the upstream end of each flume with a spillover dam provided surface water to the sediment exposure. Porewater sampling ports located laterally along each flume allowed for porewater sampling at 1.5-cm depth throughout the experiment (Figure 2.2).

The artificial stream experiments consisted of 12 flow-through streams located along the bank of Fleming Creek (Figure 2.1 map, Figure 2.2 flume). Surface water from Fleming Creek was accessed using an on-site pump; supplying flow-through exposures of hyporheic and surface water flow to the mesocosms. Creek water was delivered to a covered tank on the bank. One pump delivered water at 3.35 cm^3/second. The second pump delivered hyporheic water to 12 exposures in six flumes at flow rates averaging 0.38 cm/min (0.09 SD).

The flume experiment assessed two sediments (LBC-1 and LBC-2) and two hyporheic treatments (hyporheic and non-hyporheic), which resulted in four experimental treatments. Sediment exposure trays (same as colonization trays) were filled with either LBC-1 or LBC-2 sediments and placed in the mesocosms with Fleming Creek sediment as a filler substrate. Non-hyporheic treatments had only surface water inputs. Hyporheic treatments had an additional input of shallow oxidized hyporheic flows (similar to oxidized downwelling zones). Fleming Creek water was delivered to the mesocosm sediments via a long flat porous stone buried at the bottom of each sediment exposure tray (Figure 2.3). Hyporheic flows were forced up from the bottom of the sediment exposure tray at a rate of 11.4 cm^3/min (min 6.5, max 15.2). This rate allowed for hyporheic flow without any physical disturbance to the sediments. Two replicate sediment-hyporheic exposure baskets were placed in each flume, for six replicates per treatment.

Porewater was extracted from the sediments through time (days 1, 3, 5, 7, 13, 15, 25) using Rhizon samplers (0.19 micron) inserted into the sides of the artificial streams. Porewater

was sampled from two separate Rhizon sampling ports: (1) 11-ml was collected for pH, DO and Fe^{2+} and (2) 10-ml for dissolved metals (preserved in 2% HNO$_3$). On day 25, sediment cores were collected from the artificial streams, stored in 50-ml centrifuge tubes and frozen for analysis.

Biological endpoints were sampled throughout the flume experiments. Several commonly used toxicity test organisms (cultured in the UM laboratory) were deployed over varying exposure periods. An initial 7-day exposure of 7-14 day old *Hyalella azteca* took place, starting on day 0 and ending on day 7. A second 14-day exposure started on day 13 and ended on day 27. This exposure included ten 7-14 day old *H. azteca,* ten 1-day old *Daphnia magna* and six 14-21 day old *Lymnaea stagnalis.*

Each species was placed in a separate exposure chamber (60-ml polycarbonate) with 250-μm mesh (Costello et al. 2015). Both *H. azteca* and *L. stagnalis* were exposed to surface water and sediment and assessed for survival and growth. *D. magna* was exposed only to surface water, and was assessed for survival and reproduction.

Laboratory and data analysis

In the laboratory, sediments were thawed and analyzed for acid volatile sulfide (AVS) and simultaneously extracted metals (SEM) (Allen et al. 1991), organic carbon via loss-on-ignition (6 hour combustion at 450° C) and total metals. For the total metal digestion, 0.5-g of dried sediments was digested in 7-ml of trace metal grade HNO$_3$ in a Hot Block (Environmental Express) at 112° C for 100 minutes (EPA method 5050B), then diluted for analysis on ICP-OES. During the digestion, metal concentrations were corrected for sample handling using a procedural blank (MilliQ). The digestion recovery was verified (>80%) with standard reference materials. Porewater metal samples were preserved (2% HNO$_3$) for dissolved metal analysis (Zn,

19

Fe, Mn) on an ICP-OES. Detection limits were 50 μgL^{-1} for Fe, 25 μgL^{-1} for Zn, and 10 μgL^{-1} for Mn.

The *in situ* experiments were assessed using linear mixed effects models to determine effects of riffle location (head vs. tail) and sediment type (5 sediments) on sediment chemistry and biological responses in the *in situ* experiments, with site as a random effect. Response variables with count data (i.e., abundance, abundance of dominant taxa, Chironomid abundance, EPT taxa and sensitive taxa abundance) were analyzed with generalized linear mixed effects models with Poisson distributions. Regression analyses assessed the relationships between sediment chemistry and VHG, and assessed how both related to biological endpoints. For each regression, the relationships were compared between riffle heads and tails. For variables with non-linear relationships, log-transformations were performed.

In the mesocosm experiments, linear mixed effects models assessed the main effects of hyporheic flows, sediment type and time on porewater chemistry endpoints, accounting for the random effects of each flume. Two-way interactions between sediment and hyporheic conditions tested for variation in porewater chemistry caused by hyporheic treatment between reference sediment (LBC-1) and low Zn sediments (LBC-2). Two-way interactions between time and hyporheic conditions tested for variation in porewater chemistry caused by the hyporheic treatment over time. Two-way interactions between time and sediment type tested for the sediment specific differences in porewater chemistry over time.

Mesocosm experiment parameters that were only sampled at the end of the experiment, including biological endpoints (survival, growth, reproduction) and sediment chemistry (total metals, SEM-AVS) were also assessed using linear mixed effects and generalized linear mixed effects models (for survival data with binomial distributions). Hyporheic conditions and

sediment type were fixed effects and mesocosm sampling location was a random effect. Interactions tested for variation in effects of the sediments caused by hyporheic treatment. Regression analyses assessed relationships between continuous porewater and sediment chemistry parameters and biological parameters. For linear models, data were assessed for linearity and parameters were log-transformed when non-linear. Data analyses were performed in RStudio (Version 1.0.136).

Results

In-situ stream experiment

Hyporheic conditions were dominated by upwelling in Fleming Creek, regardless of riffle location. The VHG was predominantly positive across all sites, depths and riffle locations, ranging from -0.08 to 1.47, with an average of 0.28 ± 0.08. This suggests significant groundwater inputs from outside the stream banks. Though no significant difference in VHG was observed between riffle heads and tails, differences in chemistry were observed between the two habitats. Riffle tail sites had greater Fe^{2+} (Ferrozine method) than the riffle head sites (t=2.54, p=0.015; Figure 2.4; Table 2.2). The high variability in Fe^{2+} between sediment types is likely due to variation in total Fe and porewater Fe between sediment types, with LBC-1 having the highest total Fe and Fe^{2+} (Table 2.1).

Porewater pH in the riffle heads was significantly higher than in riffle tails (t=4.55, p <0.0001; Figure 2.5; Table 2.2), likely a product of surface water influence. A negative exponential relationship was observed between porewater pH and reduced Fe^{2+} across all treatments ($F_{1,40}$=50.66, $p < 0.001$; Figure 2.6). The LBC-1 sediment type also had higher Fe^{2+} in porewater than FC, LBC-3 and LBC-4 sediments (t=4.29; p< 0.001). There was no effect of sediment type on pH.

21

Porewater Fe was higher at riffle tails (upwelling zones), compared to riffle head sites, though not quite significant at $\alpha = 0.05$ (t=2.00, p=0.053). Porewater Fe and Fe^{2+} in porewater were highly correlated (R^2=0.79, $F_{1,43}$=166, $p<0.001$). No effects of riffle location were observed on porewater Zn, likely due to the overall low initial sediment concentrations (Table 2.1). Porewater Mn was also unaffected by riffle location. Total Zn was unaffected by riffle location and effects of sediment type did not change (Table 2.1). Total Fe (t=2.26, $p = 0.029$) and Mn (t=2.10, $p = 0.042$) in sediment were greater in the riffle head than in the riffle tail location.

The AVS fraction of SEM-AVS was less than the SEM for three of the five sediment types (LBC-2, LBC-3, LBC-4). The three sediments with positive SEM-AVS were collected from the three downstream locations along Little Black Creek, where sediment metal concentrations above PEC values were observed during a fall 2015 sediment collection and in previous studies (Cooper et al. 2001). FC and LBC-1 were collected from an uncontaminated stream and a reference site upstream of metal contamination in LBC, respectively. While unaffected by the riffle treatment, (SEM-AVS)/fOC overall was related to porewater pH and redox (Fe^{2+}). As pH increased, (SEM-AVS)/fOC increased ($F_{1,35} = 8.08$, p=0.007, $R^2 = 0.19$), and as Fe^{2+} increased, (SEM-AVS)/fOC decreased ($F_{1,35} = 11.77$, p=0.002, $R^2 = 0.25$). Despite the low Zn concentrations in the sediment, the sandy sediments in LBC had a low capacity for metals binding to sulfides and organic carbon and thus Zn may be bioavailable at low concentrations.

No direct effects of riffle location or sediment type were observed on biofilm (periphyton) structure (Chl *a*) or function (NPP). NPP decreased with increased (SEM-AVS)/fOC (p=0.008), indicating lower primary productivity with decreased metal binding capacity of the sediments (Figure 2.7). NPP also increased significantly with increased Fe^{2+} (*p*

<0.001), and decreased as pH increased from 7.0 to 8.0 ($p = 0.003$), in a similar relationship to (SEM-AVS)/fOC. No relationship between Chl *a* and (SEM-AVS)/fOC was observed.

Benthic community composition was affected by both sediment type and riffle location (Figure 2.8). There were no effects of metal chemistry (porewater metals, total metals, (SEM-AVS)/fOC) on benthic macroinvertebrate community composition; likely, due to low overall metal concentrations below threshold effect levels (TECs). Chironomids were the dominant benthic macroinvertebrate in 48 of the 50 samples; the two exceptions were dominated by oligochaetes. Both of these groups of benthic invertebrates tend to be stressor tolerant. Abundance metrics were greater at riffle tail locations, compared to riffle head locations. Total abundance was greater at downstream riffles (t=7.60, p<0.001), as was the relative abundance of the dominant taxa (t=2.16, p=0.037) and total Chironomid abundance (t=8.50, p<0.001).

Unlike abundance metrics, diversity and community sensitivity metrics were greater at riffle heads than tails (Figure 2.8). Abundance metrics can be misleading. High abundances of midges and oligochaetes, both of which tend to be pollution tolerant, can simply show a more polluted environment. The Gini-Simpson index of diversity was higher at the riffle head locations (t=2.14, p=0.039), as was Shannon's H diversity (t=3.10, p=0.004). Richness was almost significantly (α=0.05) higher at riffle heads (t=1.95, p=0.059). EPT abundance was higher at riffle heads than riffle tails (t=2.77, p=0.009) and the abundance of sensitive taxa was higher at the heads of riffles (t=2.21, p=0.033). Riffle tails, with greater influence of hyporheic upwelling, had larger abundances of organisms, largely driven by Chironomid abundances. Whereas riffle heads, characterized by downwelling zones, were better habitat for more diverse and sensitive taxa, likely due to the influence of surface water.

Artificial stream experiment

DO concentrations in the hyporheic treatment of the mesocosms averaged 5.66 ($\pm$ SE 0.25) mg/L, creating DO conditions to the shallow (< 5 cm) riffle sediments *in situ* (5.11 mg/L $\pm$ SE 1.29). Overall, treatments increased in Fe^{2+} over time as sediment equilibrated (t=6.27, p<0.001). There was a greater effect (decreased Fe^{2+}) on the LBC-2 sediments caused by the hyporheic treatment, compared to LBC-1 sediments (t=-2.35, p=0.037) (Table 2.3). The lower Fe^{2+} in hyporheic exposures indicated an oxidation, compared to non-hyporheic exposures, whose sediments were more reduced over time. A drop in Fe^{2+} across all treatments occurred on day 15. The low Fe^{2+} on day 15 for all exposures was either the result of an oxidation event that occurred across all flumes or measurement error on day 15. Measurement error is probable; as there were no weather-related events (precipitation or high flows), or variation in surface water DO, to explain the drop in Fe^{2+}.

Porewater pH decreased over time (t=-8.18, p<0.001) and pH was higher in the hyporheic exposures than non-hyporheic (t=2.45, p=0.024) (Table 2.3). The decrease in pH over time was likely related to the equilibration of the sediments with the surface water. The addition of surface water with a pH of 8.0 initially increased the sediment pH from its original 7.3 pH, and over time sediments re-equilibrated to the original sediment pH.

Though pH decreased with time across all four exposures, this trend was more pronounced for the non-hyporheic exposures (LBC-1: $F_{1,40} = 30.3$, $R^2 = 0.43$; LBC-4: $F_{1,40} = 66.7$, $R^2 = 0.63$), compared to the hyporheic exposures (LBC-1: $F_{1,40} = 13.2$, $R^2 = 0.25$; LBC-4: $F_{1,40} = 28.4$, $R^2 = 0.41$). The use of surface water for the downwelling hyporheic exposure may also explain why the decrease in pH over time was not observed as strongly in the hyporheic exposures, compared to the non-hyporheic exposures, which were only affected by surface water flowing over top of the sediments. This allowed the non-hyporheic exposures to more quickly

equilibrate over time. By day 25, the pH returned to 7.2-7.3 for all treatments. There were no differences in pH among sediment types.

Porewater iron (Fe) increased over time and was affected by interactions among treatments, similar to Fe^{2+}. Similar to Fe^{2+}, LBC-2 had a greater decrease in porewater Fe, when exposed to the hyporheic flows, compared to LBC-1 sediments (t=-2.50, p=0.028) (Table 2.3). Overtime, the LBC-1 sediments had a greater increase in porewater Fe than the LBC-2 sediments (t=2.34, p=0.021).

Similar to porewater Fe, porewater Mn was disproportionately affected by the hyporheic treatment in LBC-2 sediments, compared to LBC-1 sediments. The hyporheic treatments had lower dissolved Mn in the LBC-2 sediments than in LBC-1 sediments (t=-6.52, p<0.0001). Porewater Mn had a slight decrease over time in the LBC-2 sediments, but no change over time was observed in the LBC-1 sediments (t=-2.24, p=0.026). Porewater Mn was also unaffected by the pH, whereas Fe decreased with increasing pH. This suggests pH may be driving the Fe and Mn concentrations in the sediments. No effects of hyporheic treatment were observed on total Zn, Fe or Mn in the sediment.

The hyporheic treatment did not have any direct effects on binding ligands, but relationships between porewater chemistry (which was affected by hyporheic treatment) and metal binding ligands were observed. All (SEM-AVS)/fOC values were negative, suggesting there should be no toxicity on benthic invertebrates from sediment Zn. (SEM-AVS)/fOC increased with increased porewater pH in the hyporheic treatment (F=6.86, p=0.026, R^2=0.40), though no relationship was observed in the non-hyporheic treatment. There were no effects of treatment or porewater chemistry (pH, Fe^{2+}) on organic carbon.

The porewater and total Zn concentrations were well below the PECs for both porewater and sediment in the mesocosms. The (SEM-AVS)/fOC was negative for all treatments, thus any effects on test organisms cannot be attributed to toxicity. No effects of treatment were observed on *H. azteca* in the 7-day exposure. In the 14-day test, *H. azteca* survival declined with increased pH (F=2.32, p=0.030), similar to the 7-day experiment. There were no effects on *D. magna* or *L. stagnalis*.

Discussion

Multiple lines of evidence provided a better understanding of how hyporheic flows and bedform influence sediment geochemistry. Though the *in situ* experiments were more reflective of actual stream conditions than mesocosm experiments, both provided insight into effects of hyporheic flows. Redox conditions (Fe^{2+}) were similar between the *in situ* experiments and the oxic hyporheic exposures in the mesocosms, and similar effects of pH on (SEM-AVS)/fOC were observed between the two experiments. Future research should use the same biological endpoints in both *in situ* and mesocosm experiments. This could be done by incorporating biofilm endpoints (NPP, Chl *a*) in the mesocosms and assessments of native stream community colonization within the mesocosm, similar to other mesocosm experiments (Clements et al. 1989). It may also be important to better simulate natural surface water flow, which was much faster than could be obtained in the mesocosms. The faster surface water velocity in the *in situ* experiments could also explain the lower Fe^{2+} observed *in situ*, compared to the mesocosms.

Porewater redox conditions, indicated by Fe^{2+}, showed expected relationships in both experiments. Despite no differences in measured VHG between riffle locations, the riffle heads had higher Fe^{2+} and lower pH than the riffle tails. These results support previous research, where stream bedform location created distinct physical and chemical habitats (Hendricks and White

26

1991, Franken et al. 2001). These results suggest that bedform location and the associated redox chemistry, within Fleming Creek, could be a more sensitive metric to assess upwelling and downwelling than VHG measured via minipiezometers and manometer. Utilization of riffle locations as proxy for hyporheic conditions is limited by the stream gradient, stream substrate and the time of year. This experiment took place in October, when surface water flow is low and the location of riffles most obvious for site selection. Fleming Creek also has a cobble substrate with fine sediments filling the interstitial spaces, which also allows for easier determination of riffles than a sandy bottom stream.

The hyporheic exposures in the mesocosm experiments simulated an oxic hyporheic conditions, compared to the non-hyporheic exposures. The non-hyporheic exposure was most representative of pool habitat where there is minimal hyporheic exchange (personal observations), whereas the hyporheic exposure would be representative of a downwelling zone, due to the oxidation of sediments. In addition to downwelling zones, oxidation of upwelling zones could occur in shallow sediments (<5cm depth), due to interactions with surface water flow, especially under accelerated surface water velocities (Kaufman et al. 2017). An oxidative upwelling zone could exist naturally where hyporheic flow paths have short residence times, lower respiration or higher primary productivity (Brunke and Gonser 1997). Flow-through surface water alone has been shown to oxidize sediments down to 4.5 cm during a long-term (>200 days) study (Costello et al. 2015).

It is inherently difficult to simulate natural hyporheic flows in mesocosms. The methods in this study were not quite "passive transport", as has been used in other hyporheic flume studies (Ren and Packman 2005, Zaramella et al. 2006). Similar pumping methods to this experiment have been used to simulate hyporheic upwelling (Mathers et al. 2014). Artificial

27

stream experiments face tradeoffs between maintaining a hyporheic pumping rate slow enough for sediment microbial processes to reduce the porewater and maintaining hyporheic flow rates similar to natural conditions. Because differences in porewater chemistry were observed, the flow rates, while low, were high enough to alter sediment chemistry, similar to a downwelling exposure. Future experiments could use pumps with a higher capacity to pump water than the small aquarium pumps used in this study.

In both the *in situ* and mesocosm experiments, pH was inversely related to Fe^{2+}. The pH in the riffle heads (low Fe^{2+}) was higher than in the riffle tails (higher Fe^{2+}). This indicated a decrease in pH as surface water entered the sediment and became more reduced as it moved through the hyporheic zone. Other regional studies found similar relationships between pH and redox potential in the hyporheic zone, both in Northern Michigan (Hendricks et al. 1993) and in Ontario (Franken et al. 2001). This was likely related to the high pH buffering capacity of these streams, due to presence of calcium carbonates and associated alkalinity (~270 mg $CaCO_3$/L in Fleming Creek). The mesocosm experiment exhibited similar redox induced trends in pH; the more oxidized hyporheic exposures had a higher pH than the less oxidized non-hyporheic exposures.

Though there were no direct effects of sediment Zn or hyporheic treatment on biofilms or benthic macroinvertebrates, correlations between NPP and (SEM-AVS)/fOC suggest the hyporheic zone may play an important role in sediment toxicity, even at low metal concentrations. The metal concentrations were below toxic thresholds, yet correlated with decreased in NPP. The correlation between biofilm functional response and bioavailable metals at low concentrations suggest a potential effect at low metal concentrations for sediments with low binding capacities. As no relationships were observed between metals and benthic

macroinvertebrates, this also indicates that biofilms may be a more sensitive endpoint at low metal concentrations (Costello and Burton 2014). No relationship was observed between SEM-AVS and Chl *a*, indicating that the functional response (NPP) may be more sensitive than the structural response (Chl *a*), despite a strong correlation between NPP and Chl *a*.

This research also observed more sensitive and diverse benthic macroinvertebrate communities residing in the riffle head than tail, as was anticipated (Franken et al. 2001). This trend was related to the higher dissolved oxygen present in riffle heads, compared to tails. It could also be related to the greater potential for food production for grazers of heterotrophic biofilms, as biofilm growth can be stimulated by organic matter deposited in fine sediments with downwelling (Navel et al. 2011). Macroinvertebrate abundances, however, were higher at riffle tails, contrary to other studies which found all metrics of benthic macroinvertebrate community compositions to be higher at heads of riffles (Hendricks et al. 1993, Davy-Bowker et al. 2006). Given these abundance numbers were driven by midges and oligochaetes, it is not surprising for a less oxidized upwelling zone.

The riffle heads, with the more diverse and sensitive macroinvertebrate communities, may also be at greater risk for sediment metal contamination. Though there was no effect of riffle locations on (SEM-AVS)/*f*OC, there was greater oxidation of sediments and higher pH in the head of riffles, indicating a strong influence of the surface water on sediment chemistry. Both the higher pH and more oxidized conditions were correlated with higher (SEM-AVS)/*f*OC, resulting in more bioavailable metals (Calmano et al. 1993). Thus, the more diverse and sensitive macroinvertebrate communities in the riffle head locations are potentially at greater exposure risk from metal contaminants in sediments. This risk could be increased in urban or agricultural

streams where contaminant deposition via surface waters is more likely in the riffle head (downwelling) compared to the riffle tail (upwelling zones) (Brunke and Gonser 1997).

This study makes connections between stream bedform, sediment geochemistry and important metal binding ligands. Though metal concentrations were not high enough to see effects on biota (with the exception of biofilm Chl *a*), this research highlights the conditions in which oxic hyporheic flows decrease metal binding capacity in sediments. Multiple lines of evidence (*in situ* and mesocosm) supported similar sediment geochemistry results, which strengthens the conclusions.

Tables

Table 2.1. Physiochemical sediment properties of initial sediments (prior to experiment), including loss-on-ignition (LOI), simultaneously extracted metals (SEM) minus acid volatile sulfide (AVS) over the fraction of organic carbon (f_{OC}), and total metals concentrations.

Sediment	Experiment	LOI (% C)	AVS (μmol g^{-1})	(SEM-AVS)/f_{OC} (μmol g^{-1})	Fe (mg kg^{-1})	Mn (mg kg^{-1})	Zn (mg kg^{-1})
				SEM-AVS		**Total Metals**	
FC	*in situ*	0.75	0.78	-95.3	4176	120	19
LBC-1	*in situ* / Flume	0.85	0.83	-89.2	5731	34	12
LBC-2	*in situ* / Flume	1.32	1.04	-13.1	4815	418	59
LBC-3	*in situ*	1.09	0.40	-5.0	1816	28	46
LBC-4	*in situ*	1.87	1.91	-45.1	3390	238	161

Table 2.2. Main effects of riffle head (compared to riffle tail) and sediment type (compared to Fleming Creek sediments) at *in situ* experiment from linear mixed effects models. All p-values are reported and significant p-values are bolded. (+) indicates that the riffle head location was higher than the riffle tail, (-) indicates the riffle head had lower concentrations of the parameter.

Parameter	Riffle head	LBC1	LBC2	LBC3	LBC4
Ferrozine	(-) **p=0.015**	**p<0.001**	p=0.736	p=0.703	p=0.262
pH	(+) **p<0.001**	p=0.259	p=0.557	p=0.187	p=0.598
Zn (µg/L)	p=0.903	p=0.887	p=0.329	**p=0.007**	p=0.064
Fe (mg/L)	p=0.053	**p<0.001**	p=0.861	p=0.527	p=0.607
Mn (µg/L)	p=0.293	p=0.626	p=0.186	p=0.167	p=0.159
Zn (mg/kg)	p=0.959	p=0.985	**p<0.001**	**p=0.001**	**p=0.001**
Fe (g/kg)	(+) **p=0.029**	**p=0.011**	p=0.489	**p=0.030**	p=0.105
Mn (mg/kg)	(+) **p=0.042**	p=0.493	p=0.435	p=0.989	p=0.499
(SEM-AVS)/fOC	p=0.439	p=0.145	p=0.224	p=0.324	p=0.068
AVS (µmol/g)	p=0.598	p=0.324	**p=0.040**	p=0.594	**p=0.050**
SEM Zn (µmol/g)	p=0.969	p=0.783	**p<0.001**	p=0.121	**p<0.001**
OC (% LOI)	**p=0.051**	p=0.616	p=0.435	p=0.177	p=0.501

Table 2.3. Porewater and sediment chemistry results during the mesocosm experiment from linear mixed effects models for effects of time, hyporheic flow and sediment on porewater chemistry. Bolded text indicates significant main effect or interaction. For main effects, (+) indicates the hyporheic treatment had higher values than the non-hyporheic treatment, (-) indicates the hyporheic was lower than the non-hyporheic.

Parameter	Time	Hyp	Sed LBC-2	Time* Hyp	Time* LBC-2	Hyp* LBC-2
PW DO (mg/L)	**(-) p<0.001**	p=0.949	**(-) p=0.049**	p=0.816	p=0.328	p=0.956
PW Fe^{2+} (mg/L)	**(+) p<0.001**	p=0.431	**(+) p=0.026**	**p=0.039**	**p=0.044**	**p=0.037**
PW pH	**(-) p<0.001**	**(+) p=0.024**	p=0.806	p=0.181	p=0.545	p=0.630
PW Fe (mg/L)	**(+) p<0.001**	p=0.363	**(+) p=0.026**	**p=0.028**	**p=0.021**	**p=0.028**
PW Mn (mg/L)	p=0.311	p=0.121	**(+) p<0.001**	p=0.402	**p=0.026**	**p<0.001**
PW Zn (mg/L)	p=0.146	p=0.301	p=0.722	p=0.537	p=0.349	p=0.513
Total Fe (mg/kg)	NA	**(+) p=0.077**	**(+) p=0.037**	NA	NA	p=0.300
Total Mn (mg/kg)	NA	p=0.770	**(+) p=0.003**	NA	NA	p=0.554
Total Zn (mg/kg)	NA	p=0.866	**(+) p=0.002**	NA	NA	p=0.270
(SEM-AVS)/*f*OC	NA	p=0.582	p=0.504	NA	NA	p=0.928
SEM (µmol/g)	NA	p=0.861	**(+) p=0.002**	NA	NA	p=0.334
AVS (µmol/g)	NA	p=0.459	**(+) p=0.009**	NA	NA	p=0.643
OC (%LOI)	NA	p=0.531	**(+) p<0.001**	NA	NA	p=0.808

Figures

Figure 2.1. Locations of sites for the *in situ* experiment (starred) and artificial stream mesocosm experiments (pink box) at Fleming Creek.
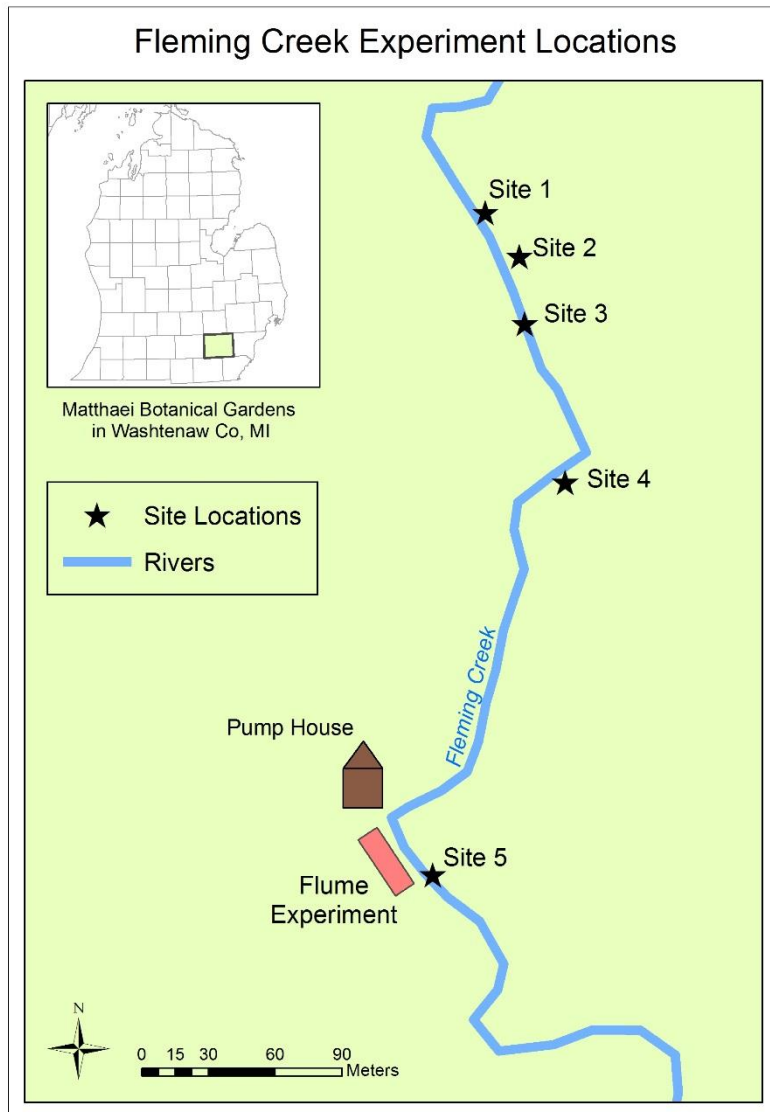
Figure 2.2. Sampling equipment deployed at each of the 10 site-riffle locations, including: minipiezometers, biofilm CES cups and benthic macroinvertebrate colonization trays.
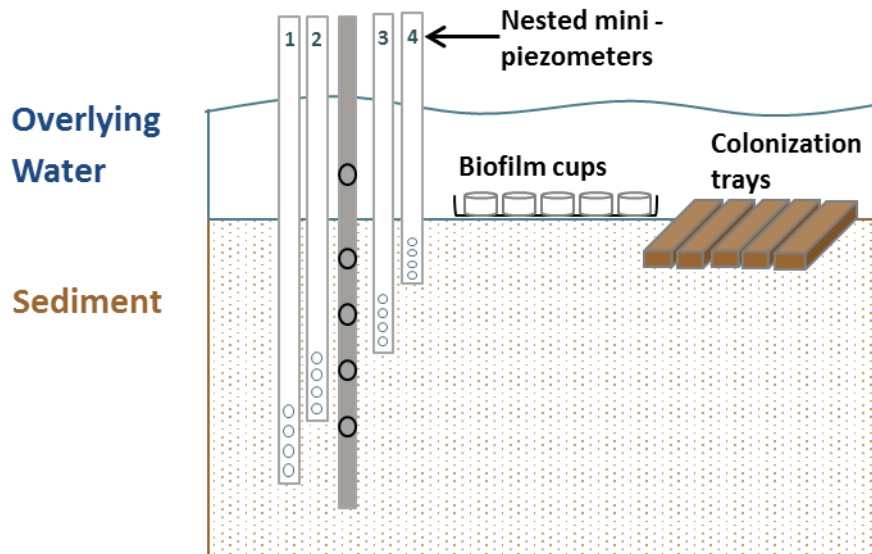
Figure 2.3. Artificial stream experimental unit (one mesocosm, lateral view). Twelve artificial streams were place side-by-side and deployed along Fleming Creek in the Matthaei Botanical Gardens. This diagram shows one of the six mesocosms with hyporheic input, the other six 'non-hyporheic' had no input of hyporheic water flow, and were only exposed to surface water input.
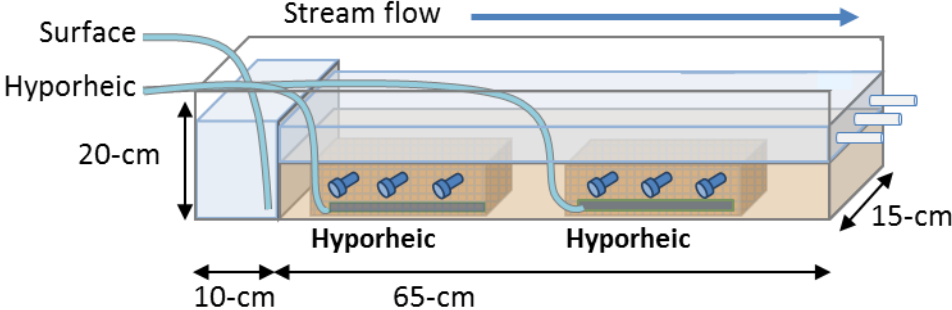
Figure 2.4. Reduced iron (Fe^{2+}) concentrations were lower in riffle heads (downwelling zones) than riffle tails (upwelling zone) in the *in situ* experiment. LBC-1 sediment has significantly greater Fe^{2+} than FC, LBC-2 and LBC-3 sediments.
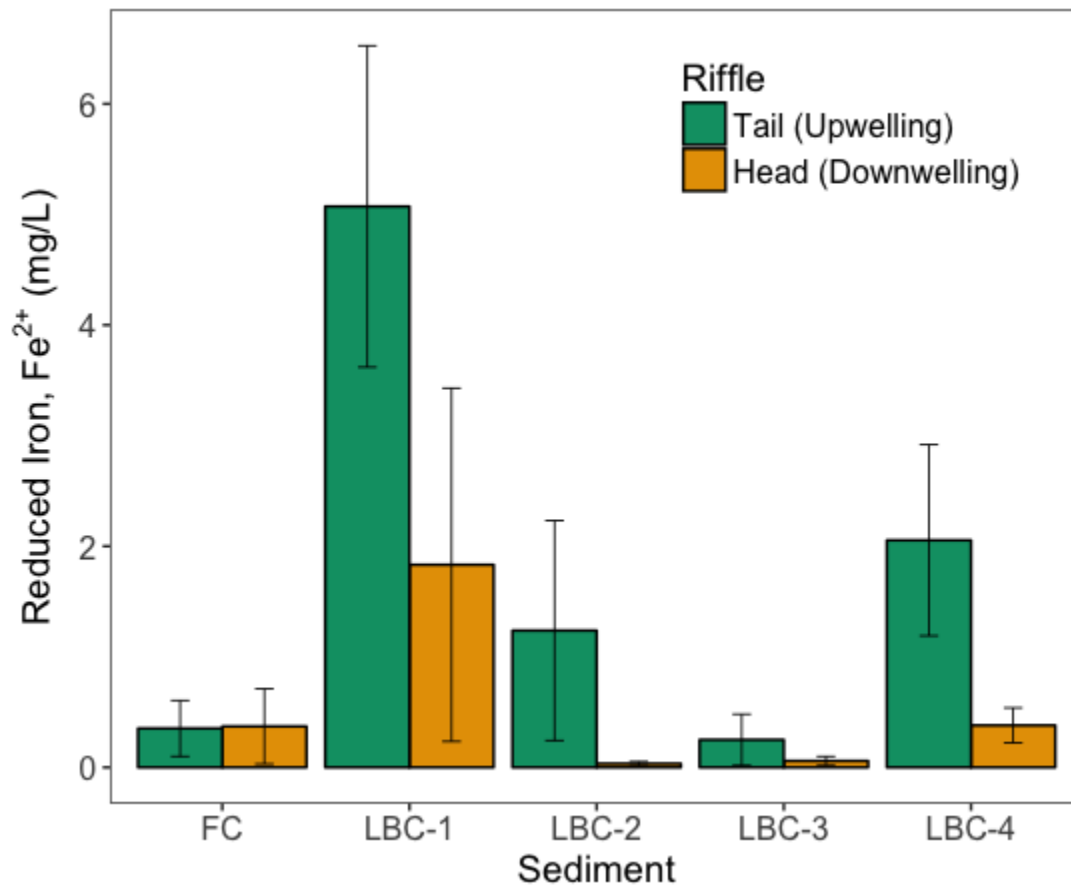
Figure 2.5. The pH was higher in riffle heads compared to riffle tails across all sediment types ($t=4.546$; $p < 0.001$) in the *in situ* experiment. No effects of sediment type on pH (LBC-1: $p=0.26$; LBC-2: $p=0.56$; LBC-3: $p=0.19$; LBC-4: $p=0.60$).
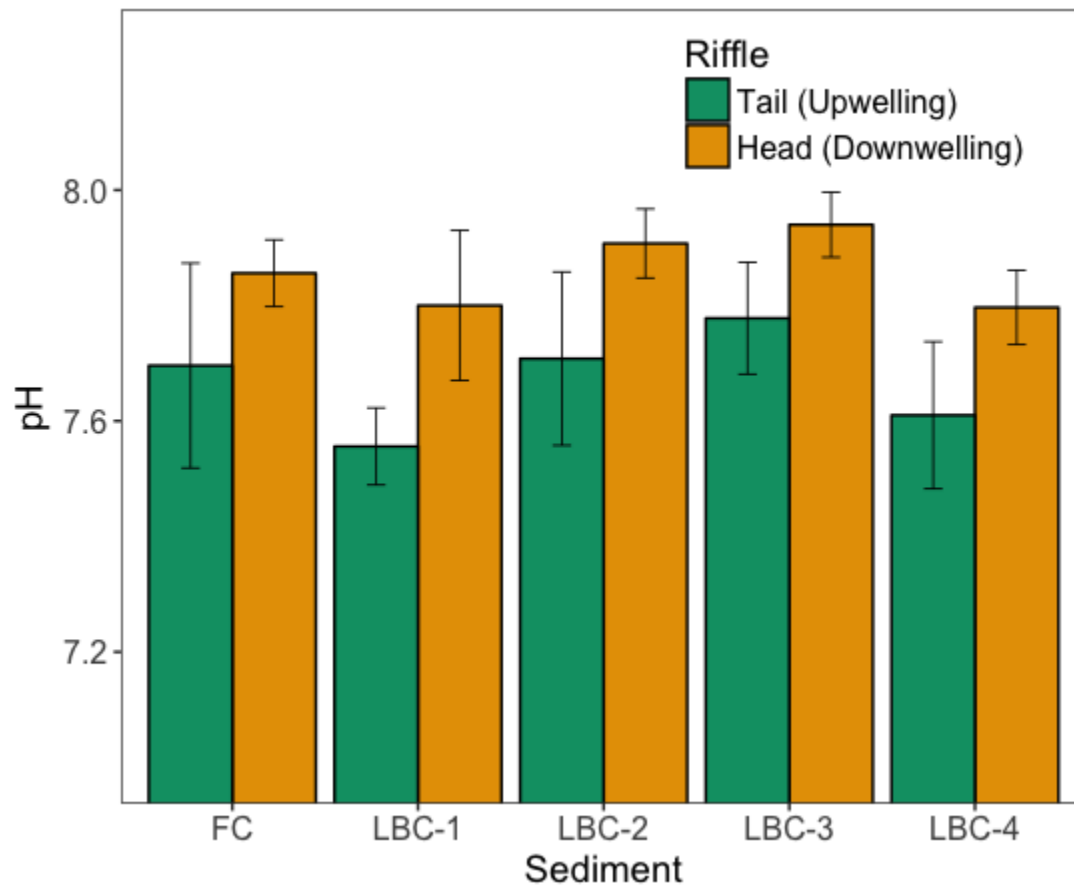
Figure 2.6. Reduced iron (Fe^{2+}) was negatively related to pH ($R^2 = 0.559$, p<0.001) in the *in situ* experiment.
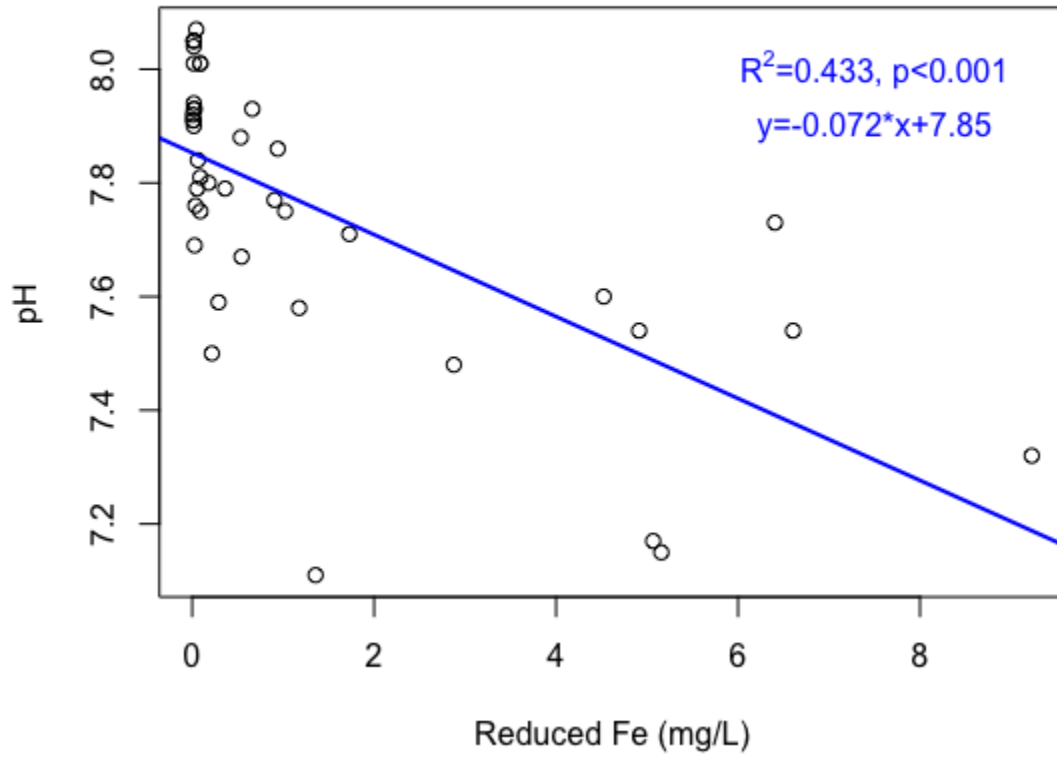
Figure 2.7. Biofilm net primary productivity declined with increased (SEM-AVS)/*f*OC during the *in situ* experiment.

The plot shows NPP (mg O_2m^{-2}h^{-1}) on the y-axis versus SEM-AVS/fOC (μmol/g) on the x-axis, with the fitted line:

$$y = -0.467*x + 46.40$$
$$R^2 = 0.157, p = 0.008$$
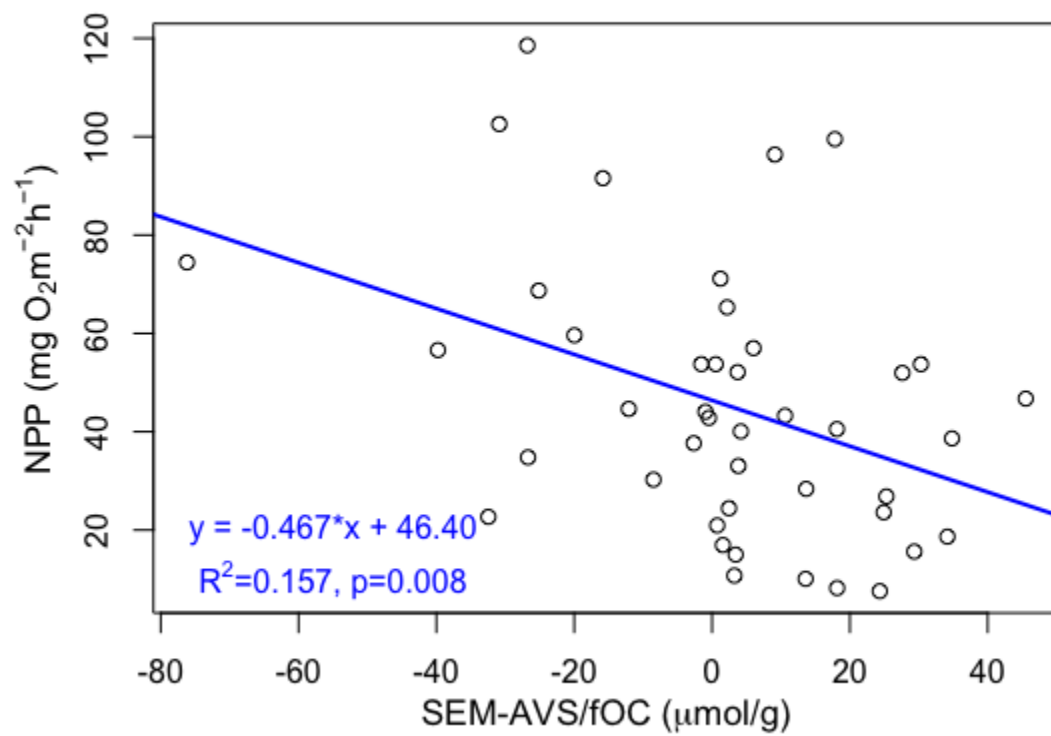
Figure 2.8. The benthic macroinvertebrate community responded to both riffle location and sediment type in *in situ* experiments. Abundance metrics were greater at riffle tails, while diversity and sensitivity metrics were greater at riffle heads.
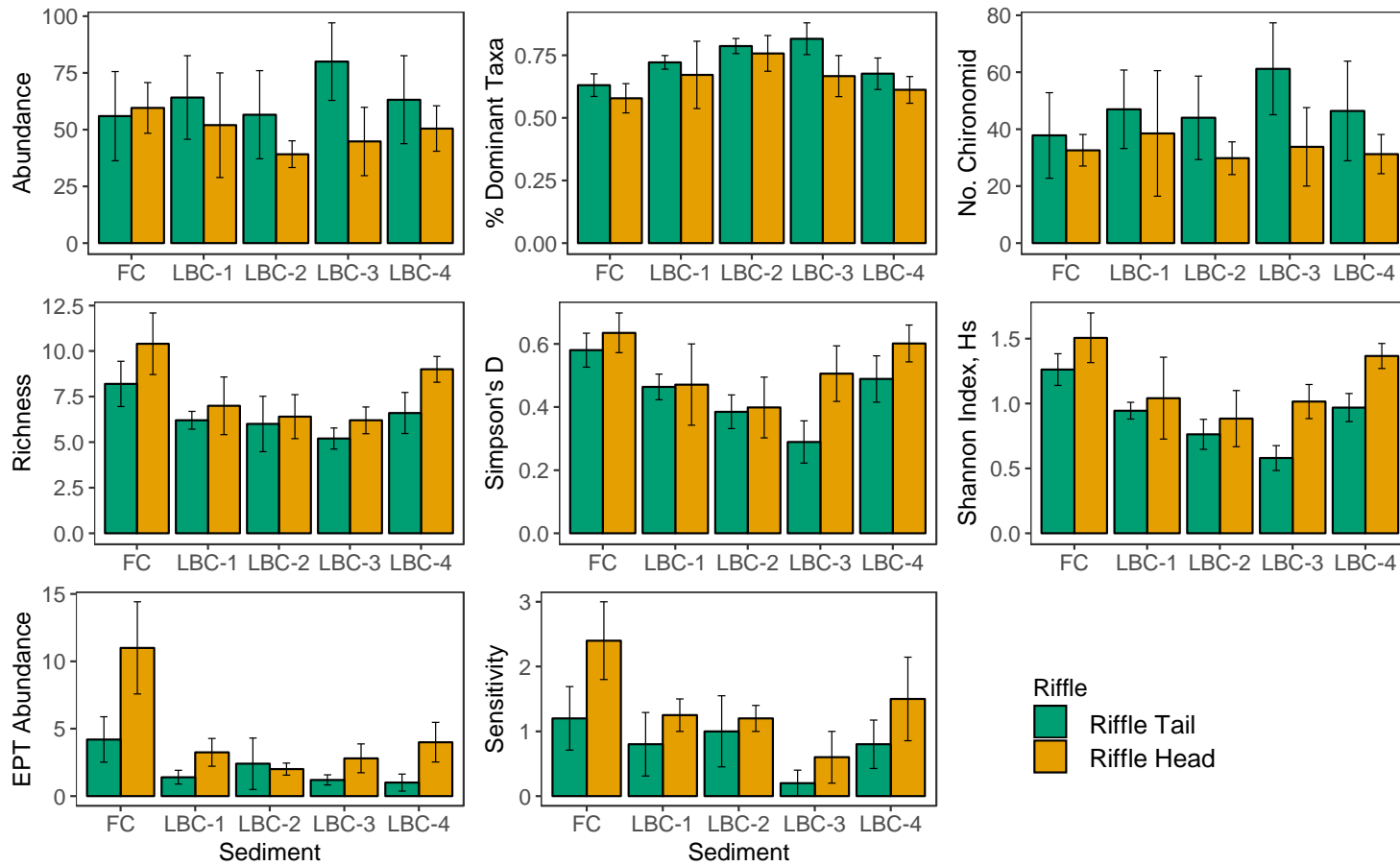
Chapter 3

Hyporheic interactions increase zinc exposure and effects to *H. azteca* in sediments under flow-through conditions

Abstract

Groundwater-surface water interactions (hyporheic flows) can influence redox conditions in stream sediments, which controls the capacity of stream sediments to store metal contaminants. Many urban and agricultural streams are contaminated with metals from stormwater runoff and legacy sources, yet little is known about the effects of hyporheic flows on metal bioavailability and the effects to aquatic benthic invertebrates. This laboratory study investigated the effects of oxic hyporheic flows and zinc-contaminated sediments on the amphipod *Hyalella azteca.* Hyporheic flows were manipulated in 12 experimental streams under flow-through conditions for 10-day exposures. Two toxicity tests were performed, an initial post-spiking test and a second aged sediment test after 80 days of saturation and flow-through conditions. Hyporheic flows altered sediment and porewater geochemistry, oxidizing the sediments and causing changes to redox sensitive endpoints. In both the initial and aged experiments, *H. azteca* survival was lowest in the exposure with zinc and hyporheic flows (compared to reference sediments and non-hyporheic exposures), despite no difference in porewater Zn in the aged exposure. Survival of *H. azteca* declined in response to porewater Zn in the initial exposure, and in response to (SEM-AVS)/fOC in the second exposure. This study suggests that hyporheic flows may play an

important role in metal bioavailability and should be further investigated to improve

environmental risk assessment.

Introduction

Groundwater-surface water interactions influence most lotic ecosystems, but their effects on contaminant bioavailability remain largely unstudied. Hyporheic flows influence sediment redox chemistry and pH (Hendricks et al. 1993, Franken et al. 2001), which in turn affect metal speciation and binding (Calmano et al. 1993). Hyporheic flows then likely affect the bioavailability of metals in contaminated sediments. This paper will address both the exposure and effects of hyporheic flows and their interaction with zinc-contaminated sediments, assessing changes in sediment chemistry and effects on the epibenthic amphipod, *Hyalella azteca.*

Hyporheic flows can influence oxidation and redox conditions in stream sediments across several scales. In streams, certain bedforms are associated with different hyporheic sediment chemistries. Upstream riffles are typically dominated by downwelling of surface waters into sediments and are more oxidized than downstream riffles, which are dominated by upwelling of hyporheic waters from the sediments (Boulton 1993). Downwelling zones are more oxidized and redox conditions are closer to surface water conditions (Hendricks and White 2000, Olsen and Townsend 2003), whereas upwelling zones are generally more reduced due to microbial respiration occurring in sediments (Brunke and Gonser 1997). Hyporheic flows can also be influenced on smaller scales. Epibenthic organisms that reside in the sediments and can create flow paths for water as they burrow and move through interstitial spaces in sediments (Gilbert et al. 2003, Sarriquet et al. 2007).

Organisms that utilize sediments for food, shelter or reproduction will be exposed to both the chemical and physical conditions in the streambed. Many benthic macroinvertebrates utilize the hyporheic zone; some epibenthic invertebrates are considered hyporheic obligate (i.e., amphipods, isopods), whereas many benthic invertebrates are opportunistic or occasional hyporheic residents (i.e., burrowing mayflies) (Boulton et al. 2010). Fish also use the hyporheic

44

zone for reproduction, as a place to lay eggs (Malcolm et al. 2005). The hyporheic zone is also hypothesized to act as a zone of refugia during hydrologic stressor events, like flooding (Williams and Hynes 1974, Dole-Olivier et al. 1997) and drought (Wood et al. 2010). These conditions could result in trade-offs for macroinvertebrate communities in contaminated streams. If hyporheic upwelling zones are refuges against flash flooding, which disturbs and oxidizes sediments, then the refuge zone may have an increased exposure of sediment contaminants to macroinvertebrates seeking refuge.

Under physically and chemically stable conditions, metals like Zn are often bound to various ligands in sediments, decreasing their bioavailability to biota. The likelihood of ligand binding is related to the presence of various binging ligands (sulfide, organic carbon, iron-oxyhydroxides) and the redox chemistry in the sediments (Calmano et al. 1993, Chapman et al. 1998). In anoxic sediments, sulfide is an important binding ligand. Organic carbon is an important binding ligand in anoxic and oxic sediments. Iron and manganese oxy-hydroxide complexes offer a binding site for divalent metals under oxic conditions (Danner et al. 2015, Costello et al. 2015), which has proven an important binding ligand in the hyporheic zone (Harvey and Fuller 1998). Physical disturbances, however, can alter the redox chemistry and ultimately release metals into sediments and surface water. Saturation of dried sediments can cause Zn oxidative release in sediments and ultimately lead to effects on aquatic invertebrates (Nedrich and Burton 2017a, 2017b). The resuspension of contaminated sediments, via propellers, can also increase metal release and increase exposure and effects to aquatic biota (Fetters et al. 2016). Thus, it is possible that the movement of oxidized porewater through the hyporheic zone will influence the binding capacity for metals.

45

To assess the impacts of hyporheic flows in metal-contaminated sediment, artificial stream experiments in the laboratory can assist with understanding metal exposure and effects. Laboratory experiments can identify mechanisms of effects between physical processes, sediment chemistry and biological endpoints, by eliminating many confounding variables present in the field. Due to difficulties associated with hyporheic flow manipulation (Palmer 1993), few studies attempt to replicate hyporheic flows in the laboratory. Laboratory flume experiments have assessed the effects of passive hyporheic flows on metal chemistry (Zaramella et al. 2006) and the effects of sedimentation on interstitial spaces in the hyporheic zone (Rehg et al. 2005). Mesocosm experiments also show the importance of both upwelling and downwelling zones for amphipod presence in systems with excess sedimentation (Mathers et al. 2014). This body of work has indicated the importance of hyporheic flows on both metals and invertebrates, yet there is limited research to connect sediment metal chemistry to ecological effects in the hyporheic zone.

Some field research has demonstrated effects of hyporheic flows on metal contaminant exposure and effects. Microbial communities of the hyporheic zone in mining impacted streams exhibited effects from metals on functional groups (Feris et al. 2003, 2009). Macroinvertebrate communities in the hyporheic zone also responded to metal contamination (Nelson and Roline 1999, Moldovan et al. 2011), but research is limited that mechanistically links hyporheic flows to metal concentrations and biotic effects. Macroinvertebrate diversity and density were higher in metal contaminated field sediments that had high hydraulic conductivity and high filtration of surface water into the streambank, essentially diluting contaminants within the hyporheic zone sediments (Gibert et al. 1995). As benthic macroinvertebrates are used to set standards for

contaminant toxicity, a better understanding of effects from hyporheic flows is needed for risk assessments.

This research assessed the influences of oxidized hyporheic flows on Zn bioavailability and effects to *H. azteca* in Zn amended sediment. We hypothesize that oxidized hyporheic flows will release bound Zn from the sediments, whereas exposures without hyporheic flow will release less Zn. This release of Zn will increase Zn exposure and potentially cause adverse effects on survival and growth of *H. azteca.* We also hypothesize that over time Zn concentrations in the hyporheic-influenced sediments will stabilize and become less toxic to *H. azteca*.

Methods

Sediment selection and spiking

Sediment was collected from an upstream reference reach of Little Black Creek (LBC) in Muskegon Heights, MI (43.216062 N, 86.180030 W). The outlet of LBC is a U.S. EPA Area of Concern due to metal contamination from a Zn smelting operation (Cooper et al. 2001, Steinman et al. 2003), with documented concentrations above probable effects concentrations (PEC) (MacDonald et al. 2000). The sediment is sandy, allowing for hyporheic exchange during the mesocosm experiments. LBC sediment has low sulfide, low organic carbon and moderate to high iron (Table 3.1). Sediment was collected in August 2016, transported to the University of Michigan and purged with N_2 gas before being sealed and stored. In November 2016, half of the sediment was amended with $ZnCl_2$, to a concentration of ~600 mg/kg, to obtain total Zn concentrations just above the PEC for Zn (459 mg/kg). Once amended with Zn, sediments were rolled twice weekly for 30 days (Simpson et al. 2004) and the pH was slightly adjusted with

NaOH to raise the pH to within 0.3 pH units of the original sediments, ~7.3 (Hutchins et al. 2009).

Experimental design

Twelve flow-through artificial streams (flumes) were used to examine the effects of oxidized hyporheic flows on Zn exposure and effects on *H. azteca.* The flumes were constructed from 0.5-inch thick clear acrylic (Figure 3.1, Figure 3.2). Surface water and hyporheic water inputs were both sourced from Ann Arbor, MI municipal water after passing through activated carbon cartridges and a biofiltration tank. Water was delivered to two separate manifold systems with 12 water supply ports each (one for each flume). One manifold supplied surface water and the second manifold supplied hyporheic flows to each flume. Surface water flowed at 2.5 cm^3/s and entered each flume through a holding tank on the upstream end of the flume. Water flowed over a spillover dam and provided surface water to the exposures in the main chamber of the flume without sediment disturbance. Hyporheic flows were set at 0.45 cm^3/s (or 1.0 cm/min velocity), to simulate shallow hyporheic flows with a low residence time, similar to a downwelling exposure. The flow rates were both high enough to supply surface and hyporheic water continuously to the sediments, but low enough to prevent erosion or movement of sediments. Both water sources flowed continuously during the experiments.

Each flume had one sediment exposure, either Zn-spiked (Zn) or reference (Ref), and two separate hyporheic exposures, hyporheic (Hyp) and no hyporheic inputs (nonHyp). The four experimental exposures were: Zn-Hyp, Zn-nonHyp, Ref-Hyp and Ref-nonHyp. Six flumes contained reference sediments and six flumes contained Zn-spiked sediments. Sediment baskets (200 cm^2 surface area, 8.3 cm deep) were used as the exposure units. Each basket was lined with mesh, filled with exposure sediments and placed in the artificial streams with sand as a filler

48

substrate (Figure 3.1). Within each flume, there were two baskets with the same sediment (Ref of Zn) and different hyporheic exposures. To prevent effects of hyporheic inputs into the shared surface water, the upstream sediment exposure basket was a non-hyporheic exposure and the downstream exposure had a hyporheic input. Hyporheic water was delivered to the flume through a long flat porous airstone buried at the bottom of the sediment exposure basket on the downstream basket in each flume. Hyporheic water was pushed through the porous stone, into the overlying sediments and ultimately into the surface water.

Two 10-day experiments were performed on the same sediments with the same hyporheic conditions: an initial experiment (d0 to d10) took place before sediment aging under flow through conditions and a second aged experiment took place 80 days later (d82 to d92). Aging of sediment under flow through conditions has shown to decrease toxicity of copper to *H. azteca* (Costello et al. 2015). Between experiments, sediments were continuously saturated with overlying water.

Chemistry sampling

Porewater sampling ports located laterally along each flume allowed for porewater sampling at 1.5-cm depth throughout the experiment (Figure 3.1, Figure 3.2). Porewater was extracted via rhizon samplers (0.19 μm filters). During the initial experiment, porewater was sampled on days 0, 1, 3, 5, 7 and 10. In the aged experiment, porewater was sampled on days 0, 2, 5 and 9. An 11-ml porewater sample was extracted from rhizon port 1 and measured for dissolved oxygen (DO) (YSI Professional Plus ODO), pH (Thermo Scientific Orion Star A121) and temperature within ten minutes of sample collection. Prior to water quality measurements, 1-ml was extracted to measure reduced iron (Fe^{2+}), a redox indicator, using the Ferrozine method (Stookey 1970, Kostka and Luther III 1994). Fe^{2+} is inversely related to DO. Absorbance was

measured on a spectrometer (Thermo Scientific Genesys 10uv scanning) the same day. From a second rhizon port, 10-ml of porewater was extracted and acidified with nitric acid to 2% for analysis of dissolved metals (Zn, Fe, Mn) on an ICP-OES. On each sampling day, one surface water sample per flume was collected using a syringe, filtered on a 0.45 µm Millipore syringe-attached filter and acidified to 2% HNO_3^- for dissolved metal analysis on an ICP-OES. Blanks (deionized water) were collected and acidified on each sampling day and sample metal concentrations were corrected for blank values. Detection limits were 50 $\mu g L^{-1}$ for Fe, 25 $\mu g L^{-1}$ for Zn, and 10 $\mu g L^{-1}$ for Mn.

Sediments were sampled at the beginning and end of both experiments. In the initial experiment, samples of both sediment types were frozen and stored upon sediment deployment, and then sediment cores were taken from each flume on day 10. In the aged experiments, sediment cores were taken from each flume on day 81 and day 92. All sediment cores were taken using a 60-ml syringe with a sawed off tip, then stored in a 50-ml centrifuge tube, the headspace purged with N_2 gas and stored frozen. Sediment samples were later thawed for acid volatile sulfide (AVS) and simultaneously extracted metals (SEM) analysis (Allen et al. 1991), dried for total metals (Zn, Fe, Mn) and combusted for organic carbon via loss-on-ignition (6 hour combustion at 450° C). For the total metal digestion, 0.5-g of dried sediment was digested in 7-ml of trace metal grade HNO_3 in a Hot Block (Environmental Express) at 112 C for 100 minutes (EPA method 3050B), then diluted 50 times for analysis on ICP-OES. During the digestion, metal concentrations were corrected for the sample analysis process using a procedural blank (MilliQ). Metal recovery from the digestion was verified (>80%) by including a NIST standard reference sediment in the digestion.

Biological sampling

In both experiments, 7 to 14 day old *H. azteca* neonates were exposed to sediment and hyporheic conditions in each flume. Ten *H. azteca* were placed into a small plastic exposure chamber with 250-μm mesh on one side, to allow for surface water and sediment exposure to organisms (Costello et al. 2015). Endpoints for *H. azteca* included survival and growth.

Statistical analyses

Data analysis was performed in RStudio (Version 1.0.136). Linear mixed effects models (package lme4) were used to assess main effects of both treatments (Zn-spike and hyporheic) over time. Main effects included sediment (Zn-spiked vs. reference), hyporheic flow (hyporheic vs. non-hyporheic) and time, with flume as a random effect. All two-way interactions between the three main effects were included in the models. Two-way interactions between sediment and hyporheic flow tested for variation in chemistry between the two sediments (Zn and Ref) caused by the hyporheic treatment. Two-way interactions between time and hyporheic flow tested for variation in porewater chemistry between the two hyporheic exposures over time. Two-way interactions between time and sediment tested for differences in porewater chemistry between sediment types over time.

Sediment chemistry endpoints with only one sampling point (total metals, SEM-AVS, OC) were assessed using linear mixed effects models. Main effects in the model included hyporheic flow and Zn-spiked sediment, with flume as the random effect. Interactions tested for variation in sediment chemistry between the two sediments caused by hyporheic flows.

Effects of hyporheic flow and Zn-spiked sediment on *H. azteca* survival were analyzed using generalized linear mixed effects models (with binomial distribution) with flume as a random effect. Sediment and porewater chemistry effects on *H. azteca* survival were assessed

51

with logistic regression models. Regression analyses assessed relationships between continuous

porewater and sediment chemistry parameters and biological parameters.

Results

Initial sediment experiment

Porewater DO was higher in the hyporheic than the non-hyporheic exposures for both

sediment types (p=0.002, Table 3.2), but not affected by sediment type. Hyporheic exposures had

an average DO of 4.65±0.18 mg/L on day 10, whereas non-hyporheic exposures had lower DO

of 3.94±0.22 mg/L (Figure 3.3).

Overall, Fe^{2+} was higher in the non-hyporheic exposures than the hyporheic exposures,

indicating less oxidation of non-hyporheic exposures (Figure 3.3). The effect of the hyporheic

treatment was greater on the reference sediments than the zinc-spiked sediments (p<0.001, Table

3.2). This is likely due to the higher overall Fe in the reference sediments (Table 3.1). There

were also interactive effects of time on the hyporheic treatment (Table 3.2). The Zn-nonHyp

exposure had constant Fe^{2+} concentrations from day 1 (2.28±0.49 mg/L) to day 10 (2.96±0.48

mg/L), while Fe^{2+} in Ref-nonHyp increased from day 1 (8.67±1.83 mg/L) to day 10 (13.3±1.97

mg/L). Fe^{2+} in the Ref-Hyp exposure decreased from day 1 (1.18±0.35 mg/L) to day 10

(0.15±0.13 mg/L), whereas in the Zn-Hyp exposure, Fe^{2+} remained near 0.0 mg/L throughout the

experiment, indicating near complete oxidation caused by the hyporheic treatment.

The hyporheic treatment increased porewater pH of the Zn-spiked sediment more than

the pH of the reference sediments (p<0.001) (Figure 3.3, Table 3.2). There was an increase in pH

over time (p<0.001), as the pH in all exposures increased over the 10-day experiment,

approaching the pH of the surface water (8.12±0.06). The pH in these systems was generally

buffered against the release of dissolved metals (Zn^{2+}), as the alkalinity of input water is

moderate (~55 mg/L CaCO$_3$/L). The pH in the Zn-nonHyp exposure increased from 7.04±0.04 on day 0 to 7.59±0.04 on day 10, whereas in the Zn-Hyp exposure, pH increased to 7.92±0.06 on day 10. The reference sediments were much closer in pH values, despite the different hyporheic treatments. Ref-nonHyp exposures ranged from pH of 7.31±0.07 on day 0 to 7.67±0.02 on day 10, while the pH in the Ref-Hyp exposure increased to 7.78±0.04 on day 10.

A significant interaction between time and hyporheic flow decreased porewater Fe in the hyporheic exposures during the first 2-3 days, whereas the non-hyporheic exposures increased porewater Fe (p<0.001) (Figure 3.4, Table 3.2). The effect of the hyporheic treatment was greater on the reference sediments than the Zn-spiked sediments (p<0.001), likely because porewater Fe was higher in the reference sediments (5.59±1.35 mg/L) than the Zn-spiked sediments (0.86±0.25 mg/L) before the experiment began. Porewater Fe in Ref-nonHyp increased on day 1 (9.67±0.88 mg/L) and remained high (reduced) through day 10 (8.42±1.28 mg/L). The Ref-Hyp porewater Fe decreased on day 1 (1.43±0.59 mg/L) and by day 10 was much lower (0.25±0.10 mg/L). Porewater Fe in the Zn-Hyp exposures decreased by day 10 (0.17±0.03 mg/L) and the Zn-nonHyp exposure had higher porewater Fe on day 10 (1.57±0.23 mg/L) than the day 0. At the end of the exposure on day 10, porewater Fe was correlated positively with Fe^{2+} (r=0.97, p<0.001) and negatively with DO (r=-0.52, p=0.008), indicating decreases in porewater Fe with sediment oxidation.

Porewater Mn declined in all exposures over time (p=0.015), though the effect of time was greater in Zn-spiked than reference sediments (p<0.005) (Figure 3.4, Table 3.2). Hyporheic flow also decreased porewater Mn in both the reference and zinc-spiked sediments (p<0.001). Zn-spiked sediments initially had higher Mn concentrations than reference sediments on day 0 (1725±209 µg/L and 878±88 µg/L, respectively). By day 1 concentrations of Mn reflected the

53

hyporheic treatment more than the sediment type, as non-hyporheic exposures had greater

porewater Mn than hyporheic exposures (Figure 3.4). On day 10, the Zn-nonHyp exposure had

the highest porewater Mn (768±81 µg/L), followed by Ref-nonHyp (587±86 µg/L), and then Zn-

Hyp (78±33 µg/L) and Ref-Hyp (19±4 µg/L). On day 10, porewater Mn concentrations

correlated positively with Fe^{2+} (r=0.56, p=0.004) and negatively with pH (r=-0.67, p<0.001).

Porewater Zn was affected by hyporheic flow, sediment and time. Day 0 Zn

concentrations in porewater averaged 2173.6±359.1 µg/L in the Zn sediments and 17.8±9.1 µg/L

in the Ref sediments. Porewater Zn decreased over time in the Zn-spiked exposures only (p

<0.001) (Figure 3.4, Table 3.2), as there was negligible Zn in the reference sediment. Porewater

Zn in the Zn-Hyp exposure decreased faster than it did in the Zn-nonHyp exposure (p<0.001).

By day 10, the Zn-nonHyp exposure had higher porewater Zn (802.1±85.4 µg/L) than the Zn-

Hyp exposure (303.0±50.5 µg/L), and both remained higher than the reference. Porewater Zn

correlated with porewater Mn (r=0.56, p=0.005), and their trends overtime were similar (Figure

3.4).

Total metals were affected by sediment and hyporheic flows. Total Zn, which was only

present in Zn-spiked sediments, was lower in the Zn-Hyp exposure (378.7±17.5 mg/kg)

compared to Zn-nonHyp by day 10 (420.7±11.8 mg/kg) (p=0.035, Table 3.2). This could be due

to a possible loss of total Zn from the system with hyporheic inputs. Total Mn was lower in the

Zn-spiked sediments than the reference sediments (p=0.013), and lower in the hyporheic

exposure than the non-hyporheic exposure (p=0.077). There was no effect of hyporheic flow on

total Fe, but total Fe was higher in the reference sediments (5.278±0.266 g/kg) than in the Zn-

spiked sediments (4.211±0.115 g/kg) (p=0.006).

Binding ligands were also affected by the hyporheic treatment. There was a significant interaction between the Zn-spiked sediment and hyporheic treatment on $(Zn_{SEM}-AVS)/fOC$ (t=-3.003, p=0.006). Post-hoc Tukey tests showed that while there was no effect of hyporheic flows on the reference sediment $(Zn_{SEM}-AVS)/fOC$, the Zn-Hyp exposure had significantly lower $(Zn_{SEM}-AVS)/fOC$ than the Zn-nonHyp exposure. Hyporheic exposures had lower AVS than non-hyporheic exposures (t=-2.358, p=0.027), but there was no difference in AVS between reference and Zn-spiked sediments. This indicates that regardless of sediment, AVS was lower in the hyporheic exposures. No effects of sediment or hyporheic exposure were observed on organic carbon.

The survival of *H. azteca* declined in response to both hyporheic exposure (z=-6.405, p<0.001) and Zn-spiked sediment (z=-2.990, p=0.003) (Figure 3.5). In the non-hyporheic exposures, there was a decrease in survival proportion in Zn-nonHyp exposure (0.43±0.11) relative to Ref-nonHyp exposure (0.82±0.11). Survival in the Zn-Hyp exposure was zero. The unexpected low survival in the Ref-Hyp exposure (0.37±0.16), compared to the Ref-nonHyp exposure (0.82±0.11), was likely due to the visible Fe oxidation on the Ref-Hyp sediments during the 10-day exposure. A thick mat of Fe flocculent developed on the sediment surface in the Ref-Hyp exposure (Figure 3.6). The iron oxidation did not occur in the Zn hyporheic exposure, possibly a product of the sediment spiking procedure and inhibition of iron oxidizing microbial communities.

Aged sediment experiment

Porewater redox conditions were more stable over time during the aged sediment experiment. The hyporheic exposures continued to have higher DO than the non-hyporheic exposures and this difference was greater in the reference sediments than the Zn-spiked

sediments (p=0.003, Figure 3.3, Table 3.3). Fe^{2+} was no longer affected by time, but there was a significant interaction between the Zn-spiked treatment and hyporheic flows (p<0.001). The lower Fe^{2+} resulting from hyporheic flows was disproportionately larger on the reference compared to Zn-spiked sediments (Figure 3.3).

Porewater pH in the aged experiment returned to the original pH of sediments before the initial experiment, ~7.3 (Figure 3.3). Porewater pH was affected by an interaction between hyporheic flows and the Zn-spike treatment (p=0.004), as the pH was higher in the Ref-nonHyp exposure than in the other three exposures. Surface water pH remained high throughout the experiment at ~7.7 to 7.8 in each flume.

Porewater Fe had a significant interaction between hyporheic exposures and Zn-spiked sediments (p<0.001), as the difference in porewater Fe was greater in the reference sediments than the Zn-spiked sediments (Figure 3.4). The hyporheic exposures had low porewater Fe throughout the experiment than the non-hyporheic exposure (Ref-Hyp = 0.023±0.009 mg/L and Zn-Hyp=0.815±0.633 mg/L on day 9). Among the non-hyporheic sediments, Ref-nonHyp exposure had higher porewater Fe (5.59±0.44 mg/L on day 9) than Zn-nonHyp (4.42±0.69 mg/L on day 9) throughout the experiment.

The aged experiment had a significant interaction between hyporheic flows and sediment type on porewater Mn ($t_{1,84}$=-3.401, p=0.001) (Figure 3.4). There was little difference in porewater Mn between the two hyporheic exposures. On day 9 Ref-Hyp was 3.3±0.3 µg/L and Zn-Hyp was 24.4±15.4 µg/L. In the non-hyporheic sediments, which had much higher porewater Mn, the Ref-nonHyp had significantly lower porewater Mn (345.2±34.3 µg/L on day 9) than Zn-nonHyp (619.9±147.1 µg/L on day 9).

There was no effect of hyporheic flows on porewater Zn, but the Zn-spiked sediments still maintained higher porewater Zn than reference sediments ($p<0.001$, Figure 3.4). Porewater Zn concentrations in the Zn-spiked sediments ranged from 135.2 ± 20.0 µg/L on day 0 to 139.1 ± 24.4 µg/L on day 9.

While total metals were unaffected by hyporheic flows, the redox sensitive binding ligands were affected by the hyporheic exposure. The significant interaction between hyporheic flows and (Zn_{SEM}-AVS)/fOC, show an effect of hyporheic flows on only the Zn-spiked sediments and not the reference sediments ($t_{1,8}=2.840$, $p=0.022$), because the reference sediments had such low Zn concentrations. Within the Zn-spiked sediments, Zn-Hyp had greater bioavailable Zn (i.e., (Zn_{SEM}-AVS)/fOC) (2.24 ± 0.24 µmol/g) than Zn-nonHyp (1.49 ± 0.36 µmol/g). SEM values were higher in Zn-Hyp than in Zn-nonHyp, whereas AVS was not influenced by hyporheic treatment in the Zn-spiked sediments, as it did not differ between Zn-Hyp and Zn-nonHyp (Table 3.1).

Despite no differences in porewater Zn or total Zn in the hyporheic exposures, there was still an effect of hyporheic flows on *H. azteca* survival on day 10. There was a significant interaction between Zn-spiked sediment and hyporheic flows ($z=2.346$, $p=0.019$). There was no difference in survival between the reference sediments caused by hyporheic flows (Ref non-hyporheic $= 0.88\pm0.03$, Ref hyporheic $= 0.90\pm0.05$), and no iron flocculent formed on the sediment surface. In the Zn-spiked sediments, survival in the Zn-Hyp exposure (0.10 ± 0.04) was lower than in the Zn non-hyporheic exposure (0.43 ± 0.11) (Figure 3.5). Sediment Zn concentrations (406 mg/kg) on day 10 were lower than the PEC (459 mg/kg) and porewater Zn concentrations (139 µg/L) were just above the PEC for freshwaters (120 µg/L) for the entire duration of the 10-day exposure. Both porewater and sediment could be contributing to toxicity.

Comparison of initial and aged experiments

Porewater chemistry was more stable during the 10-day aged experiment, compared to the initial experiment. The pH stabilized to the original pH of the sediments (~7.30), before sediment and hydrologic manipulations. Porewater metal chemistry (Zn, Fe, Mn) was stable over time in the aged experiment. Porewater Zn in the aged experiment was the same for the Zn-Hyp and Zn-nonHyp exposures, despite the differences in redox chemistry (Fe^{2+}, pH) and bioavailability (i.e., (Zn_{SEM}-AVS)/fOC) between the exposures.

The survival of *H. azteca* varied between experiments. In the initial experiment, *H. azteca* survival was impacted by hyporheic flow induced Fe-oxidation. Survival of *H. azteca* was positively correlated with Fe^{2+} (r=0.62, p=0.001), as opposed to other porewater or sediment parameters. Whereas in the aged experiment, there was no visible Fe-oxidation in the reference hyporheic exposure, and survival was high. In the aged experiment, *H. azteca* survival was more correlated with total Zn (r=-0.86, p<0.001), (Zn_{SEM}-AVS)/fOC (r=-0.74, p=0.001) and porewater Zn (r=-0.59, p=0.003). Despite similar concentrations in porewater Zn between hyporheic exposures in the aged sediments, there was still decreased survival associated with Zn-Hyp exposure, relative to Zn-nonHyp exposure. This difference was not related to porewater Zn or total Zn, but may be related to the (Zn_{SEM}-AVS)/fOC.

Discussion

These findings demonstrate the important role of hyporheic flows on sediment redox chemistry and metal bioavailability, suggesting they should be a component of sediment risk assessments in lotic systems. The laboratory experiments provided an assessment of mechanistic effects of zinc and oxic hyporheic flows. While studies have examined the important differences in redox chemistry resulting from hyporheic flows (Hendricks et al. 1993); this research linked

58

hyporheic flow processes with metal fate and biotic effects. Though these relationships are untested in the field, the redox conditions (Fe^{2+}) were similar to those in downwelling zones (Harrison Chapter 1), indicating the potential for similar effects in Zn contaminated field sediments with hyporheic flows.

Oxic hyporheic sediments were most toxic to *H. azteca.* In streams, downwelling zones are characterized by oxidized hyporheic sediments (Hendricks and White 1991, Franken et al. 2001), as simulated in our current studies. Downwelling zones typically have greater benthic macroinvertebrate community diversity and sensitivity, compared to more reduced upwelling zones (Franken et al. 2001, Harrison Dissertation Chapter 1). Based on *H. azteca* responses, less tolerant macroinvertebrate communities residing in downwelling zones could be at higher risk in metal contaminated streams, compared to communities in pools or other stream habitat with limited groundwater-surface water interaction.

H. azteca responses also showed the importance of hyporheic flows over the long-term. While the initial experiment was not yet in equilibrium (due to changing pH, D.O, Fe2+ and dissolved metals over the ten days), the aged experiment was in equilibrium, as there were no differences in porewater chemistry during the ten day exposure. Despite no variation in porewater Zn or total Zn concentrations between Zn-Hyp and Zn-nonHyp exposures, there was lower survival in the hyporheic exposure. This may be linked to (SEM-AVS)/*f*OC, which was consistently higher in the hyporheic exposure, suggesting long term effects to biota as long as AVS and organic carbon remain the same. The LBC sediments were also relatively low in sulfide and OC, thus their ability to decrease toxicity in anoxic sediments is somewhat limited. As total Fe and Mn are high in these sediments, future investigations into the role of Fe/Mn oxyhydroxides in zinc binding are warranted. In oxidized environments, Fe/Mn-oxyhydroxides

are important for metal binding (Harvey and Fuller 1998, Danner et al. 2015) and may increase

binding within the hyporheic zone specifically (Fuller and Harvey 2000).

Toxicity of the Ref-Hyp exposure during the initial experiment was unexpected, but the

visible iron flocculent on the sediment surface suggests that excess iron oxidation decreased

survival (Figure 3.6). The visual effect was similar to the oxidization of groundwater from a

spring surfacing aboveground. It is possible that the Fe-oxidation and subsequent flocculent

produced, resulted in toxicity to *H. azteca,* caused by the physical presence of the iron flocculent

on the organism body (Vuori 1995). Mayflies have been observed physically removing iron

precipitates from their bodies as well (Gerhardt 1992), which could result in toxicity from excess

ingestion. This effect was also limited to the hyporheic exposure in the reference sediments,

indicating this was a hyporheic-induced effect. It is also possible that the $ZnCl_2$ spike and

subsequent lower pH impaired or decreased the Fe-oxidizing microbial communities in the Zn-

spiked sediments, which was why we only saw the Fe flocculent form on the reference sediments

and not the Zn-spiked sediments. Soil studies have found that $ZnCl_2$ spiking can cause complete

inhibition of nitrogen fixing bacteria at 0.5 mg/L Zn Cl_2 (Cela and Sumner 2002), which was a

lower concentration than the initial porewater Zn in this experiment (2.0 mg/L). Thus, it is

possible that Fe-oxidizing bacteria were also inhibited by the $ZnCl_2$ spiking.

Monitoring of hyporheic conditions in metal contaminated ecosystems is critical to

determine if it is an important contaminant exposure route, and to understand metal speciation

and bioavailability. Without this knowledge, there will be significant uncertainty associated with

any ecological risk assessment that considers benthic invertebrate communities as receptors.

Increased exposure and effects occurred on *H. azteca,* indicating possible effects on biota *in situ*

under oxic conditions, which may be the areas of greatest ecological risk. Hyporheic flow inputs

are inexpensive and easy to measure in the *in situ* (Keery et al. 2007, Rivett et al. 2008) and inclusion in ecological risk assessments will improve risk assessments.

Tables

Table 3.1. Sediment properties (pH, OC, AVS, SEM, total Fe, Mn and Zn) during the initial and aged experiments.

Sediment/ Exposure	Experiment	pH[a]	LOI (% C)	AVS (umol/g)	(SEM-AVS)/ fOC (umol/g)	Fe (g/kg)	Mn (mg/kg)	Zn (mg/kg)
Ref	Pre-exposure	7.31	0.68	1.04	-0.308	5.4	42.1	7.6
Zn	Pre-exposure	7.04	0.57	0.80	2.774	3.8	37.7	425.9
Ref-nonHyp	Initial at d10	7.67±0.02	1.28±0.65	0.78±0.25	-0.21±0.20	5.11±0.4	39.8±2.7	7.0±0.7
Ref-Hyp	Initial at d10	7.78±0.04	0.71±0.06	0.34±0.10	-0.09±0.04	5.44±0.4	35.1±2.4	8.2±0.9
Zn-nonHyp	Initial at d10	7.60±0.04	0.52±0.09	0.56±0.08	1.82±0.13	4.15±0.1	36.4±0.5	420.7±11.8
Zn-Hyp	Initial at d10	7.92±0.06	0.36±0.04	0.36±0.06	1.44±0.21	4.28±0.2	28.2±1.5	378.7±17.5
Ref-nonHyp	Aged at d10	7.29±0.06	0.68±0.05	0.44±0.14	-0.01±0.01	6.21±0.4	53.6±3.7	15.5±1.2
Ref-Hyp	Aged at d10	7.22±0.06	1.10±0.32	0.09±0.09	-0.14±0.05	7.12±1.1	46.1±5.4	15.4±1.5
Zn-nonHyp	Aged at d10	7.19±0.05	0.53±0.13	0.43±0.04	1.49±0.36	4.42±0.4	34.3±3.2	405.9±30.4
Zn-Hyp	Aged at d10	7.20±0.05	0.34±0.01	0.44±0.14	2.24±0.24	4.32±0.2	29.1±2.9	405.6±24.6

[a] pH was measured in the porewater. The aged experiment values are from day 5.

Table 3.2. Initial experiment linear mixed effects model results for effects of time, hyporheic flow and sediment on porewater and sediment chemistry. Bolded main effects and two-way interactions were significant in the model at α = 0.05. The t-statistic and p-value are reported with a (+) or (-) to indicate effects directions of main effects (i.e., positive or negative effect of hyporheic flow or Zn-spiked sediment).

Endpoint	Time	Hyporheic	Zinc	Time*Hyp	Time*Zn	Up*Zn
Porewater DO	t=1.290 p=0.120	**(+) t=5.323 p<0.001**	t=0.036 p=0.972	**t=2.048 p=0.043**	t=0.905 p=0.367	t=0.226 p=0.822
Porewater Fe^{2+}	**(+) t=4.643 p<0.001**	**(-) t=8.132 p<0.001**	**(-) t=7.043 p<0.001**	**t=3.488 p<0.001**	*t=1.795 p=0.079*	**t=5.519 p<0.001**
Porewater pH	**(+) t=6.898 p<0.001**	t=0.767 p=0.447	**(-) t=4.713 p<0.001**	t=0.921 p=0.360	**t=3.204 p=0.002**	**t=4.279 p<0.001**
Porewater Fe	t=0.139 p=0.890	**(+) t=7.083 p<0.001**	**(-) t=9.223 p<0.001**	**t=3.819 p<0.001**	*t=1.679 p=0.096*	**t=5.530 p<0.001**
Porewater Mn	**(-) t=2.470 p=0.015**	**(+) t=4.160 p<0.001**	**(+) t=6.360 p<0.001**	t=0.840 p=0.404	**t=3.75 p<0.001**	t=1.670 p=0.096
Porewater Zn	t=0.024 p=0.981	t=0.216 p=0.83	**(+) t=14.843 p<0.001**	t=0.425 p=0.672	**t=7.140 p<0.001**	**t=4.786 p<0.001**
Total Zn	NA	t=0.081 p=0.937	**(+) t=27.136 p<0.001**	NA	NA	t=2.234 p=0.035
Total Fe	NA	t=0.846 p=0.406	**(-) t=3.020 p=0.006**	NA	NA	t=0.363 p=0.720
Total Mn	NA	t=1.851 p=0.077	**(-) t=2.698 p=0.013**	NA	NA	t=0.954 p=0.350
(SEM-AVS)/ fOC	NA	t=1.089 p=0.287	**(+) t=13.082 p<0.001**	NA	NA	t=3.033 p=0.006
AVS	NA	**(-) t=2.358 p=0.027**	t=0.104 p=0.918	NA	NA	t=0.906 p=0.374

Table 3.3. Aged e experiment linear mixed effects model results for effects of time, hyporheic flow and sediment on porewater and sediment chemistry. Bolded main effects and two-way interactions were significant in the model at α = 0.05. The t-statistic and p-value are reported with a (+) or (-) to indicate effects directions of main effects (i.e., positive or negative effect of hyporheic flow or Zn-spiked sediment).

Endpoint	Time	Hyporheic	Zinc	Time*Hyp	Time*Zn	Up*Zn
Porewater DO	t=0.729 p=0.468	**(+) t=11.627 p<0.001**	t=0.929 p=0.362	t=1.161 p=0.249	t=0.017 p=0.987	**t=3.053 p=0.003**
Porewater Fe^{2+}	t=1.481 p=0.142	**(-) t=19.429 p<0.001**	**(-) t=2.874 p=0.010**	t=1.187 p=0.239	t=0.012 p=0.991	**t=8.163 p<0.001**
Porewater pH	t=0.767 p=0.446	**(-) t=2.585 p=0.012**	t=1.611 p=0.117	t=0.139 p=0.890	t=0.658 p=0.513	**t=2.960 p=0.004**
Porewater Fe	**(-) t=2.153 p=0.034**	**(-) t=17.238 p<0.001**	**(-) t=2.916 p=0.008**	t=1.297 p=0.198	t=0.576 p=0.566	**t=5.883 p<0.001**
Porewater Mn	t=1.830 p=0.071	**(-) t=8.780 p<0.001**	**(+) t=3.286 p=0.004**	t=1.557 p=0.123	t=0.234 p=0.815	**t=4.898 p<0.001**
Porewater Zn	t=0.095 p=924	t=0.137 p=0.892	**(+) t=5.978 p<0.001**	t=0.201 p=0.841	t=0.033 p=0.974	t=0.843 p=0.402
Total Zn	NA	t=0.002 p=0.998	**(+) t=15.424 p<0.001**	NA	NA	t=0.013 p=0.990
Total Fe	NA	t=1.159 p=0.258	**(-) t=3.545 p=0.002**	NA	NA	t=0.913 p=0.370
Total Mn	NA	t=1.477 p=0.153	**(-) t=3.382 p=0.002**	NA	NA	t=0.316 p=0.755
(SEM-AVS)/ fOC	NA	t=0.811 p=0.441	**(+) t=8.439 p<0.001**	NA	NA	**t=2.840 p=0.022**
AVS	NA	**(-) t=2.678 p=0.028**	**(+) t=2.504 p=0.024**	NA	NA	t=1.952 p=0.087

Figures

Figure 3.1. Lateral view of a singular experimental stream (flume). Each of the 12 experimental streams was set-up with the same surface and hyporheic flows. Six flumes contained reference sediments in both exposure baskets and six flumes contained Zn-spiked sediments in both baskets.
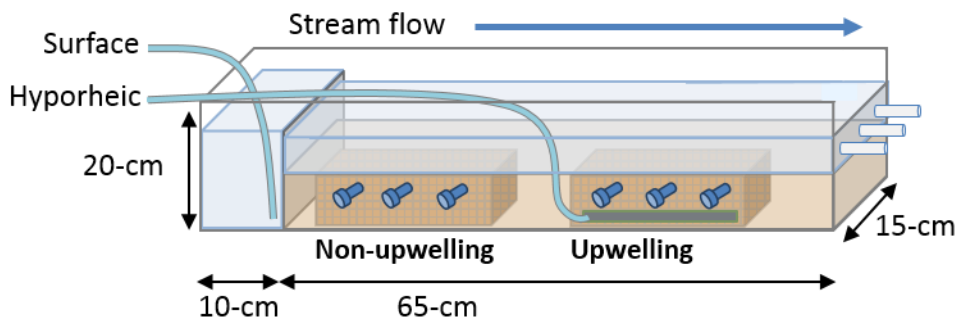
Figure 3.2. The 12-flume experiment was setup in the laboratory. The upstream end of the flume is on the right and downstream is on the left, and surface water flows from right to left. Rhizon sampling ports for temporal porewater sampling are located along the sides of each flume.

Figure 3.3. Temporal trends in porewater geochemistry chemistry over time during the initial experiment (left column) and aged experiment (right column). Time is in days on the x-axis, concentrations of porewater chemistry on the y-axis. Graphs include: reduced iron (Fe^{2+}), dissolved oxygen (DO), and pH. Error bars denote ±1 SE. Note legend: Ref-nonHyp = "Ref" and Zn-nonHyp = "Zn".
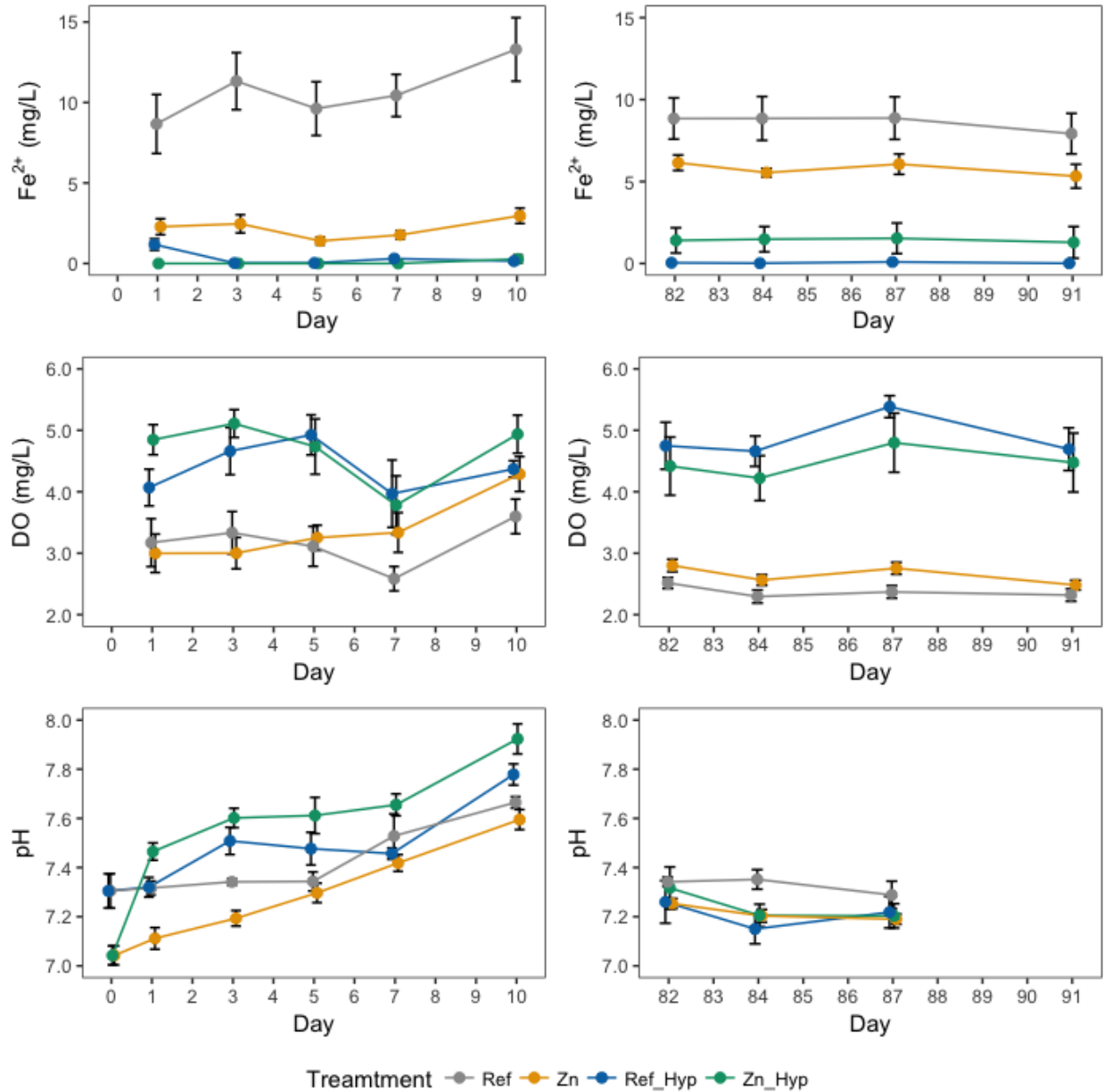
Figure 3.4. Temporal trends in porewater metal chemistry over time during the initial experiment (left column) and aged experiment (right column). Time is in days on the x-axis and concentrations of porewater metal are on the y-axis. Graphs include: reduced iron (Fe^{2+}), dissolved oxygen (DO), and pH. Error bars denote ±1 SE. Note legend: Ref-nonHyp = "Ref" and Zn-nonHyp = "Zn".
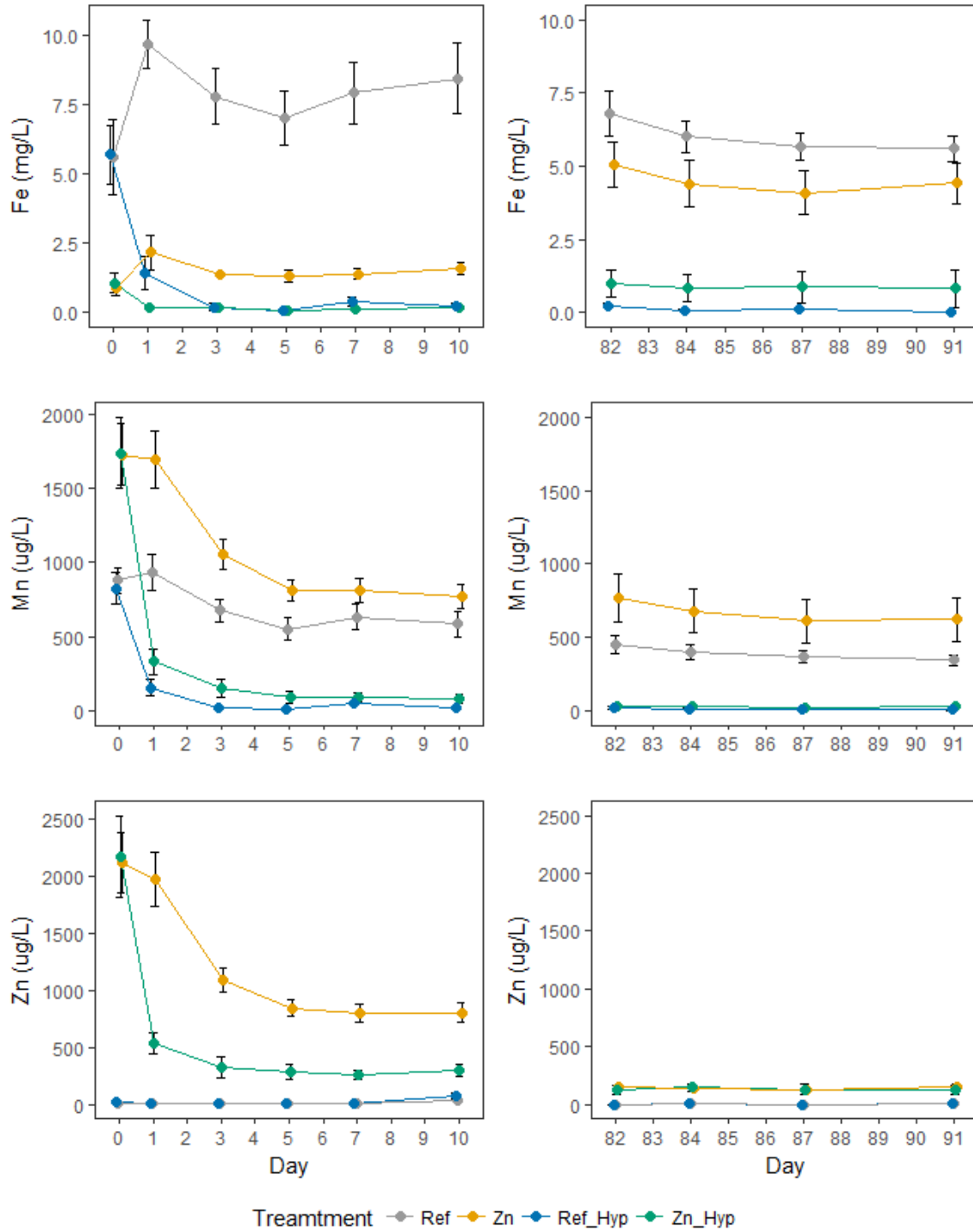
Figure 3.5. *H. azteca* survival in the initial and aged experiments was a function of sediment and hyporheic flow. Letters denote differences in survival between treatments (but within experiments).
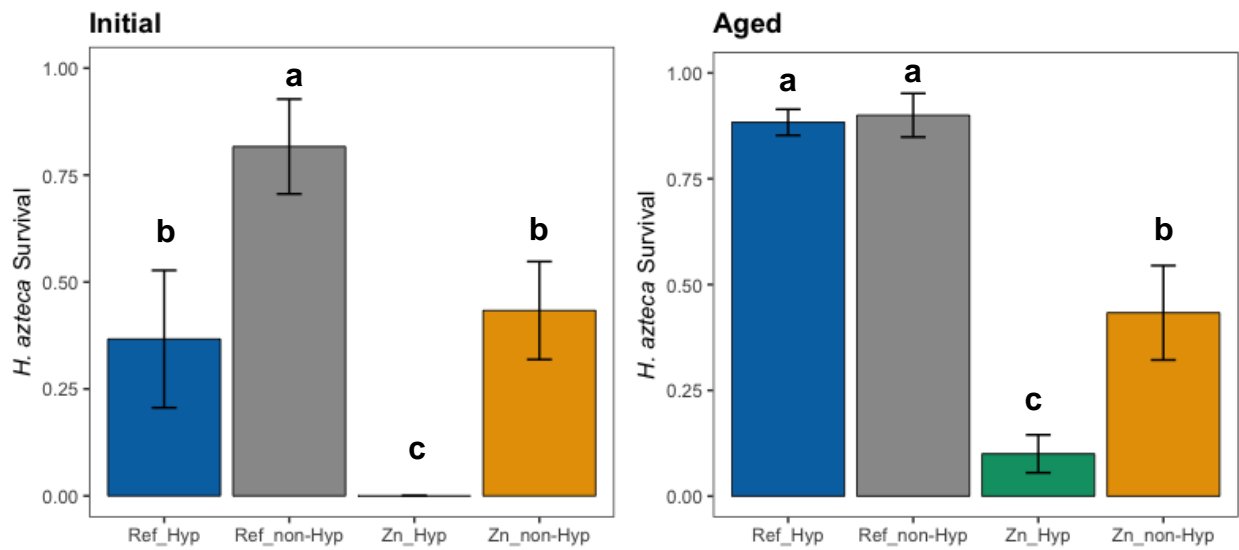
Figure 3.6. Photograph of the iron flocculent produced during the initial experiment, from Fe-oxidation on the Reference sediment hyporheic exposure (Ref-Hyp) in the upper right-hand corner of the image. The other three exposures are (clockwise) Ref-nonHyp, Zn-nonHyp and Zn-Hyp.
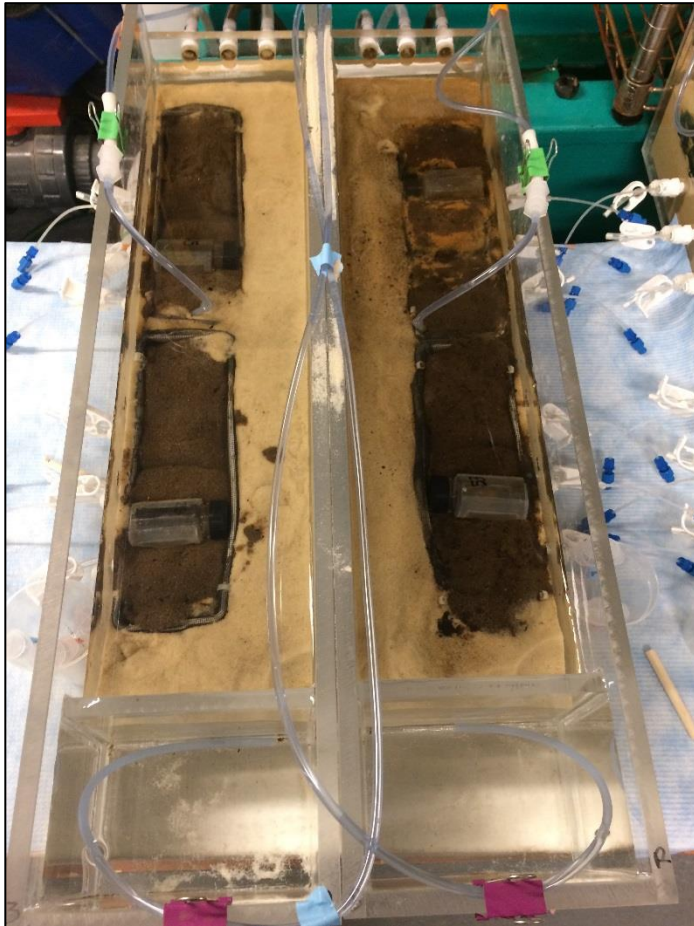
Chapter 4

The importance of hyporheic connectivity: mitigating effects of sediment drying conditions in metal contaminated sediments

Abstract

Metal contamination is common within aquatic habitats in human dominated landscapes. Physical processes, both climactic and hydrologic, can influence the exposure and effects of metals to aquatic organisms. Groundwater-surface water interactions (hyporheic flows) influence redox conditions in sediments, which partially control metal bioavailability. This research investigates the influence of hyporheic flows on the effects of two stressors (sediment zinc and drying conditions) to benthic macroinvertebrate communities and biofilm structure and function at three Great Lakes coastal wetlands. Sediment mesocosms were deployed in either saturated or dry conditions for 30 days, then inundated and sampled for porewater and sediment chemistry over the next 30 days while inundated. Sediment and porewater chemistry were predominantly affected by hydrologic conditions at each site, in addition to experimental treatments. Hyporheic connectivity mitigated effects of drying conditions on metal bioavailability at the riparian wetland site, but not at the two fringing wetland sites. Chlorophyll a biomass decreased with increased metal concentrations at two of the three sites, but also declined in response to sediment deposition at each site. Benthic macroinvertebrate endpoints did not respond to metal concentrations in sediments. The riparian wetland site may have been more susceptible to

influences of hyporheic connectivity on redox conditions due to its greater potential for

subsurface flow from the stream and stream banks.

Introduction

Freshwater ecosystems are often impacted by hydrologic and contaminant stressors, which can have interactive effects with each other. Physical stressors in freshwater ecosystems can enhance the effects of chemical stressors in sediments (Burton 2010), especially for redox sensitive contaminants like metals. Physical disturbances of sediments, such as flooding and drought, can oxidize sediments, increase the release of metals (particularly zinc) bound in sediments (Kreiling et al. 2015, Nedrich and Burton 2017b), ultimately increasing their bioavailability and toxicity to aquatic organisms. Groundwater-surface water interactions in the hyporheic zone have been suggested as a refugia for benthic invertebrates during physical disturbances, like flooding (Williams and Hynes 1974, Delucchi 1989, Dole-Olivier et al. 1997) and drought (Marchant 1988, Wood et al. 2010). The hyporheic zone can provide more stable physical habitat conditions for aquatic biota, particularly in areas with upwelling of hyporheic flows. This paper explores the influences of hyporheic connectivity as a mechanism to alleviate combined effects of sediment-associated zinc and drying conditions in coastal aquatic habitats impacted by Great Lakes water level fluctuations. Findings from this study will help to better understand the role of the hyporheic zone and local site conditions on the release of metals from drying conditions and ultimately effects on biota.

Zinc is a prevalent metal in urban and agricultural dominated ecosystems, entering aquatic ecosystems through stormwater runoff (Kayhanian et al. 2008), in addition to legacy contaminant sources. The prevalence of Zn in stormwater is due to its use in many products, including car tires, fertilizers and wood preservatives, and also as a by-product of smelting operations, coal and bottom fly ash (Burton and Pitt 2002, ATSDR 2005). In their free aqueous form, divalent metals like Zn, can bind to various ligands in sediments, which can reduce their

bioavailability to organisms. Binding capacity is often related to sediment redox chemistry and presence of redox sensitive ligands (Calmano et al. 1993, Chapman et al. 1998). In anoxic sediments, metals can bind to sulfide and organic carbon. In oxic environments, iron (Fe) and manganese (Mn) oxy-hydroxide complexes offer binding sites for divalent metals (Danner et al. 2015, Costello et al. 2015). Mn oxy-hydroxides have been documented as important metal binding ligands in hyporheic-influenced systems (Harvey and Fuller 1998, Fuller and Harvey 2000).

Binding ligands can decrease bioavailable metals under stable hydrologic conditions. Great Lakes coastal wetlands and receiving waters, however, are dynamic systems and are often affected by regional water level fluctuations. Drying and re-flooding can cause sediments to oxidize, which releases metals previously bound to anoxic ligands under stable reducing conditions. Laboratory experiments found that drying of sediments and subsequent re-flooding resulted in oxidative release of Zn from sediments and toxicity to invertebrates (Nedrich and Burton 2017a, 2017b). Other studies have shown that other physical disturbances, like resuspension, can increase sediment oxidation and ultimately release metals, increasing toxicity to biota (Fetters et al. 2016).

Biofilms are important for ecosystem processes (primary productivity and respiration) and as a basal food resource, yet they are an understudied biological endpoint for contaminant toxicity. In periphyton, Zn absorbs onto algal cells, particularly if total organic carbon concentrations are high (Kashian et al. 2004). This can result in Zn uptake by periphyton and facilitate the transfer of Zn to consumer invertebrates. In field experiments, biofilm NPP and Chl *a* responded to copper and nickel contamination in sediments when benthic invertebrate community endpoints indicated minimal effects (Costello and Burton 2014). In mining

contaminated streams, metal concentrations in biofilms have been measured at similar concentrations to bulk sediments, indicating an accumulation at elevated sediment concentrations (Farag et al. 1998). Increases in stormwater Zn can also result in greater accumulation of Zn in periphyton (Meylan et al. 2003, Ancion et al. 2010a). Accumulation can lead to shifts in biofilm species composition changes in response to elevated (>50 µg/L) metal concentrations (Genter et al. 1987).

Biofilm processes (photosynthesis and respiration) can also influence metal fluxes. Metal fluxes in streams have diel fluctuations, increasing at night when pH is lower (Nimick et al. 2005, Tercier-Waeber et al. 2009), this process is likely mediated by nighttime respiration of biofilms, which alters pH and redox at the sediment surface (Burton 2010).

Sediment exposures in mesocosm experiments that are connected to the hyporheic zone are expected to provide more realistic environmental conditions for aquatic biota than unconnected exposures. When sediments are exposed to drying conditions, the connectivity to the hyporheic zone in areas with reduced hyporheic upwelling may mitigate metal contaminant release, compared to exposures closed to the hyporheic zone. Upwelling hyporheic conditions are typically reduced, thus metals will remain bound to anoxic binding ligands. To assess the role of hyporheic upwelling on metal bioavailability, sediment exposures were either open to surrounding sediments or closed off from surrounding sediments. It is expected that closed exposures under drying conditions will have greater effects of metals on benthic and hyporheic communities than the exposures that are open to hyporheic exchange. The treatment (open versus closed) also allows for a comparison between field and laboratory conditions, where open exposures simulate field conditions and closed exposures simulate laboratory exposures.

The objectives in this research are to investigate the effects of hyporheic connectivity on sediment redox conditions, metal chemistry and effects on aquatic biota. The primary object is to assess the influence of hyporheic connectivity on sediment chemistry, metal bioavailability and biota *in situ* at metal contaminated aquatic ecosystems. A second objective is to assess the importance of hyporheic connectivity for sediment chemistry and biota during a simulated drying event, as the research aims to determine if connectivity to the hyporheic zone can decrease effects of drying conditions, as has been suggested in hyporheic literature. The third objective of this research uses biofilms as a biological endpoint and aims to understand biofilm sensitivity to environmental stressors, in addition to traditional benthic macroinvertebrate community metrics.

Methods

Site selection

The field experiment was performed at three sites: Little Black Creek (LBC) in Muskegon Heights, MI (43.185705°N, -86.245844°W), East Traverse Bay (EB) in Traverse City, MI (44.762122°N, -85.575644°W) and Quanicassee Wildlife Refuge (QC) in Big Bay, MI (43.636102°N, -83.815163°W) (Figure 4.1). The LBC site is in a riparian wetland of a cold-water stream in a suburban landscape. The EB and QC wetlands are lacustrine fringe wetlands. EB is located in a high-energy, wave-influenced bay, surrounded by residential and urban land use. The QC site is in a conservation area with standing water (low dissolved oxygen) and dense grasses (*Phragmites spp.*), adjacent to a coal ash plant. Sites were selected for accessibility, elevated sediment metal concentrations, variation in hyporheic connectivity (Figure 4.1 – groundwater potential), variable sediment properties (Table 4.1.) and a high likelihood of being affected by water level fluctuations due to proximity to the Great Lakes. In addition to the field

contaminated sediment at each site, a reference sediment was also deployed from the Raisin

River in Manchester MI (42.168521°N, -84.123712°W).

Experimental design

At each site, the influences of hyporheic connectivity on metal-contaminated sediments

and drying conditions were measured. Two sediments were deployed, a natural sediment from

the field contaminated site and a reference sediment from the Raisin River. The hyporheic

connectivity treatments included sediments either connected (open) to hyporheic exchange or

unconnected (closed). Two levels were used to assess effects of drying: sediments were either

continuously saturated for 60 days or dried in an upland area for 30 days prior to a 30-day

inundation. In this experiment, the 'open-saturated' exposure is considered the reference

exposure, as the sediments are both connected to hyporheic flows and never experience oxidation

associated with drying conditions.

Sediments were deployed into two containers, one for chemistry sampling and a second

for biological sampling. Porewater and sediment chemistry samples were taken from round

polycarbonate containers (11.4 L) with rhizon sampling ports (0.19 μm filters) at 1-cm depth.

Sediment was filled within 2-cm of the top of the mesocosm (~10-L), and when deployed, the

sediment was level with surrounding sediment surface. Holes were drilled along the side of the

mesocosms, to maintain water levels equal to that of the site, in case of rain during the drying

exposure. For biological sampling, sediment was deployed into sediment colonization trays (200

cm^2 surface area, 8.3 cm deep) (Nguyen et al. 2011, Costello et al. 2011). Colonization trays

were filled to the top with sediment and placed flush with the sediment surface for benthic

macroinvertebrate colonization.

Natural sediments were collected on site the day before the drying deployment, which began on day -30 (Figure 4.2). Reference sediment from the Raisin River, used at all three sites, was collected in November 2015, stored in buckets and purged with N_2 gas to prevent oxidation of sediments. At each site, two wooden, removable docks were constructed before mesocosm and colonization tray deployment on day -30. The docks allowed for mesocosm chemistry sampling without disturbing the surrounding sediments.

To assess the influence of hyporheic connectivity, both the mesocosms and the colonization trays had connected (open) and disconnected (closed) exposures. For the mesocosms, the 'open' mesocosm exposure had two sides and the bottom removed and replaced with window-screen mesh (Burton et al. 2005, Costello et al. 2011). The 'open' colonization trays were also lined with same mesh, whereas the 'closed' trays were additionally lined with a plastic covering, to prevent hyporheic and porewater exchange with the surrounding sediments. The mesh size allowed for exchange with porewater and hyporheic in sediments, but prevented macroinvertebrates from moving into the sides or bottom of the mesocosms and colonization trays.

To assess the effects of sediment drying conditions, both a saturated and dry exposure were included. The combined hyporheic connectivity and drying treatments had four exposures: open-saturated, open-dry, closed-saturated, closed-dry. Deployment locations for the saturated and dry exposures had to be accessible for equipment and sampling, but low visibility by the public, to minimize the likelihood of human disturbances. Saturated and dry exposures were located within close proximity of each other (within 20-m). On day -30, half of the mesocosms and colonization trays were deployed in a saturating environment (Figure 4.2). The other half was deployed in a dry, mudflat area upland of the inundated area. For 30 days (day -30 to day 0),

78

the 'saturated' sediments remained saturated and 'dry' sediments remained dry. The dry sediments incurred some inundation, due to precipitation and an extremely wet summer 2016. On day 0, the dry exposures were moved into the saturated area for porewater and sediment sampling.

Hyporheic sampling

Minipiezometers were deployed at each site at 3 locations within the saturated area and sampled on two dates between day 1 and day 10. The vertical hydraulic gradient (VHG) was measured with a manometer, assessing the difference in hydraulic pressure in the sediments compared to the surface waters via height on the manometer (Winter et al. 1988). Four depths were sampled for porewater metals and reduced iron (Fe^{2+}) (5-cm, 10-cm, 15-cm and 20-cm). VHG was measured at 10-cm and 20-cm. Porewater samples were extracted using a hand pump, then filtered on a 0.45-µm polycarbonate syringe filter. Dissolved metal samples were acidified to 2% trace metal grade HNO_3^- and stored for analysis on an ICP-OES. Reduced iron (Fe^{2+}) was measured using the ferrozine method as described in the porewater chemistry section below.

Chemistry sampling

Porewater chemistry sampling began on day 1 after inundation. Surface water and porewater were sampled three times over the first ten days of inundation, on day 1, day 5 or 6 and day 9 or 10. Porewater was additionally sampled on day 26 or 30, but without replicates for reference sediments. On site, the pH, Eh, dissolved oxygen (DO), conductivity and temperature were measured with a YSI multi-meter. Three replicate surface water samples were taken, one at each minipiezometer, on each day at each site and stored at 4°C before analysis for alkalinity. Dissolved metal samples for surface water were filtered onsite with 0.45-µm polycarbonate syringe filter and acidified to 2% HNO_3^- for Ca, Mn, Fe, Mn and Zn on ICP-OES.

A maximum of 15-mL porewater was extracted per mesocosm from 2 or 3 Rhizon samplers within each mesocosm per sampling day. Porewater was collected into 6-ml vacutainers, to minimize oxidation of porewater before sample analysis. Porewater was added to a 50-ml tube and immediately sampled for dissolved oxygen (YSI Professional Plus ODO), pH (Thermo Scientific Orion Star A121) and Eh. Reduced iron (Fe^{2+}), a redox indicator, was measured using the ferrozine method (Stookey 1970, Kostka and Luther 1994). Reduced iron reagents were added to samples and standards in the field upon sample collection. Samples and standards were stored in the dark at 4°C and the absorbance measured on a spectrometer within 48 hours of sample collection. Reduced iron was used as the primary redox indicator in this experiment for porewater, as both DO and Eh oxidized quickly during sampling. A separate porewater sample from each mesocosm was extracted for dissolved metals (Zn, Fe, Mn, Ca, Mg) and analyzed on an ICP-OES. Detection limits were 3 mgL^{-1} for Mg and Ca, 50 µgL^{-1} for Fe, 25 µgL^{-1} for Zn, and 10 µgL^{-1} for Mn.

Sediment cores were extracted three times from each mesocosm, on day 0, day 9/d10 and day 26/d30. Upon collection, sediment cores were wrapped in parafilm and stored in 4°C upright until cores could be separated in the laboratory. If sedimentation was present, the depth was recorded and the layer of fine, organic material was removed from the sediment core. The top 2-cm of sediment was frozen in a 50-ml tube for sediment analyses. Sediments were processed for acid volatile sulfides (AVS) and simultaneously extracted metals (SEM) (Allen et al. 1991), total metals (Zn, Fe, Mn) and organic carbon via loss-on-ignition (*f*OC) (combusted at 450º C for 6 hours). The (SEM-AVS)/*f*OC is the bioavailable fraction of metals in the sediments and is used as the primary predictor of Zn toxicity to benthic organisms (U.S. EPA 2005). For the total metal digestion, 0.5 g dried sediment was digested in 7-ml of trace metal grade HNO_3 in a Hot Block

(Environmental Express) at 112°C for 100 minutes, according to EPA method 3050B (US EPA 1996). Samples were then diluted 50x for analysis on ICP-OES. Sediment digestions included a procedural blank (MilliQ) and NIST reference sediments. Metal recovery was verified >80%.

Biological sampling

Benthic macroinvertebrate colonization trays were deployed alongside the mesocosms to characterize stressor effects on benthic macroinvertebrate communities and on biofilm structure and function. Sediment trays were used for benthic colonization and biofilm colonization, as opposed to mesocosms. Mesocosms were not ideal for colonization because their top was elevated above the surficial sediment layer, possibly impeding invertebrate colonization. The recurring porewater and sediment sampling would also have potentially impaired invertebrate colonization. To prevent colonization on the saturated sediment exposures (from day -30 to d0), but allow for exchange with surface water, the tops of both colonization trays and mesocosms in the saturating exposure were covered with 250-µm mesh. The mesh was removed on day 0 (end of drying exposure) to allow for equal colonization time among treatments.

To assess biofilm endpoints, fritted glass discs were deployed atop the colonization trays on day 0. On day 28, trays were recovered from inundated area, biofilm colonization discs removed and sediments sieved to collect benthic macroinvertebrates. If discs were not visible due to sedimentation, then a plastic ruler was used to locate the discs by touch and the depth of sedimentation measured. Biofilm discs were removed from sediments and gently rinsed in site water to remove excess sediment (without disturbing attached biofilms).

Biofilm structure and function was measured on each disc. Function was measured by net primary productivity (NPP). To measure NPP, discs were then placed in clear 120-ml plastic specimen cups, capped and incubated in site water in direct sunlight for approximately four

81

hours (Costello and Burton 2014). Dissolved oxygen (DO) was measured on at least four replicate discs for each treatment combination, using a YSI Professional Plus ODO meter. DO concentrations (mg/L) were measured in stream water prior to disc addition (DO_{stream}), after 4-hour incubation ($DO_{biofilm}$), corrected for site water only ($DO_{control}$) and adjusted for volume of water (L) and area of disc (m^2) (Equation 1). Biofilm structure was assessed as Chlorophyll a (Chl *a*). Chl *a* was extracted from discs in 90% ethanol and absorbance measured at 750 nm (and 665 nm to correct for turbidity) on a Thermo Scientific Genesys 10uv scanning spectrometer (Steinman et al. 2007).

Equation 1: $$NPP = \left(\frac{DO_{biofilm} - DO_{stream}}{time_{biofilm}} - \frac{DO_{control} - DO_{stream}}{time_{control}} \right) \times \frac{Volume}{Area}$$

After removal of biofilm discs, sediments in each colonization tray were sieved using a 595-micron sieve bucket. Colonized macroinvertebrates were collected and preserved in 70% ethanol. Macroinvertebrates were sorted from sediment and debris in the laboratory and identified to family. Invertebrate community composition was characterized by total abundance, richness, Gini-Simpson diversity, Shannon's H diversity and the relative abundance of dominant taxa.

Statistical analyses

Statistics were performed in RStudio (Version 1.0.136). ANOVAs and post-hoc Tukey tests were used to assess effects of treatments (hyporheic connectivity & drying) on sediment chemistry, porewater chemistry and biological endpoints. Response variables were log-transformed for non-parametric data. The natural sediment exposures had three replicates sampled each day, and the ANOVA models assessed main effects of time, hyporheic connectivity and drying, with an interaction between connectivity and drying. Significant

interactions indicated that hyporheic connectivity changes the effects of the drying stressor. Reference mesocosms had three replicates for porewater sampling through day 10, but only one replicate on day 26/30 and only one replicate for sediment endpoints. Averages for reference sediment endpoints were obtained by averaging across the three days. Averages are reported with standard errors (SE), unless otherwise noted. The ANOVAs for the reference sediments assess main effects of hyporheic connectivity and drying conditions, and their interaction. Regression analyses were used to assess effects of sediment and porewater chemistry parameters on biological responses. Many of these relationships were not linear and were analyzed using exponential functions.

Results

Hyporheic conditions and chemistry

The three sites varied in VHG, but not significantly from one another, due to variability between minipiezometers and at different depths within each site. At both depths (10-cm and 20-cm), LBC had the highest VHG, followed by EB, then QC (Table 4.2). Porewater Zn concentrations were also highest at LBC ($305.67 \pm$ SE 253.83), though not significantly higher than EB ($39.50 \pm$ SE 19.85) or QC ($65.45 \pm$ SE 19.89). Porewater Fe, Mn, and Fe^{2+} were significantly higher at both QC and LBC, compared to EB (Table 4.2). As VHG increased, so did Fe^{2+} concentrations in the sediments ($R^2 = 0.52$, $F_{1,15} = 16.37$, $p = 0.001$), indicating that greater upwelling had a reducing effect on sediment porewater.

Porewater general chemistry indicators

Porewater chemistry varied across the three sites (Table 4.3). Results from the mesocosm experiments indicated effects of hyporheic connectivity on porewater redox conditions in LBC. In LBC natural sediments, the porewater redox indicator Fe^{2+} was lower in the closed treatment

compared to the open treatment ($F_{1,30}$=8.85, p=0.006), indicating more oxidized conditions in the closed treatments (Figure 4.3). There was also a significant interaction between drying and hyporheic connectivity ($F_{1,30}$=7.44, p=0.01), as the closed-dry exposure was lower than the saturated exposures and the open-dry exposure. Porewater pH was higher in the closed treatments compared to the open treatments ($F_{1,30}$=12.11, p=0.002), but there were no interactive effects (Figure 4.3). Porewater sulfide (S^{2-}) in the natural sediments was lower in the closed treatments, compared to open treatments ($F_{1,30}$=29.29, p<0.001), also indicating oxidation of the closed treatment sediments. There was also a significant interaction between drying and hyporheic connectivity, as the closed-dry exposure had lower S^{2-} than the other three ($F_{1,30}$=5.20, p=0.030), similar to Fe^{2+} results.

Reference sediments at LBC responded similarly to the natural sediments, as Fe^{2+} was lower in the closed treatments overall ($F_{1,22}$=25.84, p<0.001), and there was an interactive decrease of Fe^{2+} in the dry-closed exposures ($F_{1,22}$=16.33, p<0.001). The pH in the reference sediments was higher in the closed exposures compared to open exposures ($F_{1,8}$=6.52, p=0.034). No effects were found from either treatment on sulfide in the reference sediments.

Porewater chemistry in EB natural sediments was unaffected by hyporheic connectivity, and only changed due to the drying exposure (Figure 4.3). Natural sediments exposed to drying conditions were more oxidized ($F_{1,31}$=19.98, p<0.001), had higher pH ($F_{1,31}$=12.95, p=0.001) and lower S^{2-} ($F_{1,31}$=21.58, p<0.001). The dried sediments were more oxidized, resulting in higher pH and lower S^{2-}.

Reference sediments at EB were affected by both drying and hyporheic connectivity. Saturated exposures were more reduced than dry exposures ($F_{1,31}$=32.59, p<0.001), and the open-saturated exposure were more reduced (higher Fe^{2+}) than the open-dry and both closed exposures

($F_{1,31}=9.14$, p=0.005). There was a significant interaction between hyporheic connectivity and drying on pH ($F_{1,31}=14.33$, p=0.005). The pH in the open-saturated exposure was significantly lower than open-dry and closed-saturated exposures. There were no effects of treatment on S^{2-}. Redox and pH relationships indicate effects of both drying and hyporheic connectivity, as all exposures with physical stressor treatments were more oxidized.

There were no trends in porewater chemistry at QC related to hyporheic connectivity. The natural sediments were more reduced in the closed exposures than the open exposures ($F_{1,18}=7.96$, p=0.011), which is the opposite trend observed at LBC and EB (Figure 4.3). No effects of treatment were observed on reference sediments at QC.

Porewater metal chemistry

LBC natural sediment porewater metals were affected by both hyporheic connectivity and by drying over the 30-day inundation (Table 4.4). The closed-dry treatment had significantly higher porewater Zn (167.3±85.7 µg/L) than the other three treatments (Table 4.3). Porewater Fe was higher in open exposures than closed exposures, and the closed-dry exposure was significantly lower than the other 3 treatments (Figure 4.4). Porewater Mn was initially affected by drying conditions, but by day 9, the closed exposures had higher porewater Mn than the open exposures.

Porewater in the reference sediment at LBC responded similarly to the LBC natural sediments (Table 4.4). Porewater Fe was lower in closed exposures compared to the open exposures, and the closed-dry exposures had the lowest porewater Fe. Reference sediment porewater manganese was not affected by hyporheic connectivity, but was higher in the dry exposure compared to the saturated.

85

At EB, the porewater metal response was more varied than LBC, but was driven primarily in the drying treatment (Figure 4.4). Natural sediment porewater Zn was unaffected by hyporheic connectivity, but was higher in dry sediments than in saturated sediments (Table 4.4), indicating oxidative release of metals from drying and re-flooding. Porewater Zn concentrations were low overall, generally near or below the detection limit of the ICP-OES. There were no effects of treatments on porewater Fe, but Fe did increase overtime in the dry treatments (Table 4.3). Porewater Mn decreased over time in all treatments, except for the open-dry.

The reference sediments at EB were impacted by both hyporheic connectivity and drying conditions. The dry sediments had lower porewater Fe than the saturated sediments, but the open-saturated had higher Fe than the closed-saturated. Porewater Mn was highest in the closed-dry exposure and lowest in the closed-sat exposure.

Natural sediments at QC had low porewater Zn and it was not affected by hyporheic connections or drying (Table 4.4). Porewater Fe was higher overall in the closed exposures than the open exposures, concentrations remained stable, with the exception of open-dry which increased from day 1 to day 9 (Figure 4.4). Porewater Mn responded similarly to Fe, as closed exposures had higher Mn than open, and the closed-dry exposure was higher throughout the inundated exposure. There were no significant relationships between treatment and porewater metals in the reference sediment porewater at QC.

Sediment metal chemistry

Total metals in sediment varied between sites, as did the effect of hyporheic connectivity on sediment chemistry. Total Zn was highest at LBC, compared to EB, QC and the Reference sediments (Table 4.3). Total Fe was highest in the Reference sediments, and higher at LBC than at EB and QC. Total Mn was higher at LBC and the Reference sediments than EB or QC. Total

86

Zn at LBC was higher in the open exposure than the closed exposure ($F_{1,24}=6.63$, p=0.017), despite higher porewater Zn in closed exposures (Table 4.3). There were no effects of treatment on total Zn at QC or EB.

Bioavailable metals were affected by treatments and differed between sites. Due to replicates, only open-dry and closed-dry were compared (as they each had at least 3 replicates). LBC sediments had higher (SEM-AVS)/fOC in closed exposures than in open exposures ($F_{1,12}=22.65$, p<0.001) (Figure 4.5). The (SEM-AVS)/fOC decreased over time in the open-dry treatments, but remained consistently higher (SEM exceeding AVS) in the closed treatments, indicating greater potential toxicity in closed treatments. This was likely caused by the lower overall AVS in the closed treatments ($F_{1,14}=19.92$, p<0.001), whereas the open treatments increased in AVS over time ($F_{1,14}=8.37$, p=0.012). Based on the elevated SEM fraction relative to AVS, it is possible that LBC sediments would be toxic to aquatic organisms in the closed-dry treatments because the metals exceed sulfide concentrations.

At EB and QC there was no effect of hyporheic connectivity on (SEM-AVS)/fOC, but concentrations decreased over time. At EB the (SEM-AVS)/fOC dropped from d0 to d10 remained low through d30 ($F_{2,12}=7.10$, p=0.009). This trend is unrelated to SEM at EB, but is related to increased AVS ($F_{2,12}=4.73$, p=0.031) and fOC ($F_{2,12}=14.02$, p<0.001) over time. QC bioavailable metals and binding ligands behaved similarly to EB, as the SEM fraction exceeded AVS and fOC on day 0, but by day 10 through day 30, SEM was lower than AVS ($F_{1,12}=5.37$, p=0.022). This trend also coincided with increased AVS over time ($F_{2,14}=5.82$ p=0.015) and increased fOC over time ($F_{2,14}=14.27$, p<0.001).

Biological effects

Biofilm biomass (Chl *a*) and productivity (NPP) varied between the three sites. In the natural sediments, NPP was highest at QC, followed by LBC and EB ($F_{2,51}$=7.23, p=0.002). Chl *a* also differed between sites ($F_{2,51}$=8.87, p<0.001). Despite having the lowest NPP of the three sites, EB had the highest Chl *a*, compared to both QC and LBC. Among the reference sediments, NPP varied between the sites ($F_{2,35}$=21.07 p<0.001). NPP was higher at QC compared to LBC and EB. NPP was often negative at EB, suggesting that respiration likely exceeded NPP. There were no effects of site location on Chl *a* in the reference sediments.

No effects of treatments (drying or hyporheic connectivity) were observed on biofilms at EB or LBC, but at QC there was lower NPP in closed treatments compared to open treatments ($F_{1,10}$=7.91, p=0.018), and the closed-dry exposure was significantly lower NPP than the open-saturated exposure. At all sites, there were responses of biofilm Chl *a* and/or NPP from exposure to sediment metals. At LBC, Chl *a* production decreased with increased SEM Zn (R^2=0.544, p=0.023) (Figure 4.6). At EB, both NPP (R^2=0.545, p=0.004) and Chl *a* (R^2=0.354, p=0.032) declined in response to increased total SEM (Figure 4.6). Similar, but slightly weaker, relationships were found with SEM_{Zn} at EB. No relationships with SEM were found with biofilms at QC. No effects of porewater Zn in natural sediments were found on biofilms.

An additional, unexpected, stressor on biofilm structure and function was sediment deposition at each site. Sedimentation depths ranged from 0-1cm at LBC, and 0-2cm at EB and QC. Chl *a* declined at all three sites with increased depth of sedimentation (LBC: R^2=0.296, p<0.001; EB: R^2=0.212, p=0.003; QC: R^2=0.196 p=0.018) (Figure 4.7). At EB, NPP also declined with increased sedimentation depth (R^2=0.318, p<0.001) (Figure 4.7).

Benthic macroinvertebrates were not affected by hyporheic connectivity and drying conditions at any of the 3 sites. Natural sediment richness was greater at LBC and EB than QC

($F_{2,33}$=4.56, p=0.018). Relative abundance of dominant taxa was highest at QC, compared to EB and LBC (Table 4.6). The Gini-Simpson Diversity index was greater at LBC than QC, and Shannon's H diversity was greater at EB and LBC than QC. Within the reference sediments, there were no differences between the three sites for any benthic macroinvertebrate metrics. There were no effects of elevated sediment metals or porewater metals on benthos, given that total and dissolved metal concentrations mostly fell below threshold values for toxicity.

Discussion

There were some limitations to the study design. The sediment chemistry and biological endpoints were taken from separate sediment exposures (mesocosms and colonization baskets, respectively). This introduces the uncertainty of whether there was variability between the two units. For data analysis, chemical and biological samples were paired together based on sample ID designated upon deployment, or averaged across treatments. The number of replicates in the study (n=3) was an additional limitation, as it reduced the statistical power of the data analysis and often resulted in higher variability within treatments.

Hyporheic connectivity and sediment metals

In the fringe wetland ecosystems (EB and QC), the importance of hyporheic connectivity is much less obvious than in the riparian wetland at LBC. At QC, neither hyporheic connectivity nor drying conditions affected porewater redox chemistry. The surface water at QC had very low DO (< 1 mg/L). This continuously reduced environment likely had the greatest effect on the low metal bioavailability during the inundated exposure from day 0 to 30, as any oxidation from drying was reduced upon inundation in the low DO surface water. EB, the high-energy lake system, was dominated by surface water conditions (wave action, sediment resuspension). The

sediments *in situ* were highly oxidized, as indicated by low Fe^{2+} relative to other sites (Table 4.2), despite similar total Fe concentrations (Table 4.1.).

The importance of hyporheic connectivity to mitigate effects of drying varied among the three sites. At LBC, the connection to the hyporheic zone influenced most physiochemical porewater endpoints. The closed-dry exposure was more oxidized and had the lowest sulfide concentrations. These redox trends occurred in both natural and reference sediments. The similarity in porewater chemistry between treatments in the natural and reference sediments indicated that effects of the site (not sediment) might be driving the porewater chemistry. The importance of hyporheic connectivity at LBC may be due to its higher VHG than the other sites. Additionally, LBC was the only site located within a riverine system, which are often influenced by groundwater-surface water interactions (Boulton et al. 1998).

Sediment binding ligands responded to the redox conditions, as they differed between open and closed exposures under drying conditions. AVS and *f*OC were both higher at LBC in the open exposures compared to the closed exposures, despite no difference in SEM between the exposures. Though SEM was unaffected by groundwater connectivity, the important binding ligands, *f*OC and the redox sensitive AVS, were higher when connected to the hyporheic zone. This also suggests a hyporheic influence, as studies on sulfur in hyporheic zone showed sulfate reduction occurs in upwelling zones, due to reducing conditions (Ng et al. 2017). The upwelling at LBC may be responsible for the reduced conditions in the open exposures, as upwelling zones are characterized by reduced conditions (Hendricks et al. 1993). If hyporheic upwelling was taking place at LBC, then the closed-dry exposure was cut off from the reduced upwelling porewater, resulting in oxidized sediments throughout the exposure.

Porewater Zn at LBC was also impacted by interactions between hyporheic connectivity and drying. Porewater Zn was high throughout the experiment in the closed-dry exposures, compared to the open and/or saturated exposures. Concentrations averaged 162.4±40.0 µg/L, above the probable effects levels for Zn in surface waters (120 µg/L). Despite elevated concentrations, no relationships were observed between porewater Zn and effects on biota.

This research emphasizes an important limitation to mesocosm and laboratory studies that are unconnected to natural hyporheic and porewater exchange. Particularly in lotic system sediments, where hyporheic flows can dominate sediment redox conditions (Boulton 1993, Franken et al. 2001), laboratory tests may find artificially high metal toxicity, compared to what would be occurring naturally. The artifact of being unconnected to hyporheic flows can be avoided in natural settings by using mesocosms and exposures that are open to the surrounding sediments, but cannot be avoided in laboratory experiments.

Accurate characterization of redox sensitive contaminant exposure and effects in laboratory tests may be more difficult for sediments that originate from sites with hyporheic influences, like LBC. Laboratory tests and closed off mesocosms better simulate sites with minimal hyporheic flows (i.e., QC), but are unable to mimic the exchange that takes place in sites like LBC. For example, a previous laboratory test using these same sediments to test the effects of drying accurately concluded that after 30 days, the AVS fraction exceeded the SEM for QC and EB (Nedrich and Burton 2017b). In the same study, SEM exceeded AVS at LBC after 30 days of inundation. In the present field study at LBC, the closed-dry field exposure (most similar to laboratory mesocosm) found similar SEM > AVS, but in the open-dry exposure AVS exceeds SEM (Figure 4.5). Laboratory experiment results suggest continuously elevated (SEM-AVS)/fOC at LBC in dried (drought-affected) sediments, but in a field test, connected to the

hyporheic zone, bioavailable metals decrease overtime and are no longer bioavailable after 10 days.

Biofilms as exposure endpoint

Biofilm structure and function were useful endpoints for ecosystems stressors in this experiment, and were more sensitive to metals than any of the benthic macroinvertebrate endpoints. Biofilm Chl *a* biomass declined at both EB and LBC in response to increased SEM. At EB, biofilm function (NPP) decreased with increased SEM. These results were inhibited by sedimentation, which occurred across all three sites on the biofilm colonization discs. Chl *a* at all three sites decreased with increased depth of sedimentation. At EB, NPP also decreased as depth of sedimentation increased.

Biofilms are increasingly being used in ecotoxicology field studies, to better understand both structural and functional responses to contaminants. Using biofilms as an endpoint helps to explain how crucial processes in aquatic habitats (respiration, primary production, and other microbial mediated processes) can be altered by contaminants. Biofilms are also an important food source for benthic invertebrates, and thus a transport pathway for metal accumulation into invertebrates (Farag et al. 1998, Rhea et al. 2006, Kim et al. 2012). Though benthic macroinvertebrates are the established endpoint to assess habitat quality, this study and others suggest that biofilms may be more sensitive to metals than macroinvertebrates at lower metal concentrations (Ancion et al. 2010b, 2013, Costello and Burton 2014). Easy and inexpensive techniques have been developed to assess other biofilm functional endpoints, like respiration (Tiegs et al. 2013). Biofilm samples are also small and many replicates can be deployed, allowing for versatility in sample design and treatments.

Acknowledgement of hyporheic conditions is important for assessments of ecological risk and management of contaminated sites. While it is not possible to simulate hyporheic flows during toxicity testing, it is important for researchers and managers to understand the ecosystem from which the metals originate. Much of what is known about metal toxicity and ecological risk was developed in closed exposure chambers without realistic site conditions (U.S. EPA 2000). These bench-top laboratory exposures lack ecological and physical realism and do not take into account the site conditions. If physical processes in the hyporheic zone influence sediment redox conditions, then a traditional toxicity test will not accurately characterize the metal exposure, as was observed in the LBC closed treatments. Comprehensive research should include multiple lines of evidence, both laboratory and *in situ* testing, to understand realistic exposures to aquatic organisms.

Tables

Table 4.1. Sediment chemistry for each site. Values are averaged across treatments and sample days (d0, d10, d30).

Sediment	LOI (% C)	AVS (μmol/g)	(SEM-AVS)/ *f*OC	Total Fe (mg/kg)	Total Mn (mg/kg)	Total Zn (mg/kg)	Total Ni (mg/kg)	Total Cu (mg/kg)	Total Cr (mg/kg)
EB	2.9 ± 0.4	2.90 ± 0.68	-74.64 ± 19.30	2288.99[a] ± 156.92	63.88[a] ± 4.51	0.19[a] ± 0.13	0.65[a] ± 0.25	5.14[a] ± 2.94	3.08[a] ± 1.03
LBC	5.6 ± 1.6	2.13 ± 0.38	2.44 ± 6.98	3003.53[b] ± 245.00	180.45[b] ±12.22	78.42[b] ± 17.50	0.00[a] ± 0.00	33.65[b] ± 6.50	25.74[b] ± 5.41
QC	2.3 ± 0.3	0.59 ± 0.09	-14.88 ± 3.99	1867.34[a] ± 88.58	35.19[a] ± 2.47	10.51[a] ± 1.06	3.33[b] ± 1.13	2.87[a] ± 0.34	1.50[a] ± 0.28
Reference	2.5 ± 0.4	2.03 ± 0.64	-43.40 ± 12.30	6383.06[c] ± 241.55	210.39[b] ± 6.35	11.52[a] ±3.94	2.86[b] ± 0.66	31.97[b] ± 6.58	7.64[a] ± 1.80

[a,b,c] Indicate significant differences between sediment types.

Table 4.2. Hyporheic data collected from minipiezometers (n=3) at each site at 2 depths (10cm and 20cm), including: vertical hydraulic gradient (VHG), reduced iron (Fe^{2+}), porewater iron, manganese and zinc (± SE).

Site	Depth (cm)	VHG	Fe^{2+} (mg/L)	Fe (mg/L)	Mn (ug/L)	Zn (ug/L)
EB	10	0.183[a] ± 0.061	0.04[a] ± 0.03	4.16[a] ± 0.43	271.33[a] ± 26.90	39.50[a] ± 19.85
EB	20	0.138[a] ± 0.025	0.04[a] ± 0.03	2.29[a] ± 0.14	170.70[a] ± 9.96	84.53[a] ± 84.53
LBC	10	0.227[a] ± 0.027	4.17[b] ± 0.60	17.89[b] ± 2.49	1311.00[b] ± 460.62	305.67[a] ± 253.83
LBC	20	0.107[a] ± 0.030	1.84[b] ± 1.39	10.90[b] ± 4.18	973.87[b] ± 336.62	193.83[a] ± 144.99
QC	10	0.115[a] ± 0.105	1.56[b] ± 0.84	14.79[b] ± 5.31	1521.22[b] ± 212.39	65.45[a] ± 19.89
QC	20	0.103[a] ± 0.023	1.40[b] ± 0.27	16.34[b] ± 8.59	1678.42[b] ± 242.56	110.78[a] ± 58.61

[a,b] Differences between sites

Table 4.3. Porewater physiochemical properties of natural and reference sediments, averaged (±1 standard error) for each sediment type across all treatments.

Sediment	pH	DO (mg/L)	Eh (mV)	Fe^{2+} (mg/L)	Fe (mg/L)	Mn (mg/L)	Zn (µg/L)	Alkalinity (mg/L $CaCO_3$)	Hardness (mg/L $CaCO_3$)
EB (n=36)	6.86 ± 0.03	2.83 ± 0.15	-94.93 ± 4.58	2.71 ± 0.38	20.92 ± 1.55	0.80 ± 0.04	13.19 ± 1.19	0.212 ± 0.014	587. 62 ± 59.51
LBC (n=36)	6.70 ± 0.25	2.56 ± 0.13	-100.49 ± 5.09	7.12 ± 0.92	44.26 ± 2.98	4.31 ± 0.22	408.82 ± 209.36	0.266 ± 0.129	1278.95 ± 87.33
QC (n=24)	6.48 ± 0.12	3.32 ± 0.14	-81.82 ± 2.38	2.98 ± 0.52	16.64 ± 0.85	1.13 ± 0.04	18.70 ± 2.86	0.343 ± 0.012	1304.16 ± 24.39
Reference (n=32)	6.88 ± 0.04	2.17 ± 0.16	-116.45 ±5.47	5.14 ± 0.76	37.66 ± 2.71	6.61 ± 0.36	20.66 ± 4.20	0.255 ± 0.015	1224.62 ± 57.13

Table 4.4. Summary of porewater ANOVA models and significance of treatment effects from inundation exposure day 1 to 10. All p-values less than 0.1 were reported. In the main effects columns, (-) indicates that porewater metals concentrations were lower in the closed or drying treatments (relative to open or saturated, respectively), and (+) indicates that they were higher. In the INT column, bolded values indicate the closed-dry treatment varied from the other three treatments. Day was also included in the model to account for changes over time.

Site	Sediment	Porewater metal	Day	Closed to Hyporheic		Drying		INT: Hyporheic X Drying
LBC	Natural	Zn	x	(+)	0.031	(+)	0.014	**<0.001**
LBC	Natural	Fe	x	(-)	<0.001	(-)	<0.001	**<0.001**
LBC	Natural	Mn	x		x	(-)	0.006	x
LBC	Reference	Fe	x	(-)	<0.001	(-)	<0.001	**<0.001**
LBC	Reference	Mn	x	(-)	*0.092*	(+)	0.011	x
EB	Natural	Zn	0.009		x	(+)	0.003	x
EB	Natural	Fe	0.007		x		x	x
EB	Natural	Mn	x		x	(-)	0.012	x
EB	Reference	Fe	0.013		x	(-)	<0.001	<0.001
EB	Reference	Mn	<0.001		x		x	**<0.001**
QC	Natural	Zn	x		x		x	X
QC	Natural	Fe	x	(+)	0.001		x	<0.001
QC	Natural	Mn	x		x		x	<0.001
QC	Reference	Fe	<0.001	(-)	<0.001	(-)	<0.001	<0.001
QC	Reference	Mn	<0.001		x		x	0.002

Table 4.5. Surface water physiochemical properties of each site. Values are averaged (±1 standard error) across the 3 replicate sampling locations sampled on 4 separate sampling days (day 1, day 5/6, day 9, day 28/30) at each site.

Sediment	pH	DO (mg/L)	Conductivity (µS/cm)	Temp (°C)	Fe (mg/L)	Mn (mg/L)	Zn (µg/L)	Alkalinity (mg/L CaCO₃)	Hardness (mg/L CaCO₃)
EB	8.31 ± 0.11	9.50 ± 0.67	318.43 ± 3.69	25.49 ± 0.87	0.010 ±0.002	0.007 ± 0.002	0.004 ± 0.001	0.093 ± 0.002	160.0 ± 3.6
LBC	7.21 ± 0.06	3.66 ± 0.42	753.83 ± 15.85	16.67 ± 0.25	0.038 ±0.007	0.095 ± 0.011	0.003 ± 0.002	0.145 ± 0.020	89.2 ± 2.6
QC	7.30 ± 0.03	0.75 ± 0.11	782.08 ± 6.69	22.21 ± 0.58	0.113 ±0.009	0.107 ± 0.024	0.009 ± 0.001	0.251 ± 0.003	222.0 ± 1.1

Table 4.6. Averages (±SE) of biotic endpoints (biofilms and benthic macroinvertebrates) for both sediments (natural and reference) at each site. Superscripts indicate significant differences from one-way ANOVA between sites within each sediment type.

Site	Sediment	NPP (mg O_2m^{-2}h^{-1})	Chl a (mg m^{-2})	Abundance	Richness	% Dominant	Gini-Simpson Diversity	Shannon Diversity
EB	Natural	7.8 ± 4.3 [a]	26.3 ± 5.0 [a]	21.4 ± 3.5	4.6 ± 0.5[a]	0.56 ± 0.06[ab]	0.56 ± 0.05[ab]	1.10 ± 0.11[a]
LBC	Natural	17.9 ± 4.9[ab]	7.2 ± 1.7 [b]	31.9 ± 7.5	5.1 ± 0.5[a]	0.45 ± 0.04[a]	0.64 ± 0.03[a]	1.22 ± 0.07[a]
QC	Natural	30.8 ± 2.9 [b]	9.2 ± 2.5 [b]	9.2 ± 4.4	2.5 ± 0.4[b]	0.75 ± 0.09[b]	0.40 ± 0.10[b]	0.67 ± 0.17[b]
EB	Reference	-2.4 ± 1.3 [a]	12.7 ± 2.9	23.4 ± 7.3	4.1 ± 0.7	0.67 ± 0.06	0.45 ± 0.07	0.86 ± 0.14
LBC	Reference	18.5 ± 5.7 [b]	17.0 ± 5.6	76.4 ± 25.4	6.4 ± 0.7	0.57 ± 0.06	0.58 ± 0.05	1.19 ± 0.11
QC	Reference	45.0 ± 4.3 [c]	19.7 ± 5.2	26.8 ± 3.1	4.3 ± 0.8	0.55 ± 0.13	0.55 ± 0.12	1.04 ± 0.25

[a,b] Indicate significant differences between sites, within each sediment type (i.e., natural or reference)

Figures

Figure 4.1. Map of three field experiment locations (EB, LBC and QC), with groundwater connectivity overlay. The dark purple indicates low groundwater connectivity, and pink/red is higher groundwater connectivity. Groundwater connectivity map layer was obtained from the State of Michigan GIS Open Data (http://gis-michigan.opendata.arcgis.com).
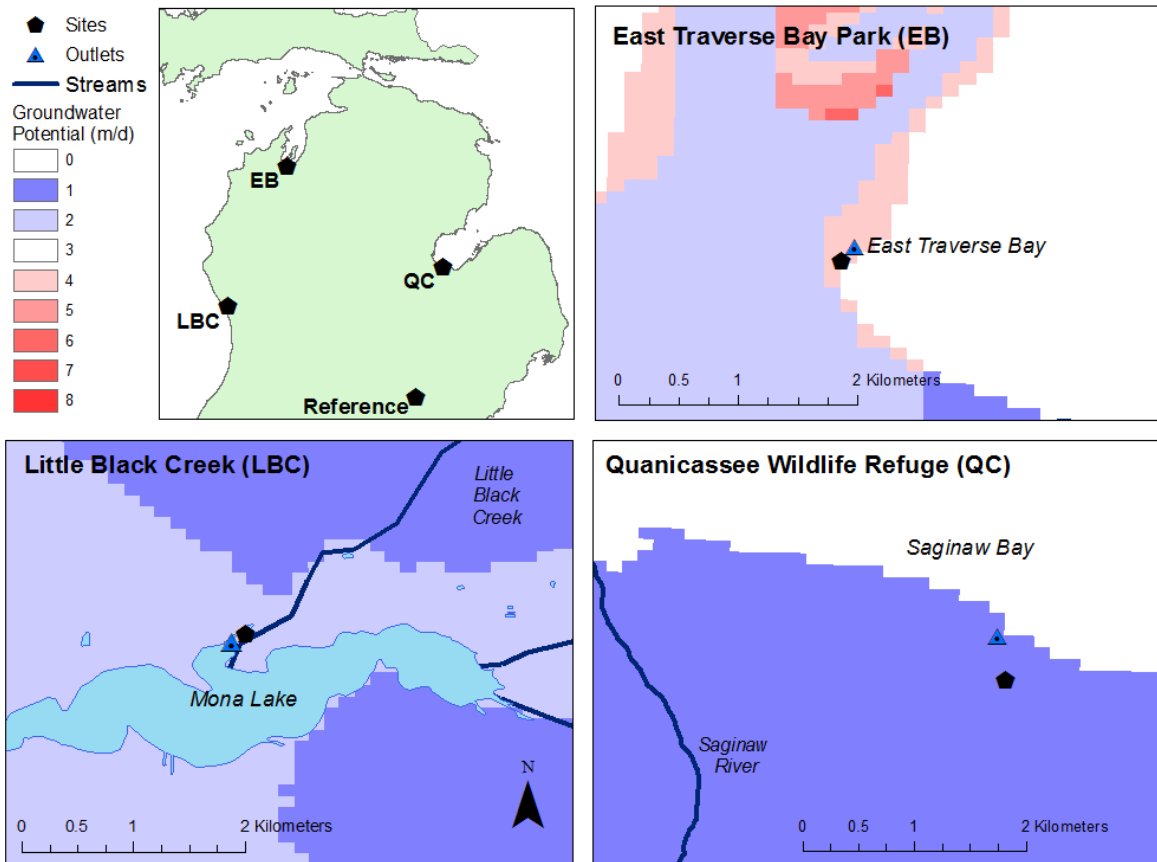
Figure 4.2. Timeline of the 60-day sediment exposure and sampling schedule, repeated for each site.
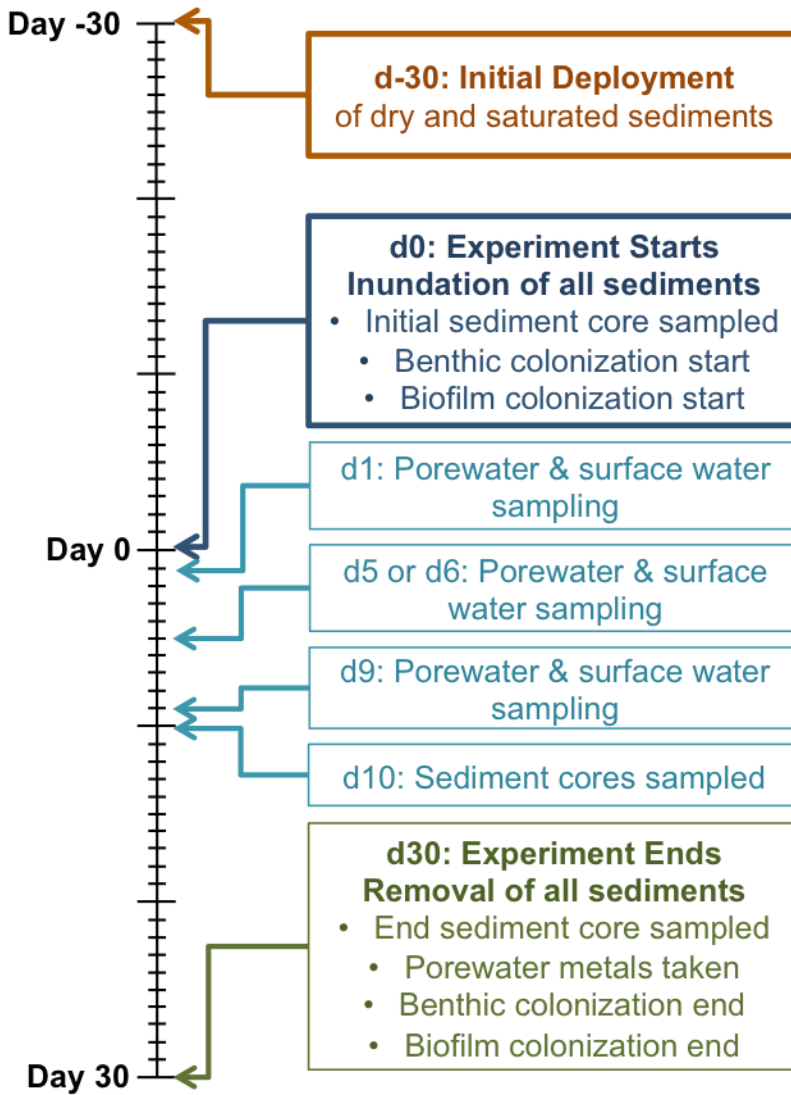
Figure 4.3. Site porewater pH and Fe^{2+} over the 10-day inundation period, in response to drying and hyporheic connectivity (± SE on 3 replicates). Note y-axis variation for each site.
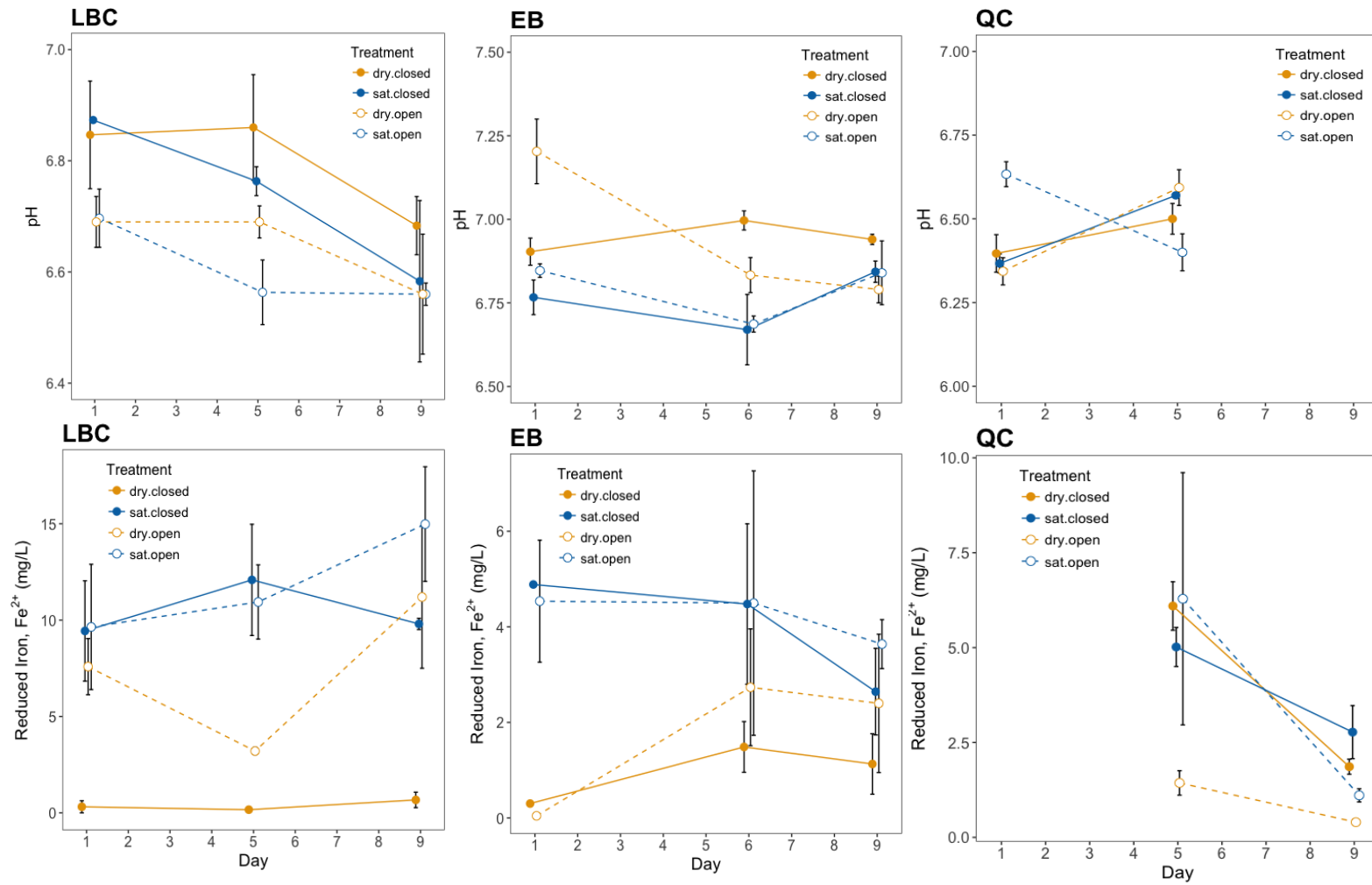
Figure 4.4. Site porewater Zn and Fe over the 10-day inundation period, in response to drying and hyporheic connectivity (± SE on 3 replicates). Note y-axis variation in zinc graphs (0-250 µg/L for LBC and 0-30 µg/L for EB and QC).
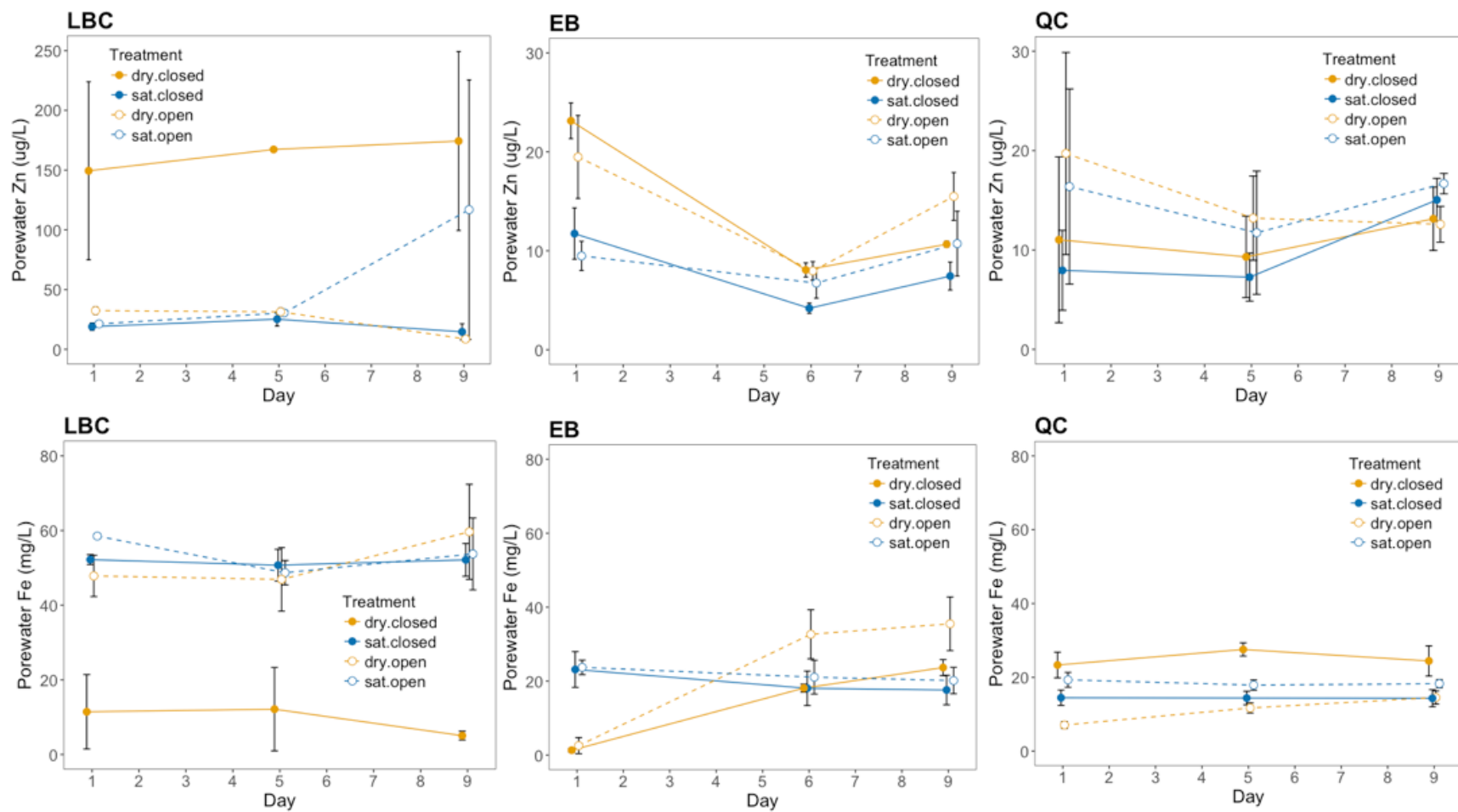
Figure 4.5. (SEM-AVS)/f_{OC} (±SE of 3 replicates) at each site for dry sediments only from d0 to d30. Y-axis varies for each site. EB and QC have AVS exceeding SEM after day 0. At LBC, the closed treatments have SEM exceeding AVS, whereas open treatments have declining bioavailable fraction over time.
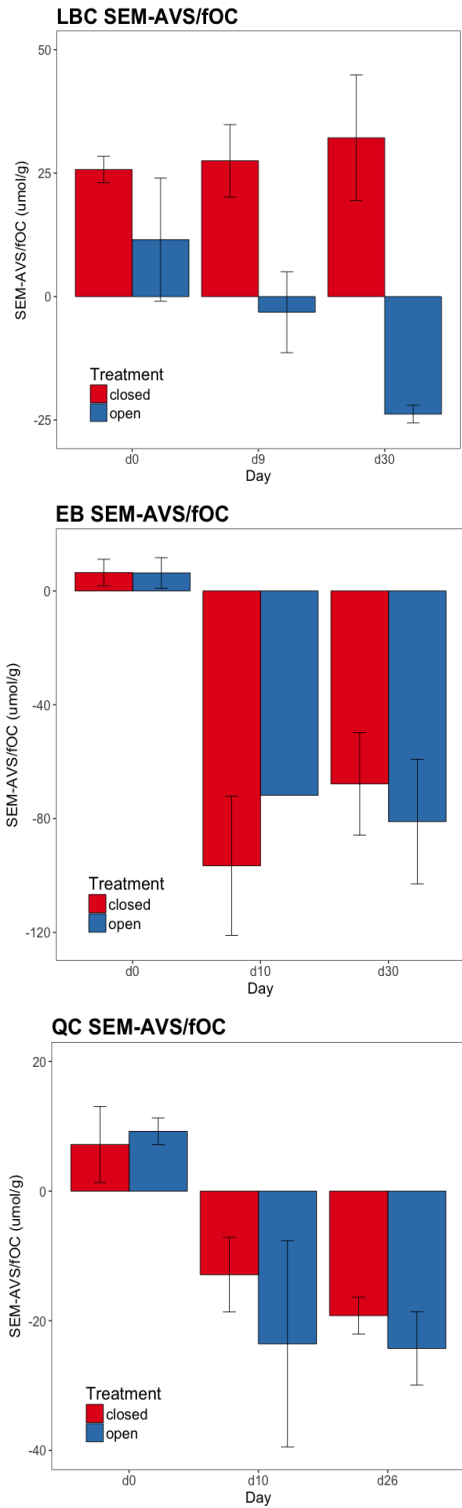
Figure 4.6. Biofilms responses (negative exponential) to sediment metals at LBC and EB. Total Zn was used for LBC sites because concentrations of Zn were relatively high. At EB, total Zn concentrations were low, but other metals were detected, and thus the SEM (simultaneously extracted metals) fraction was used for analysis.
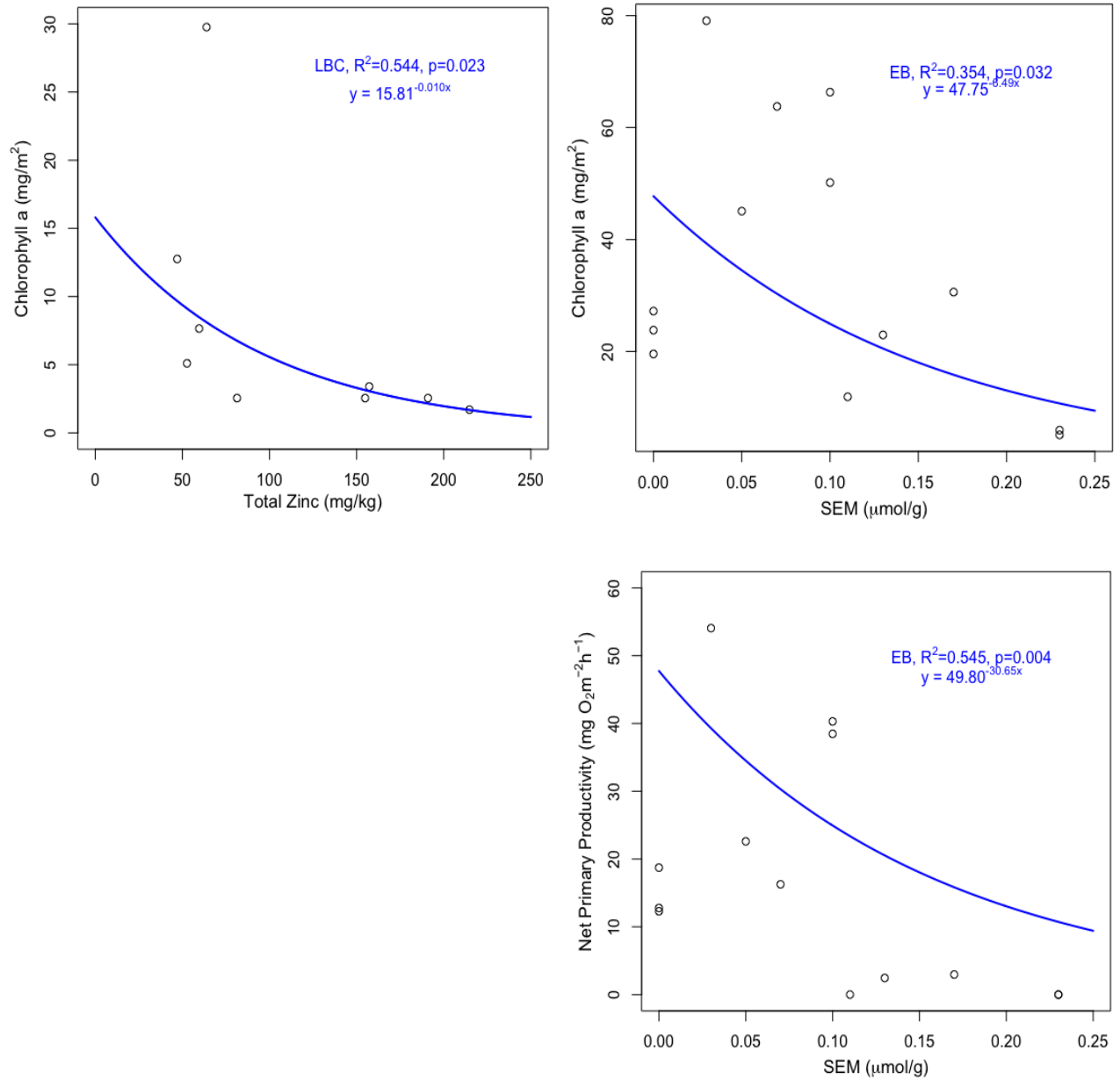
Figure 4.7. Biofilm Chl *a* declines in response to sedimentation at each of the 3 sites.
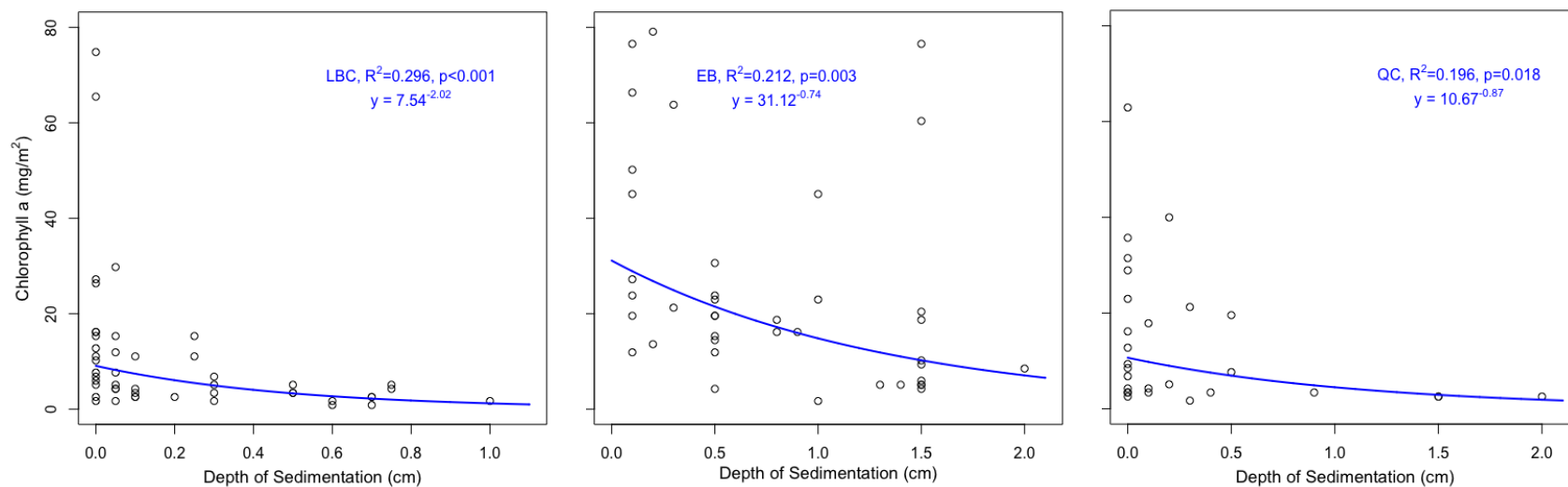
Chapter 5

Conclusions

Summary of key findings

This dissertation explored the effects of hyporheic flows on sediment geochemistry and zinc exposure and effects to aquatic organisms. Hyporheic flows influenced redox conditions and pH in sediments, but were dependent on type of hyporheic flow (Figure 5.1). Downwelling exposures resulted in increased Zn exposure via both porewater Zn and (SEM-AVS)/fOC, ultimately resulting in effects on aquatic biota. Upwelling exposures, conversely, were more reduced and had less bioavailable metals, which resulted in lower risk from metal contamination, but not necessarily in better habitat quality for benthic organisms (due to lower dissolved oxygen and less influence of surface water inputs).

Across all experiments, both in the field and the laboratory, the hyporheic zone affected sediment redox chemistry and metal chemistry. Inclusion of hyporheic flow characterization (using minipiezometers to measure VHG or temperature loggers to measure influence of surface water) would improve ecological risk assessments, as hyporheic flows can alter the bioavailability of metals in contaminated sediments. This dissertation also demonstrated that biofilms are an important endpoint for ecotoxicology studies in the field, as they were often more sensitive to low concentrations of metals than benthic macroinvertebrates.

In Chapter 2, the effects of stream bedform location in the *in situ* experiments were compared to artificial stream mesocosms with an oxic hyporheic flow manipulation. In the *in situ*

experiments, stream bedform (head vs. tail riffle) influenced redox chemistry, which in turn influenced sediment metal chemistry. As expected from previous literature, benthic macroinvertebrate species diversity and richness were higher at the upstream riffle (head) where surface water downwells into sediments (Pepin and Hauer 2002, Davy-Bowker et al. 2006). As sediment oxidation increased, so did the (SEM-AVS)/fOC in sediments (Calmano et al. 1993). This indicated that metal bioavailability might be higher in head riffles (or in downwelling zones), thus potentially exposing sensitive benthic communities of the head riffle to metals more than less sensitive communities in the tail riffle. This research cannot determine if decreased risk in tail riffles trumps the better habitat quality (oxic conditions) in the head riffles. The low sediment Zn concentrations (<150 mg/kg) did not result in any effects to benthic macroinvertebrates. Biofilm NPP, however, decreased with increased (SEM-AVS)/fOC, suggesting that biofilms may be a more sensitive endpoint for metals than benthic macroinvertebrates (Genter et al. 1987, Costello and Burton 2014).

In Chapter 3, a laboratory experiment explored impacts of sediment Zn and oxic hyporheic conditions on *Hyalella azteca*. Porewater and sediment chemistry changed over time, and eventually porewater Zn concentrations stabilized and were equal between the hyporheic and non-hyporheic exposures. Despite similar porewater Zn concentrations after 80 days, survival of *H. azteca* was lower in the hyporheic exposure than in the non-hyporheic exposure. These long-term effects appear to be influenced by (SEM-AVS)/fOC, which was higher in the hyporheic exposure compared to the non-hyporheic exposure. We know from Chapter 2 results and other literature (Davy-Bowker et al. 2006), that more sensitive and diverse communities exist in oxic downwelling environments (compared to upwelling). If metal concentrations like those observed

in Chapter 3 were found in field sediments, then these sensitive communities would potentially

be at higher risk for effects from metal contamination, as were observed in the *H. azteca.*

The importance of hyporheic flows on the effects of drying conditions in contaminated

field sites was explored in Chapter 4. The only site to exhibit effects of hyporheic connectivity

(LBC) also had the most reduced porewater and the highest VHG. Effects were observed only on

sediment exposures re-oxidized from drying conditions without hyporheic connectivity (closed-

dry). This suggests that hyporheic connectivity may decrease the effects of sediment drying on

metal bioavailability in systems where hyporheic flows (upwelling specifically) are present.

Though no direct links were found between hyporheic connectivity and biological endpoints,

(SEM-AVS)/*f*OC was lower in the open hyporheic exposures, and biofilm community biomass

(Chl *a*) decreased with higher metal concentrations at both LBC and EB. As in Chapter 2, this

suggests greater sensitivity of biofilm endpoints, compared to benthic macroinvertebrates, at low

metal concentrations in sediments.

When results from each chapter are assessed together, hyporheic flows are an important

influence on redox chemistry and redox sensitive binding ligands (Figure 5.1). Hyporheic flows

do not appear to impact total concentrations of metals in sediments, but they do influence the

binding capacity of sediments to decrease bioavailable metals. This was observed indirectly in

Chapter 2 *in situ* when head riffles (typically downwelling conditions) were more oxidized than

tail riffles (typically upwelling conditions), which correlated with increased (SEM-AVS)/*f*OC. In

Chapter 4, the reduced hyporheic field conditions at the riparian wetland site (LBC) likely

decreased the bioavailable fraction of metals in the drying-influenced sediments of the open

(open-dry) mesocosm compared to closed mesocosms (closed-dry). While direct links between

treatment and biological effects primarily only occurred in Chapter 3, effects of treatment were

observed on sediment redox chemistry and metal chemistry. Subsequent trends in sediment chemistry were observed and correlated with effects on the biological endpoints.

Throughout this dissertation, the pH trends in the oxic hyporheic treatments were initially unexpected. In Chapters 2 and 3, the pH was higher in the oxidized exposures (compared to the non-hyporheic and more reduced exposures), which is the opposite of what is expected with oxidation-pH relationships. Generally, when sediment is oxidized and metals are released, there is also a release of protons (H^+), which decreases the pH. In this experiment, however, the oxidation is driven by surface water downwelling, which is well-buffered from any drop in pH associated with metal oxidation, due to the moderate to high alkalinity of the field sites and laboratory experimental systems.

Future directions of research & recommendations

In Chapter 2, the implications of effects from riffle location and hyporheic exchange indicate that inclusion of hyporheic flows and bedform location could improve ecological risk assessments. The importance of groundwater-surface water interactions has been directly addressed by the U.S. EPA in a report suggesting the need for increased characterization of groundwater-surface water interactions in contaminated receiving waters (U.S. EPA 2008). Many techniques exist for monitoring hyporheic flows and water chemistry, even in locations without obvious riffle locations. In this experiment we used only minipiezometers and VHG, but other research has paired minipiezometers for porewater and groundwater sampling with time series temperature loggers to assess hyporheic flows over time, which may provide more fine scale VHG differences (Hatch et al. 2006). Alternatively, drive-point piezometers can be installed and sampled on the same day (Winter et al. 1988, Rivett et al. 2008) which allows for monitoring of flows and porewater chemistry sampling at multiple locations.

The effects of hyporheic flows and bedform on geochemistry will also be different for various sources of contaminants (i.e., groundwater) and different types of contaminants (e.g., organics). Each of the experiments in this dissertation assessed potential effects of metals in sediments, though much of the metal contamination associated with hyporheic flows is related to upwelling of metal contaminated groundwater. In other experiments, downwelling hyporheic flows often mitigated effects of metal contaminants in groundwater through dilution by clean surface waters (Brunke and Gonser 1997, Gandy et al. 2007). In assessments of hyporheic (upwelling vs. downwelling) influences on an organic contaminant (chlorobenzenes) from groundwater and sediment sources, sites with upwelling had the most negative effects on aquatic invertebrates (Greenberg et al. 2002). Further investigations into the effects of hyporheic flows on sediment chemistry and biological communities will help to inform management and remediation of contaminated groundwater and sediments.

Future artificial stream experiments could also explore different types of hyporheic flows. To accurately mimic hyporheic flow paths in a low gradient stream like Fleming Creek, a longer flow path and residence time in sediments would be necessary for microbial respiration to remove oxygen from the interstitial water. This type of exposure would require larger experimental systems to maintain realistic hyporheic flow rates (Ren and Packman 2005, Mathers et al. 2014). The experiments in this dissertation assessed effects of oxic hyporheic conditions in the stream mesocosms by comparing them to exposures without hyporheic interactions (surface water influence only). The laboratory exposures are chemically and physically comparable a pool habitat (non-hyporheic) and downwelling zone (hyporheic) in a natural stream. Oxic exposures are important for metals especially, as metal bioavailability can be higher in oxic sediments without reduced sulfide present (Calmano et al. 1993), though this

also depends on the stability of the system and whether sediments are in equilibrium (Costello et al. 2015).

An extension of this research would be to assess the effects of reduced hyporheic flows on metal contaminants and biological effects. A reduced hyporheic exposure would better simulate an upwelling exposure from a natural stream. This could be manipulated by purging hyporheic water with nitrogen gas to reduce the porewater. A reduced upwelling hyporheic input would also decrease the likelihood of the sediment oxidation that was observed in the initial experiment of Chapter 3. Ideally, an experiment could include upwelling (riffle tail feature), downwelling (riffle head feature) and a non-hyporheic treatment (pool feature) to better reflect natural habitats in streams. Using the conceptual model in Figure 5.1, a study would look at both sides of the diagram and add a third "Direction of Flow", which would be the pool habitat. Much research is needed to better understand how the hyporheic zone influences contaminants and their exposure to aquatic ecosystems.

Figures

Figure 5.1. Conceptual diagram of major findings in the dissertation. Chapters and experiments/exposures associated with significant relationships are in italics below chemical and biological endpoints (bold, underlined). Regarding Chapter 2 *in situ* experiment, the tail riffle exposure could have been added to the "Upwelling" side of the flow chart (as opposed to the current flow chart with the head riffle exposure on the "Downwelling" side of the flow chart). Arrows indicate significant relationships between variables.
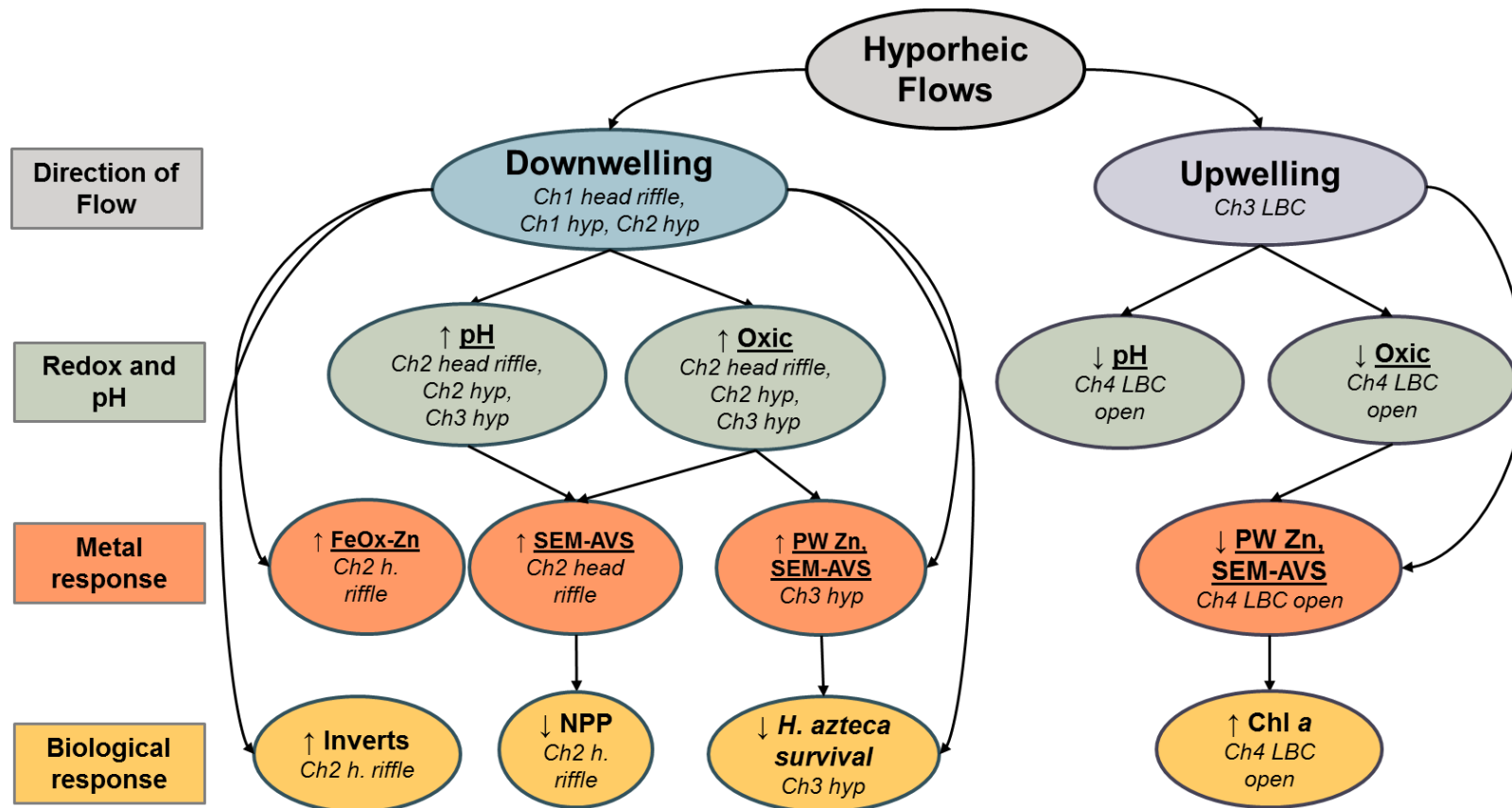
Appendices

Appendix A. Chapter 2 *in situ* experiment benthic macroinvertebrate summary data for each sediment basket (n=50), organized by site, riffle and sediment.

Site	Riffle	Sediment	Abund-ance	Rich-ness	Dominate Taxa	Relative Abund	Chironomid Abund	EPT Abund	Simpson Diversity	Gini-Simpson Diversity	Shannon H Diversity	Even-ness	Sensi-tive
1	Up	FC	85	11	Chironomidae	0.518	44	11	0.305	0.695	1.660	0.692	3
1	Up	Evans	33	11	Oligochaeta	0.273	8	3	0.179	0.821	1.983	0.827	1
1	Up	McGary	22	8	Chironomidae	0.545	12	1	0.331	0.669	1.547	0.744	0
1	Up	Summit	50	8	Chironomidae	0.720	36	3	0.542	0.458	1.032	0.496	1
1	Up	Hoyt	34	5	Chironomidae	0.618	21	0	0.424	0.576	1.165	0.724	0
1	Down	FC	91	10	Chironomidae	0.659	60	5	0.467	0.533	1.216	0.528	1
1	Down	Evans	83	6	Chironomidae	0.723	60	0	0.558	0.442	0.886	0.495	0
1	Down	McGary	61	9	Chironomidae	0.557	34	2	0.393	0.607	1.279	0.582	1
1	Down	Summit	62	7	Chironomidae	0.726	45	0	0.547	0.453	1.002	0.515	0
1	Down	Hoyt	67	4	Chironomidae	0.881	59	1	0.784	0.216	0.454	0.327	1
2	Up	FC	53	14	Chironomidae	0.528	28	11	0.302	0.698	1.829	0.693	3
2	Up	Evans											
2	Up	McGary	64	8	Chironomidae	0.500	32	3	0.313	0.688	1.491	0.717	2
2	Up	Summit	41	10	Chironomidae	0.512	21	3	0.315	0.685	1.588	0.690	2
2	Up	Hoyt	18	5	Chironomidae	0.389	7	6	0.290	0.710	1.382	0.859	0
2	Down	FC	26	4	Chironomidae	0.692	18	0	0.518	0.482	0.917	0.661	0
2	Down	Evans	51	6	Chironomidae	0.667	34	1	0.471	0.529	1.060	0.592	0
2	Down	McGary	38	5	Chironomidae	0.553	21	0	0.398	0.602	1.152	0.715	0
2	Down	Summit	68	6	Chironomidae	0.794	54	1	0.642	0.358	0.804	0.449	1
2	Down	Hoyt	97	7	Oligochaeta	0.567	37	1	0.468	0.532	0.925	0.475	0
3	Up	FC	67	12	Chironomidae	0.672	45	8	0.464	0.536	1.363	0.549	3
3	Up	Evans	121	8	Chironomidae	0.860	104	6	0.743	0.257	0.653	0.314	2
3	Up	McGary	51	9	Chironomidae	0.725	37	4	0.539	0.461	1.118	0.509	1
3	Up	Summit	50	3	Chironomidae	0.940	47	1	0.886	0.114	0.265	0.241	1
3	Up	Hoyt	71	8	Chironomidae	0.831	59	3	0.699	0.301	0.723	0.348	2
3	Down	FC	18	7	Chironomidae	0.556	10	2	0.352	0.648	1.428	0.734	1
3	Down	Evans	124	8	Chironomidae	0.742	92	3	0.568	0.432	0.969	0.466	2
3	Down	McGary	76	8	Chironomidae	0.829	63	0	0.693	0.307	0.762	0.366	1
3	Down	Summit	4	2	Chironomidae	0.750	3	0	0.625	0.375	0.562	0.811	0
3	Down	Hoyt	113	6	Chironomidae	0.867	98	0	0.759	0.241	0.547	0.305	0

4	Up	FC	20	4	Chironomidae	0.750	15	2	0.585	0.415	0.826	0.596	0
4	Up	Evans	27	4	Chironomidae	0.778	21	1	0.630	0.370	0.722	0.521	1
4	Up	McGary											
4	Up	Summit	37	6	Chironomidae	0.838	31	1	0.708	0.292	0.696	0.389	1
4	Up	Hoyt	12	5	Chironomidae	0.667	8	1	0.472	0.528	1.099	0.683	0
4	Down	FC	30	9	Chironomidae	0.500	15	4	0.298	0.702	1.623	0.739	1
4	Down	Evans	15	5	Chironomidae	0.667	10	2	0.476	0.524	1.081	0.671	2
4	Down	McGary	13	3	Chironomidae	0.615	8	0	0.456	0.544	0.925	0.842	0
4	Down	Summit	30	4	Chironomidae	0.900	27	1	0.813	0.187	0.435	0.314	1
4	Down	Hoyt	19	4	Chironomidae	0.842	16	2	0.717	0.283	0.610	0.440	0
5	Up	FC	73	11	Chironomidae	0.425	31	23	0.231	0.769	1.855	0.774	3
5	Up	Evans	27	5	Chironomidae	0.778	21	3	0.621	0.379	0.806	0.501	1
5	Up	McGary	65	11	Chironomidae	0.677	44	8	0.473	0.527	1.310	0.546	3
5	Up	Summit	18	5	Chironomidae	0.778	14	2	0.617	0.383	0.838	0.521	1
5	Up	Hoyt	89	8	Chironomidae	0.831	74	4	0.701	0.299	0.707	0.340	1
5	Down	FC	115	11	Chironomidae	0.748	86	10	0.556	0.444	1.127	0.470	3
5	Down	Evans	48	6	Chironomidae	0.813	39	1	0.673	0.327	0.727	0.406	0
5	Down	McGary	128	8	Chironomidae	0.828	106	3	0.695	0.305	0.726	0.349	2
5	Down	Summit	119	11	Chironomidae	0.765	91	10	0.595	0.405	1.011	0.422	3
5	Down	Hoyt	104	5	Chironomidae	0.923	96	2	0.854	0.146	0.364	0.226	0

Note: Evans = LBC-1, McGary = LBC-4, Summit = LBC-2, Hoyt = LBC-3.

Appendix B. Chapter 2 *in situ* experiment biofilm Net Primary Productivity (NPP) and Chlorophyll (Chl a).

Site	Sediment	Riffle	Depth (mm)	NPP (mg $O_2m^{-2}h^{-1}$)	Chla (mg/m²)	Biomass (g)
1	FC	Up	2.0	24.43	90.134	0.0787
1	Evans	Up	0.5	68.69	202.376	0.0599
1	McGary	Up	1.0	15.63	125.847	0.1065
1	Summit	Up	1.0	18.66	82.481	0.0930
1	Hoyt	Up	1.0	30.25	17.006	0.0969
1	FC	Down	0.5	20.94	0.850	0.0319
1	Evans	Down	1.0	22.69	23.809	0.0970
1	McGary	Down	1.0	46.72	50.169	0.1307
1	Summit	Down	1.0	28.37	62.073	0.1362
1	Hoyt	Down	2.0	23.61	18.707	0.0887
2	FC	Up	0.5	71.13	246.592	0.1372
2	Evans	Up	2.0	16.95	216.831	0.1495
2	McGary	Up	1.0	53.73	260.197	0.1424
2	Summit	Up	2.0	34.79	34.013	0.1253
2	Hoyt	Up	1.0	7.59	9.354	0.0783
2	FC	Down	1.0	44.06	153.057	0.1081
2	Evans	Down	1.0	56.60	156.459	0.1152
2	McGary	Down	0.0	40.53	157.309	0.0791
2	Summit	Down	1.0	43.26	130.099	0.1028
2	Hoyt	Down	1.0	23.16	28.061	0.0592
3	FC	Up	0.0	15.01	28.911	0.0657
3	Evans	Up	0.5	102.56	210.879	0.1420
3	McGary	Up	1.0	99.50	229.586	0.1511
3	Summit	Up	1.0	65.29	221.933	0.1403
3	Hoyt	Up	1.0	42.05	214.280	0.1168
3	FC	Down	2.0	91.56	34.863	0.3463
3	Evans	Down	1.0	118.56	267.000	0.2577
3	McGary	Down	1.0	74.44	133.500	0.1746
3	Summit	Down	1.0	96.36	199.825	0.1713
3	Hoyt	Down	1.0	91.20	231.287	0.3006
4	FC	Up	1.0	44.63	141.153	0.1415
4	Evans	Up	1.0	59.60	157.309	0.1149
4	McGary	Up	0.5	26.84	61.223	0.0799
4	Summit	Up	1.0	51.96	187.920	0.1215
4	Hoyt	Up	1.0	79.84	198.975	0.1131
4	FC	Down	0.5	53.74	196.424	0.1469
4	Evans	Down	2.0	57.00	176.866	0.1851

4	McGary	Down	0.5	52.12	98.637	0.1101
4	Summit	Down	0.5	42.81	129.248	0.0950
4	Hoyt	Down	1.0	18.46	265.299	0.1882
5	FC	Up	0.5	53.73	113.092	0.1608
5	Evans	Up	0.5	33.05	58.672	0.1640
5	McGary	Up	0.5	8.21	117.344	0.1333
5	Summit	Up	0.5	40.06	76.529	0.5594
5	Hoyt	Up	0.5	44.96	75.678	0.0610
5	FC	Down	0.5	37.66	59.522	0.0972
5	Evans	Down	2.0	10.74	14.455	0.1130
5	McGary	Down	0.5	38.63	90.984	0.1035
5	Summit	Down	0.5	10.08	167.513	0.0000
5	Hoyt	Down	0.5	40.97	100.338	0.1099
Blank1						1.701
Blank2						0.850
Blank3						2.551
Blank4						-1.701
Blank5						0.000

Note: Evans = LBC-1, McGary = LBC-4, Summit = LBC-2, Hoyt = LBC-3.

Appendix C. Chapter 2 *in situ* experiment sediment chemistry (total Zn, Fe, Mn, AVS, SEM, *f*OC).

Site	Sediment	Riffle	*f*OC	Total metals			(SEM-AVS)/*f*OC		
				Zn (mg/kg)	Fe (g/kg)	Mn (mg/kg)	AVS (umol /g)	SEM-Zn (umol /g)	SEM-AVS /*f*OC
1	FC	UP	0.013	18.345	3.965	123.958	0.009	0.042	2.457
1	EVANS	UP	0.016	22.364	7.763	157.915	0.470	0.072	-25.152
1	MCGARY	UP	0.011	80.893	2.457	174.260	0.236	0.562	29.350
1	SUMMIT	UP	0.010	77.600	6.546	268.768	0.407	0.755	34.151
1	HOYT	UP	0.012	47.154	4.010	164.558	0.372	0.270	-8.500
1	FC	DOWN	0.013	17.285	5.373	294.375	0.034	0.044	0.749
1	EVANS	DOWN	0.012	13.057	5.540	69.145	0.408	0.034	-32.463
1	MCGARY	DOWN	0.008	94.748	2.400	127.548	0.131	0.518	45.526
1	SUMMIT	DOWN	0.014	94.113	6.274	247.785	0.410	0.601	13.654
1	HOYT	DOWN	0.009	40.370	2.459	80.323	0.093	0.318	24.912
2	FC	UP	0.010	14.881	3.812	142.628	0.019	0.031	1.212
2	EVANS	UP	0.052	38.841	18.406	1173.188	0.038	0.120	1.568
2	MCGARY	UP	0.010	68.736	5.577	544.070	0.147	0.457	30.305
2	SUMMIT	UP	0.006	70.400	6.301	306.672	0.827	0.663	-26.704
2	HOYT	UP	0.007	33.771	3.081	241.431	0.074	0.240	24.345
2	FC	DOWN	0.011	17.844	5.500	286.354	0.046	0.036	-0.961
2	EVANS	DOWN	0.008	12.672	5.596	45.077	0.391	0.064	-39.777
2	MCGARY	DOWN	0.010	75.936	2.927	155.995	0.440	0.620	18.119
2	SUMMIT	DOWN	0.006	98.953	5.997	175.868	0.370	0.437	10.591
2	HOYT	DOWN	0.008	48.075	3.535	128.731	0.275		
3	FC	UP	0.008	16.693	4.568	224.067	0.007	0.033	3.428
3	EVANS	UP	0.010	18.226	7.440	78.807	0.358	0.039	-30.876
3	MCGARY	UP	0.009	52.797	3.195	208.139	0.193	0.360	17.823
3	SUMMIT	UP	0.011	29.336	6.466	362.196	0.074	0.098	2.180
3	HOYT	UP	0.008	26.441	3.180	140.691	0.042		
3	FC	DOWN	0.008	17.757	3.852	119.300	0.128	0.000	-15.831
3	EVANS	DOWN	0.007	12.488	5.397	69.245	0.179	0.000	-26.805
3	MCGARY	DOWN	0.010	64.151	3.814	143.896	2.298	1.560	-76.193
3	SUMMIT	DOWN	0.006	51.094	3.661	89.020	0.501	0.553	9.113
3	HOYT	DOWN	0.007	39.104	2.100	46.774			
4	FC	UP	0.022	22.153	5.836	256.212	0.345	0.078	-12.088
4	EVANS	UP	0.016	19.830	8.464	95.879	0.392	0.066	-19.969
4	MCGARY	UP	0.012	64.615	2.399	90.367	0.173	0.487	25.295
4	SUMMIT	UP	0.010	60.409	7.812	299.099	0.852	1.115	27.619
4	HOYT	UP	0.013	39.157	2.300	88.625			
4	FC	DOWN	0.011	19.716	5.625	286.189	0.017	0.000	-1.559

4	EVANS	DOWN	0.007	16.904	5.155	36.474	0.028	0.068	6.009
4	MCGARY	DOWN	0.009	17.810	6.258	66.136	0.075	0.107	3.716
4	SUMMIT	DOWN	0.013	53.436	4.029	159.754	0.368	0.362	-0.460
4	HOYT	DOWN	0.005	32.023	1.435	39.947			
5	FC	UP	0.014	21.366	6.554	224.723	0.031	0.039	0.536
5	EVANS	UP	0.010	16.062	5.061	83.133	0.017	0.057	3.817
5	MCGARY	UP	0.020	44.163	4.240	246.280	0.124	0.494	18.149
5	SUMMIT	UP	0.022	62.008	6.030	264.344	0.242	0.335	4.179
5	HOYT	UP		50.192	5.854	262.663			
5	FC	DOWN	0.023	19.843	5.991	466.222	0.061	0.000	-2.652
5	EVANS	DOWN	0.010	14.344	6.300	98.990	0.041	0.074	3.240
5	MCGARY	DOWN	0.011	65.016	2.858	140.396	0.168	0.554	34.818
5	SUMMIT	DOWN	0.010	52.058	4.227	243.413	0.112	0.249	13.586
5	HOYT	DOWN	0.009	32.333	2.787	125.868			
initial	FC		0.008	18.700	4.176	120.440	0.781	0.064	-95.297
initial	EVANS		0.009	12.434	5.731	33.748	0.827	0.065	-89.241
initial	MCGARY		0.019	161.770	3.390	238.494	1.913	1.068	-45.132
initial	SUMMIT		0.013	59.811	4.815	417.519	1.043	0.871	-13.114
initial	HOYT		0.011	46.324	1.816	28.199	0.372	0.381	0.851
initial	HOYT		0.011	46.324	1.816	28.199	0.402	0.347	-5.000

^fOC – fraction of organic carbon in sediment
Note: Evans = LBC-1, McGary = LBC-4, Summit = LBC-2, Hoyt = LBC-3.

Appendix D. Chapter 2 *in situ* experiment porewater chemistry, collected from porous stone in sediment basket (Zn, Mn, Fe, Fe^{2+}, pH). Filtered on 0.45-micron syringe filter.

Site	Sediment	Riffle	Zn (µg/L)	Mn (µg/L)	Fe (mg/L)	Ferrozine (Fe^{2+} mg/L)	pH	Temp (ºC)
1	FC	UP	0.278	0.000	0.000	0.000	7.8	15.5
1	EVANS	UP	0.000	180.208	0.376	0.036		
1	MCGARY	UP	13.585	0.000	0.058	0.063	7.84	14.2
1	SUMMIT	UP	9.614	0.000	0.000	0.009	7.91	14.3
1	HOYT	UP	19.666	0.000	0.000	0.018	8.01	15.1
1	FC	DOWN	0.329	356.799	0.399	0.054	7.79	18.2
1	EVANS	DOWN	0.000	918.814	14.531	4.913	7.54	19
1	MCGARY	DOWN	27.619	140.308	1.922	1.022	7.75	17
1	SUMMIT	DOWN	3.115	0.000	0.000	0.009	7.92	15.9
1	HOYT	DOWN	16.361	0.000	0.000	0.018	7.94	15.5
2	FC	UP	2.077	0.000	0.017	0.018	8.05	18.5
2	EVANS	UP						
2	MCGARY	UP						
2	SUMMIT	UP						
2	HOYT	UP						
2	FC	DOWN	1.612	28.650	0.018	0.090	8.01	17.7
2	EVANS	DOWN	0.000	758.733	12.332	4.524	7.6	17.4
2	MCGARY	DOWN	60.885	50.497	0.656	0.362	7.79	15.3
2	SUMMIT	DOWN	2.762	435.696	1.352	0.905	7.77	15
2	HOYT	DOWN	16.989	1114.312	1.303	1.176	7.58	15.5
3	FC	UP	0.284	0.000	0.000	0.090	7.81	13.3
3	EVANS	UP	0.000	757.577	11.752	6.605	7.54	13.6
3	MCGARY	UP	6.121	37.955	0.782	0.543	7.67	13.4
3	SUMMIT	UP	119.525	0.000	0.000	0.090	7.75	13
3	HOYT	UP	24.455	0.000	0.000	0.181	7.8	13.1
3	FC	DOWN	2.780	458.279	1.612	1.357	7.11	13.1
3	EVANS	DOWN	0.000	514.876	9.778	9.229	7.32	14.5
3	MCGARY	DOWN	182.598	263.532	5.412	5.067	7.17	12.5
3	SUMMIT	DOWN	5.103	181.194	5.194	5.157	7.15	11.7
3	HOYT	DOWN	1.912	0.000	0.179	0.000	7.56	13.7
4	FC	UP	5.906	2385.942	6.143	1.728	7.71	13.4
4	EVANS	UP	13.190	230.419	2.766	0.661	7.93	11.3
4	MCGARY	UP						
4	SUMMIT	UP	25.329	3.819	0.028	0.018	8.04	10.5
4	HOYT	UP	19.720	0.000	0.000	0.018	8.05	12.2
4	FC	DOWN	8.790	1615.897	0.273	0.045	8.07	14.7
4	EVANS	DOWN	0.000	272.355	9.957	6.406	7.73	10.2
4	MCGARY	DOWN	30.314	91.886	1.309	0.941	7.86	10.1
4	SUMMIT	DOWN	10.736	326.105	0.266	0.090	8.01	10.8

4	HOYT	DOWN	12.788	0.000	0.000	0.018	8.05	10.6
5	FC	UP	16.151	40.476	0.023	0.018	7.91	11.4
5	EVANS	UP	2.143	0.000	0.021	0.027	7.93	9.8
5	MCGARY	UP	42.894	36.271	0.740	0.534	7.88	9.4
5	SUMMIT	UP	13.795	0.000	0.000	0.018	7.93	9.3
5	HOYT	UP	25.870	12.103	0.000	0.018	7.9	9.8
5	FC	DOWN	0.000	149.392	0.530	0.217	7.5	10.6
5	EVANS	DOWN	0.000	46.293	1.166	0.290	7.59	14.4
5	MCGARY	DOWN	0.000	176.926	3.427	2.877	7.48	10.8
5	SUMMIT	DOWN	79.864	10.517	0.021	0.027	7.69	10.3
5	HOYT	DOWN	9.600	0.000	0.037	0.036	7.76	11.8

Note: Evans = LBC-1, McGary = LBC-4, Summit = LBC-2, Hoyt = LBC-3.

Appendix E. Chapter 2 *in situ* experiment minipiezometers data, vertical hydraulic gradient (VHG).

Site	Riffle	Depth	VHG_1	VHG_2	VHG_Ave	Notes
5	Down	5	-0.008	x	-0.008	(2) tubing cut
5	Down	10	0.166	x	0.166	(2) tubing cut
5	Down	15	0.164	x	0.164	(2) tubing cut
5	Up	5	1.472	x	1.472	(2) tubing cut
5	Up	10	0.116	x	0.116	(2) tubing cut
5	Up	15	0.111	x	0.111	(2) tubing cut
5	Up	20	0.118	0.093	0.106	(2) tubing cut
4	Down	5	x	x		All tubing cut, no data
4	Down	10	x	x		All tubing cut, no data
4	Down	15	x	x		All tubing cut, no data
4	Down	20	x	x		All tubing cut, no data
4	Up	5	0.472	x	0.472	
4	Up	10	0.266	0.226	0.246	
4	Up	20	0.088	-0.017	0.035	
3	Down	5	-0.048	x	-0.048	
3	Down	10	0.036	0.096	0.066	
3	Down	20	0.058	0.128	0.093	
3	Up	5	0.092	x	0.092	
3	Up	10	0.216	0.506	0.361	
3	Up	20	0.083	0.338	0.211	
2	Down	5	0.272	x	0.272	
2	Down	10	0.376	0.656	0.516	
2	Down	15	0.411	x	0.411	
2	Down	20	1.388	1.503	1.446	
2	Up	5	0.272	x	0.272	
2	Up	10	0.326	0.306	0.316	
2	Up	20	0.093	0.173	0.133	
1	Down	5	0.472	0.572	0.522	out of the water??
1	Down	10	-0.084	x	-0.084	(2) tubing cut
1	Down	15	-0.036	x	-0.036	(2) tubing cut
1	Down	20	x	x		(1) tubing cut
1	Up	5	0.072	x	0.072	
1	Up	10	0.076	0.066	0.071	
1	Up	15	0.011	x	0.011	
1	Up	20	-0.017	0.063	0.023	

Appendix F. Chapter 2 artificial stream (flume) experiment porewater chemistry (Zn, Mn, Fe, Fe^{2+}, pH, dissolved oxygen and Eh).

Flume	Basket	Sediment	Hyporheic	Day	Zn (µg/L)	Mn (µg/L)	Fe (mg/L)	Ferrozine Fe^{2+} (mg/L)	pH	DO (mg/L)	Eh (mV)
3	A	LBC-1	Y	d1	0.555	291.412	1.644		7.72	6.63	-73
3	B	LBC-1	Y	d1	0.000	266.475	2.975		7.76	6.37	-67.7
4	A	LBC-1	N	d1	0.000	733.946	3.261		7.66	6.8	-101.5
4	B	LBC-1	N	d1	0.520	366.681	4.834		7.65	6.38	-84.9
5	A	LBC-2	N	d1	0.000	5113.674	6.754		7.51	5.08	-101.1
5	B	LBC-2	N	d1	2.055	4208.412	10.696		7.51	4.82	-69.5
6	A	LBC-2	Y	d1	13.396	358.850	0.309		7.48	4.06	-62
6	B	LBC-2	Y	d1	0.000	1775.186	2.361		7.5	4.37	-55.8
7	A	LBC-1	Y	d1	0.000	531.768	2.606		7.84	6.47	-62.8
7	B	LBC-1	Y	d1	0.000	535.149	4.515		7.89	6.32	-73.7
8	A	LBC-1	N	d1	88.977	966.343	4.321		7.53	6.29	-72.5
8	B	LBC-1	N	d1	0.588	1201.914	6.337		7.4	5.96	-69.7
9	A	LBC-2	N	d1	87.238	5434.956	3.341		7.42	4.54	-92.6
9	B	LBC-2	N	d1	0.462	4439.134	10.136		7.45	5.05	-84.1
10	A	LBC-2	Y	d1	120.401	1505.606	1.034		7.75	5.9	-78.1
10	B	LBC-2	Y	d1	0.000	2138.570	3.987		7.63	6.11	-77.3
11	A	LBC-1	Y	d1	0.003	409.343	4.662		7.83	6	-73.1
11	B	LBC-1	Y	d1	0.000	661.308	4.356		7.64	5.66	-81.5
12	A	LBC-1	N	d1	0.000	1122.072	6.609		7.53	5.48	-84.3
12	B	LBC-1	N	d1	0.778	1666.103	7.101		7.43	5.87	-47.4
13	A	LBC-2	Y	d1	0.125	1962.991	2.124		7.4	4.9	-78.9
13	B	LBC-2	Y	d1	3.204	1457.494	3.339		7.55	5.14	-82.3
14	A	LBC-2	N	d1	2.592	6090.816	17.639		7.34	4.97	-67.9
14	B	LBC-2	N	d1	1.070	8157.143	13.886		7.42	5.87	-74.3
3	A	LBC-1	Y	d3	0.000	326.821	2.869	1.091	7.23	6.1	-57.2
3	B	LBC-1	Y	d3	0.000	320.018	4.100	1.389	7.29	6.82	-54.7
4	A	LBC-1	N	d3	0.000	730.330	4.490	2.858	7.2	6.34	-40.6

4	B	LBC-1	N	d3	0.000	354.428	6.070	3.274	7.26	6.38	-42.3
5	A	LBC-2	N	d3	0.000	4686.383	8.272	6.737	7.4	7.05	-24.8
5	B	LBC-2	N	d3	0.000	3784.102	11.383	10.201	7.39	6.71	-41.5
6	A	LBC-2	Y	d3	2.019	232.046	0.351	0.109	7.32	5.51	-61.1
6	B	LBC-2	Y	d3	0.000	2457.253	3.421	3.403	7.28	5.3	-60.9
7	A	LBC-1	Y	d3	0.000	597.943	4.017	3.870	7.36	6.59	-41.5
7	B	LBC-1	Y	d3	0.000	656.545	6.269	4.902	7.33	6.48	-36.9
8	A	LBC-1	N	d3	18.589	991.825	5.518	3.314	7.24	6.49	-43.2
8	B	LBC-1	N	d3	0.000	1188.785	6.442	3.493	7.19	5.94	-58.1
9	A	LBC-2	N	d3	19.470	4443.732	4.056	2.262	7.28	6.18	-62.3
9	B	LBC-2	N	d3	0.000	4413.405	10.850	6.152	7.38	6.06	-62.8
10	A	LBC-2	Y	d3	11.888	935.604	0.823	0.516	7.59	6.43	-44.5
10	B	LBC-2	Y	d3	0.000	770.630	1.279	1.250	7.65	6.01	-40.9
11	A	LBC-1	Y	d3	0.000	491.181	6.629	2.877	7.41	5.76	-57
11	B	LBC-1	Y	d3	0.000	729.761	5.586	3.195	7.37	5.87	-57
12	A	LBC-1	N	d3	0.000	1143.078	7.895	6.400	7.27	5.95	-66
12	B	LBC-1	N	d3	0.000	1677.847	8.579	8.186	7.28	5.14	-76
13	A	LBC-2	Y	d3	0.000	1460.646	3.910	3.195	7.59	5.27	-80.6
13	B	LBC-2	Y	d3	0.000	1482.821	4.268	2.867	7.56	5.54	-71.5
14	A	LBC-2	N	d3	6.086	4921.255	16.203	13.674	7.34	4.78	-69.7
14	B	LBC-2	N	d3	0.000	6098.242	13.133	11.173	7.32	4.31	-89.8
3	A	LBC-1	Y	d5	0.000	281.734	3.635	2.398	6.72	7.55	8.7
3	B	LBC-1	Y	d5	0.000	379.572	5.262	3.184	6.81	7.1	-9.7
4	A	LBC-1	N	d5	0.000	752.803	5.536	4.694	7.07	6.87	-35.4
4	B	LBC-1	N	d5	0.000	347.065	6.789	4.477	7.19	6.6	-37.2
5	A	LBC-2	N	d5	0.000	4710.612	9.079	4.301	7.38	6.92	-39.8
5	B	LBC-2	N	d5	0.000	3484.678	10.428	5.191	7.35	5.63	-53.6
6	A	LBC-2	Y	d5	0.000	73.659	0.330	0.000	7.29	4.68	-71.9
6	B	LBC-2	Y	d5	0.000	2782.062	4.278	2.398	7.13	4.64	-79.5
7	A	LBC-1	Y	d5	0.000	675.217	5.167	3.432	7.29	4.92	-78.1
7	B	LBC-1	Y	d5	0.000	363.539	3.823	2.760	7.25	4.75	-75.6

8	A	LBC-1	N	d5	18.138	1103.377	6.879	3.960	7.18	6.72	-7
8	B	LBC-1	N	d5	0.000	1251.180	7.341	4.115	7.09	6.13	-55.1
9	A	LBC-2	N	d5	14.534	4804.095	5.041	2.542	7.23	4.96	-73.3
9	B	LBC-2	N	d5	0.000	4301.833	10.963	6.401	7.28	5.04	-74.3
10	A	LBC-2	Y	d5	11.499	332.418	0.396	0.122	7.62	5.32	-73.6
10	B	LBC-2	Y	d5	0.000	949.114	2.224	1.311	7.55	5.29	-56.9
11	A	LBC-1	Y	d5	4.205	579.571	8.116	2.439	7.16	4.94	-83.9
11	B	LBC-1	Y	d5	0.000	757.464	6.469	1.756	7.23	5.15	-81.1
12	A	LBC-1	N	d5	0.000	1160.508	8.615	5.108	7.19	5.24	-90.5
12	B	LBC-1	N	d5	0.000	1643.521	9.263	7.819	7.26	4.48	-91.5
13	A	LBC-2	Y	d5	0.000	1865.265	6.165	3.008	7.24	4.94	-54.3
13	B	LBC-2	Y	d5	0.000	1574.437	5.245	1.508	7.2	4.69	-51.8
14	A	LBC-2	N	d5	0.000	4914.408	17.440	8.274	7.11	3.55	-79.6
14	B	LBC-2	N	d5	0.000	5847.714	12.776	7.291	7.26	3.3	-97.2
3	A	LBC-1	Y	d7	4.472	274.726	3.738	5.853	7.3	6.03	-57.4
3	B	LBC-1	Y	d7	12.046	3713.315	10.991	6.018	7.22	5.33	-77.7
4	A	LBC-1	N	d7	1.974	762.507	6.669	5.211	7.29	5.44	-77.4
4	B	LBC-1	N	d7	2.900	352.621	7.862	3.887	7.34	5.09	-73.6
5	A	LBC-2	N	d7	1.920	4580.930	9.450	2.687	7.46	5.2	-72.1
5	B	LBC-2	N	d7	2.700	3980.397	10.952	7.404	7.39	5.12	-72.3
6	A	LBC-2	Y	d7	0.000	71.801	0.253	0.000	7.44	4.45	-73.4
6	B	LBC-2	Y	d7	0.000	2485.552	4.199	3.629	7.36	4.48	-73.9
7	A	LBC-1	Y	d7	0.353	707.647	6.353	2.781	7.39	4.53	-79.1
7	B	LBC-1	Y	d7	3.078	300.481	3.799	2.346	7.32	4.51	-77.6
8	A	LBC-1	N	d7	43.568	1019.467	7.113	3.918	7.4	5.43	-68.6
8	B	LBC-1	N	d7	3.992	1312.493	8.315	5.873	7.24	4.84	-70.5
9	A	LBC-2	N	d7	15.595	5115.633	6.152	4.715	7.31	4.35	-76.5
9	B	LBC-2	N	d7	0.623	4161.144	11.085	10.332	7.41	4.51	-73.2
10	A	LBC-2	Y	d7	12.983	610.008	0.986	0.670	7.68	4.92	-70.6
10	B	LBC-2	Y	d7	0.535	729.667	2.621	2.056	7.61	5.26	-64
11	A	LBC-1	Y	d7	1.987	594.255	8.594	1.912	7.21	4.96	-46.1

11	B	LBC-1	Y	d7	4.727	750.661	6.202	1.156	7.24	5.08	-53
12	A	LBC-1	N	d7	1.053	1144.907	9.234	3.732	7.24	4.92	-66
12	B	LBC-1	N	d7	8.669	1666.555	10.256	8.718	7.28	4.49	-63.4
13	A	LBC-2	Y	d7	0.000	2218.186	8.499	5.770	7.41	4.6	-63
13	B	LBC-2	Y	d7				3.349	7.4	4.17	-51.5
14	A	LBC-2	N	d7	8.522	4892.164	17.154	13.797	7.29	3.32	-59.7
14	B	LBC-2	N	d7	0.000	5533.670	12.714	9.990	7.32	3.21	-79.9
3	A	LBC-1	Y	d13	0.023	209.076	5.565	3.243	7.25		
3	B	LBC-1	Y	d13	0.024	502.396	9.122	5.014	7.17		
4	A	LBC-1	N	d13	0.030	816.540	9.946	5.200	7.12		
4	B	LBC-1	N	d13	0.026	240.305	7.454	3.243	7.14		
5	A	LBC-2	N	d13	0.025	4150.502	10.031	5.293	7.16		
5	B	LBC-2	N	d13	0.023	3662.600	11.227	5.387	7.25		
6	A	LBC-2	Y	d13	0.020	28.203	0.137	0.000	7.26		
6	B	LBC-2	Y	d13	0.027	2233.918	4.905	2.590	7.26		
7	A	LBC-1	Y	d13	0.025	711.343	8.543	5.666	7.27		
7	B	LBC-1	Y	d13	0.023	386.066	5.845	4.548	7.28		
8	A	LBC-1	N	d13	0.043	1162.280	10.426	6.971	7.11		
8	B	LBC-1	N	d13	0.027	1489.770	11.409	7.251	7.13		
9	A	LBC-2	N	d13	0.035	4237.329	7.323	5.014	7.08		
9	B	LBC-2	N	d13	0.023	4340.294	12.843	9.861	7.13		
10	A	LBC-2	Y	d13	0.026	236.860	0.981	0.539	7.64		
10	B	LBC-2	Y	d13	0.022	1088.229	4.940	1.658	7.66		
11	A	LBC-1	Y	d13	0.022	721.990	11.904	3.802	7.39		
11	B	LBC-1	Y	d13	0.023	798.802	8.613	5.014	7.33		
12	A	LBC-1	N	d13	0.025	1226.064	11.648	6.878	7.26		
12	B	LBC-1	N	d13	0.028	1470.687	11.520	7.344	7.26		
13	A	LBC-2	Y	d13	0.023	3072.397	14.935	9.208	7.34		
13	B	LBC-2	Y	d13	0.023	2214.773	8.495	3.895	7.38		
14	A	LBC-2	N	d13	0.025	4236.331	16.525	9.954	7.3		
14	B	LBC-2	N	d13	0.021	5232.336	13.451	7.158	7.31		

3	A	LBC-1	Y	d15	0.028	243.324	6.376	0.353	7.28
3	B	LBC-1	Y	d15	0.022	513.129	9.781	0.539	7.22
4	A	LBC-1	N	d15	0.027	757.331	10.112	0.632	7.14
4	B	LBC-1	N	d15	0.028	255.182	9.499	0.297	7.2
5	A	LBC-2	N	d15	0.022	4153.160	10.653		7.25
5	B	LBC-2	N	d15	0.022	3495.661	11.290	0.502	7.36
6	A	LBC-2	Y	d15	0.020	31.443	0.116	0.000	7.37
6	B	LBC-2	Y	d15	0.022	2360.866	5.428	0.157	7.37
7	A	LBC-1	Y	d15	0.022	752.554	9.189	0.399	7.22
7	B	LBC-1	Y	d15	0.024	432.632	6.692	0.465	7.26
8	A	LBC-1	N	d15	0.037	1243.191	11.620	1.257	7.3
8	B	LBC-1	N	d15	0.024	1521.659	12.093	1.723	7.3
9	A	LBC-2	N	d15	0.029	4687.045	8.437	1.490	7.25
9	B	LBC-2	N	d15	0.023	4429.653	13.059	3.597	7.32
10	A	LBC-2	Y	d15	0.027	201.928	1.020	0.036	7.42
10	B	LBC-2	Y	d15	0.022	1246.894	5.930	0.604	7.47
11	A	LBC-1	Y	d15	0.023	735.445	12.279	0.759	7.38
11	B	LBC-1	Y	d15	0.021	784.806	8.467	1.033	7.38
12	A	LBC-1	N	d15	0.021	1146.751	11.061	2.124	7.3
12	B	LBC-1	N	d15	0.022	1024.844	9.386	3.112	7.3
13	A	LBC-2	Y	d15	0.024	3259.462	15.321	6.300	7.22
13	B	LBC-2	Y	d15	0.023	2313.415	8.832	1.732	7.28
14	A	LBC-2	N	d15	0.029	4105.437	15.756	5.461	7.24
14	B	LBC-2	N	d15	0.023	5232.216	13.103	4.920	7.26
3	A	LBC-1	Y	d25	0.023	173.551	6.317	5.144	7.02
3	B	LBC-1	Y	d25	0.021	94.266	2.424	10.364	6.94
4	A	LBC-1	N	d25	0.022	654.533	10.276	7.596	6.87
4	B	LBC-1	N	d25	0.021	341.074	11.165	2.040	6.85
5	A	LBC-2	N	d25	0.022	4053.814	12.148	9.675	6.91
5	B	LBC-2	N	d25	0.025	3791.758	13.238	11.343	6.98
6	A	LBC-2	Y	d25	0.023	21.045	0.038	4.005	7.06

6	B	LBC-2	Y	d25	0.023	1635.146	5.334	0.000	7.09
7	A	LBC-1	Y	d25	0.022	544.464	8.118	8.090	7.16
7	B	LBC-1	Y	d25	0.022	414.735	7.016	7.167	7.17
8	A	LBC-1	N	d25	0.031	1308.054	14.196	14.354	7.16
8	B	LBC-1	N	d25	0.024	1591.088	15.187	12.900	7.11
9	A	LBC-2	N	d25	0.030	3115.465	6.504	5.927	7.12
9	B	LBC-2	N	d25	0.023	4505.027	14.812	14.298	7.17
10	A	LBC-2	Y	d25	0.028	176.143	0.611	0.530	7.14
10	B	LBC-2	Y	d25	0.022	479.966	3.050	2.618	7.2
11	A	LBC-1	Y	d25	0.025	499.915	9.641	8.770	7.11
11	B	LBC-1	Y	d25	0.022	139.715	1.861	1.546	7.18
12	A	LBC-1	N	d25	0.023	1091.392	11.996	12.061	7.07
12	B	LBC-1	N	d25	0.028	733.449	10.205	10.150	7.05
13	A	LBC-2	Y	d25	0.024	482.308	0.684	0.716	7.04
13	B	LBC-2	Y	d25	0.023	1583.553	6.976	6.822	7.06
14	A	LBC-2	N	d25	0.027	4320.674	18.099	16.228	7.03
14	B	LBC-2	N	d25	0.023	5113.510	14.345	13.012	7.03

Note: LBC-1 = Evans and LBC-2 = Summit

Appendix G. Chapter 2 artificial stream experiment sediment chemistry (total Zn, Fe, Mn, dw/ww, S^{2-}, AVS, SEM-Zn, fOC).

Sediment	Flume	Hypo-rheic	Day	fOC^	Zn (mg/kg)	Fe (g/kg)	Mn (mg/kg)	dw/ ww*	S^{2-} (umol)	AVS dw* (umol/g)	Zn dw* (ug/g)	Zn dw* (umol/g)	SEM-AVS /fOC
LBC-1	initial		0	0.0163	16.733	8.083	49.223	0.670	1.680	0.722	8.420	0.129	-36.285
LBC-1	initial		0	0.0088	8.779	3.283	14.678	0.784	0.664	0.271	1.064	0.016	-28.820
LBC-1	initial		0	0.0018	7.317	1.964	8.077	0.787	0.895	0.320	-0.128	-0.002	-176.265
LBC-1	initial		0	0.0039	10.790	4.263	21.612	0.773	0.110	0.041	0.404	0.006	-8.978
LBC-3	initial		0	0.0032	47.865	4.832	125.111	0.777					
LBC-3	initial		0	0.0062	65.281	2.945	62.157	0.778					
LBC-2	initial		0	0.0125	96.340	7.897	291.804	0.766					
LBC-2	initial		0	0.0064	190.947	14.208	455.999	0.775	2.214	0.828	70.859	1.084	39.719
LBC-1	3	Y	25	0.0048	9.634	8.800	58.050	0.785	1.191	0.490	2.491	0.038	-94.535
LBC-1	3	Y	25	0.0077	16.098	7.065	59.676	0.744	2.590	1.057	4.067	0.062	-129.496
LBC-1	4	N	25	0.0057	7.526	5.487	53.850	0.752	0.224	0.089	1.857	0.028	-10.659
LBC-1	4	N	25	0.0042	10.095	4.679	36.026	0.766	0.186	0.057	1.934	0.030	-6.544
LBC-2	5	N	25	0.0110	65.025	4.104	186.881	0.766	5.130	1.710	34.793	0.532	-107.479
LBC-2	5	N	25	0.0115	71.986	7.185	231.259	0.766	4.322	1.366	56.223	0.860	-44.057
LBC-2	6	Y	25	0.0105	88.938	6.312	162.354	0.760	2.044	0.707	39.046	0.597	-10.455
LBC-2	6	Y	25	0.0132	92.927	11.863	620.222	0.758	4.322	1.791	43.493	0.665	-85.486
LBC-1	7	Y	25	0.0062	14.089	5.121	83.989	0.746	0.125	0.050	6.317	0.097	7.518
LBC-1	7	Y	25	0.0052	17.715	10.005	62.257	0.764	0.349	0.129	3.979	0.061	-13.214
LBC-1	8	N	25	0.0036	11.086	4.397	32.835	0.801	0.550	0.183	1.930	0.030	-42.091
LBC-1	8	N	25	0.0046	8.920	4.862	47.869	0.763	0.739	0.262	2.906	0.044	-47.531
LBC-2	9	N	25	0.0170	103.674	7.700	331.462	0.748	1.915	0.659	54.824	0.838	10.527
LBC-2	9	N	25	0.0120	79.784	9.171	172.809	0.757	1.490	0.587	49.754	0.761	14.547
LBC-2	10	Y	25	0.0098	68.896	5.696	345.771	0.772	2.203	0.938	113.820	1.741	81.748
LBC-2	10	Y	25	0.0142	250.394	8.562	171.453	0.754	5.272	1.764	57.775	0.884	-61.775
LBC-1	11	Y	25	0.0064	13.816	5.218	41.400	0.772	0.830	0.281	3.705	0.057	-34.949

LBC-1	11	Y	25	0.0044	5.391	4.357	38.404	0.771	0.148	0.060	4.107	0.063	0.651
LBC-1	12	N	25	0.0075	9.323	4.785	39.662	0.778	0.474	0.179	3.282	0.050	-17.114
LBC-1	12	N	25	0.0045	9.346	4.259	37.524	0.770	0.250	0.100	2.301	0.035	-14.450
LBC-2	13	Y	25	0.0117	91.049	6.544	208.309	0.761	5.462	1.957	57.224	0.875	-92.138
LBC-2	13	Y	25	0.0125	92.511	6.202	209.279	0.742	2.817	1.177	56.082	0.858	-25.636
LBC-2	14	N	25	0.0073	75.137	6.306	245.073	0.771	2.309	0.890	35.644	0.545	-47.068
LBC-2	14	N	25	0.0111	77.607	8.471	177.932	0.776	2.563	0.877	41.599	0.636	-21.690

^fOC – fraction of organic carbon in sediment

*dw, ww – dry weight and wet weight, respectively

Note: LBC-1 = Evans and LBC-2 = Summit

Appendix H. Chapter 2 artificial stream experiment, *Hyalella azteca* survival and growth from day-0 to day-7. Control samples were in beakers in the laboratory for the 7-day exposure. Control organisms were fed and had a water was change every 2 days. Initial mass samples were collected and desiccated on day 1, to get an initial mass of the *H. azteca* used in the experiment.

Flume	Basket	Sediment	Hyporheic	No. Alive	Mass (mg)	Average Mass mg)	RGR*
3	A	Ev	Y	9	0.427	0.0474	0.0037
3	B	Ev	Y	6	0.257	0.0428	0.0030
4	A	Ev	N	10	0.369	0.0369	0.0022
4	B	Ev	N	10	0.422	0.0422	0.0029
5	A	Su	N	1	0.049	0.0490	0.0039
5	B	Su	N	8	0.323	0.0404	0.0027
6	A	Su	Y	8	0.313	0.0391	0.0025
6	B	Su	Y	6	0.254	0.0423	0.0029
7	A	Ev	Y	8	0.232	0.0290	0.0010
7	B	Ev	Y	8	0.36	0.0450	0.0033
8	A	Ev	N	8	0.333	0.0416	0.0028
8	B	Ev	N	8	0.348	0.0435	0.0031
9	A	Su	N	10	0.361	0.0361	0.0020
9	B	Su	N	7	0.277	0.0396	0.0025
10	A	Su	Y	3	0.125	0.0417	0.0028
10	B	Su	Y	10	0.356	0.0356	0.0020
11	A	Ev	Y	8	0.242	0.0303	0.0012
11	B	Ev	Y	8	0.228	0.0285	0.0010
12	A	Ev	N	7	0.26	0.0371	0.0022
12	B	Ev	N	6	0.229	0.0382	0.0023
13	A	Su	Y	9	0.319	0.0354	0.0020
13	B	Su	Y	9	0.308	0.0342	0.0018
14	A	Su	N	8	0.261	0.0326	0.0016
14	B	Su	N	10	0.37	0.0370	0.0022
Control1				10	0.486	0.0486	0.0038
Control2				10	0.348	0.0348	0.0019
Control3				10	0.445	0.0445	0.0032
Control4				10	0.377	0.0377	0.0023
Control5				9	0.282	0.0313	0.0014
Initial1				10	0.213	0.0213	
Initial2				10	0.202	0.0202	
Initial3				10	0.225	0.0225	
Initial4				10	0.241	0.0241	
Initial5				10	0.207	0.0207	

*RGR = Relative Growth Rate

Note: LBC-1 = Evans and LBC-2 = Summit

Appendix I. Chapter 2 artificial stream experiment test organism results from day-14 to day-28, including: *Hyalella azteca* survival and growth, *Daphnia magna* survival and reproduction (neonates after 2 weeks), and *Lymnaea stagnalis* survival and growth. Control samples were in beakers in the laboratory for the 14-day exposure. Control organisms were fed and had a water was change every 2 days. Initial mass samples were collected and desiccated on day 1, to get an initial mass of the *H. azteca* and *L. stagnalis* used in the experiment.

Flume	Basket	Sediment	Hypo-rheic	*Hyalella azteca*				*Daphnia magna*			*Lymnaea stagnalis*		
				No. Survival (n=10)	Total Mass (mg)	Average Mass (mg)	RGR*	No. Survival (n=10)	No. neonate	No. Survival (n=6)	Total Mass (mg)	Average Mass (mg)	RGR*
3	A	Ev	Y	8	0.208	0.0260	0.0020	10	7	6	2.715	0.453	0.0208
3	B	Ev	Y	5	0.117	0.0234	0.0017	10		6	2.392	0.399	0.0170
4	A	Ev	N	9	0.249	0.0277	0.0023	9	16	6	1.473	0.246	0.0060
4	B	Ev	N	9	0.277	0.0308	0.0027	9	9	6	2.742	0.457	0.0211
5	A	Su	N	0				3	3	6	2.521	0.420	0.0185
5	B	Su	N	5	0.107	0.0214	0.0014	2	10	6	2.393	0.399	0.0170
6	A	Su	Y	8	0.208	0.0260	0.0020	9	5	6	2.731	0.455	0.0210
6	B	Su	Y	9	0.223	0.0248	0.0019	0		6	4.205	0.701	0.0386
7	A	Ev	Y	8	0.166	0.0208	0.0013	10	1	6	2.739	0.457	0.0211
7	B	Ev	Y	6	0.127	0.0212	0.0014	10	8	5	2.006	0.401	0.0172
8	A	Ev	N	8	0.207	0.0259	0.0020	9	24	6	3.179	0.530	0.0264
8	B	Ev	N	8	0.197	0.0246	0.0019	7	10	6	3.446	0.574	0.0295
9	A	Su	N	4	0.075	0.0188	0.0010	8	10	6	3.924	0.654	0.0352
9	B	Su	N	8	0.189	0.0236	0.0017	9	9	6	2.77	0.462	0.0215
10	A	Su	Y	2	0.053	0.0265	0.0021	6	15	6	2.698	0.450	0.0206
10	B	Su	Y	1	0.024	0.0240	0.0018	7	6	6	2.907	0.485	0.0231
11	A	Ev	Y	4	0.108	0.0270	0.0022	10	8	6	4.523	0.754	0.0424
11	B	Ev	Y	1	0.021	0.0210	0.0013	8	6	6	4.686	0.781	0.0443
12	A	Ev	N	8	0.194	0.0243	0.0018	9	6	5	3.553	0.711	0.0393
12	B	Ev	N	5	0.093	0.0186	0.0010	10	10	6	4.157	0.693	0.0380
13	A	Su	Y	3	0.086	0.0287	0.0024	10	9	6	2.797	0.466	0.0218

13	B	Su	Y	8	0.203	0.0254	0.0020	0		6	2.997	0.500	0.0242
14	A	Su	N	8	0.205	0.0256	0.0020	7	8	6	3	0.500	0.0242
14	B	Su	N	6	0.138	0.0230	0.0016	10	25	6	2.287	0.381	0.0157
Control	1			10	0.554	0.0554	0.0062	3	35	5	2.619	0.524	0.0259
Control	2			9	0.505	0.0561	0.0063	3	22	6	6.504	1.084	0.0659
Control	3			9	0.442	0.0491	0.0053	7	53	4	1.08	0.270	0.0078
Control	4			9	0.541	0.0601	0.0069	4	17	5	1.557	0.311	0.0107
Control	5			10	0.698	0.0698	0.0083	7	21				
Initial	1			9	0.11	0.0122				6	0.982	0.164	
Initial	2			10	0.118	0.0118				6	1.098	0.183	
Initial	3			9	0.1	0.0111				6	0.876	0.146	
Initial	4			10	0.124	0.0124				6	0.906	0.151	
Initial	5			10	0.108	0.0108							

*RGR = Relative Growth Rate

Note: LBC-1 = Evans and LBC-2 = Summit

Appendix J. Chapter 3 initial experiment *Hyalella azteca* survival and growth data. Control samples were in beakers in the laboratory for the 10-day exposure. Control organisms were fed and had a water was change every 2 days. Initial mass samples were collected and desiccated on day 1, to get an initial mass of the *H. azteca* used in the experiment.

Ha3_ID	Sample	Trmt	Rep	No. Alive	After Depuration	Survival	Total Mass (mg)	Average Mass (mg)
1	1-A	nonHyp	1	7	7	0.7	0.217	0.031
2	1-B	Hyp	1	0	0	0		
3	2-A	nonHyp	1	10	10	1	0.286	0.029
4	2-B	Hyp	1	7	7	0.7	0.211	0.030
5	3-A	nonHyp	2	10	8	0.8	0.172	0.022
6	3-B	Hyp	2	2	2	0.2	0.097	0.049
7	4-A	nonHyp	2	3	3	0.3	0.063	0.021
8	4-B	Hyp	2	0	0	0		
9	5-A	nonHyp	3	3	3	0.3	0.084	0.028
10	5-B	Hyp	3	0	0	0		
11	6-A	nonHyp	3	0	0	0		
12	6-B	Hyp	3	0	0	0		
13	7-A	nonHyp	4	7	7	0.7	0.203	0.029
14	7-B	Hyp	4	0	0	0		
15	8-A	nonHyp	4	8	6	0.6	0.175	0.029
16	8-B	Hyp	4	10	10	1	0.264	0.026
17	9-A	nonHyp	5	3	2	0.2	0.053	0.027
18	9-B	Hyp	5	0	0	0		
19	10-A	nonHyp	5	10	9	0.9	0.260	0.029
20	10-B	Hyp	5	1	1	0.1	0.029	0.029
21	11-A	nonHyp	6	8	8	0.8	0.254	0.032
22	11-B	Hyp	6	2	2	0.2	0.053	0.027
23	12-A	nonHyp	6	6	5	0.5	0.149	0.030
24	12-B	Hyp	6	0	0	0		
25	Ha_C1	Control	1	9	9	0.9	0.429	0.048
26	Ha_C2	Control	2	10	10	1	0.515	0.052
27	Ha_C3	Control	3	10	9	0.9	0.709	0.079
28	Ha_C4	Control	4	10	9	0.9	0.617	0.069
29	Ha_C5	Control	5	10	10	1	0.524	0.052
30	Ha_A	Initial mass	1		10		0.228	0.023
31	Ha_B	Initial mass	2		10		0.210	0.021
32	Ha_C	Initial mass	3		10		0.180	0.018
33	Ha_D	Initial mass	4		10		0.241	0.024
34	Ha_E	Initial mass	5		10		0.189	0.019

Appendix K. Chapter 3 aged experiment *Hyalella azteca* survival and growth data. Control samples were in beakers in the laboratory for the 10-day exposure. Control organisms were fed and had a water was change every 2 days. Initial mass samples were collected and desiccated on day 1, to get an initial mass of the *H. azteca* used in the experiment.

Ha3_ID	Sample	Trmt	Replicate	No. Alive	Survival	Total Mass (mg)	Average Mass (mg)
1	1-A	nonHyp	1	6	0.6	0.130	0.022
2	1-B	Hyp	1	0	0.0		
3	2-A	nonHyp	1	12	1.0	0.498	0.042
4	2-B	Hyp	1	9	0.9	0.217	0.024
5	3-A	nonHyp	2	8	0.8	0.156	0.020
6	3-B	Hyp	2	8	0.8	0.142	0.018
7	4-A	nonHyp	2	3	0.3	0.059	0.020
8	4-B	Hyp	2	0	0.0		
9	5-A	nonHyp	3	10	1.0	0.252	0.025
10	5-B	Hyp	3	8	0.8	0.234	0.029
11	6-A	nonHyp	3	2	0.2	0.033	0.017
12	6-B	Hyp	3	0	0.0		
13	7-A	nonHyp	4	6	0.6	0.107	0.018
14	7-B	Hyp	4	2	0.2	0.057	0.029
15	8-A	nonHyp	4	7	0.7	0.118	0.017
16	8-B	Hyp	4	10	1.0	0.195	0.020
17	9-A	nonHyp	5	1	0.1	0.021	0.021
18	9-B	Hyp	5	2	0.2	0.048	0.024
19	10-A	nonHyp	5	10	1.0	0.156	0.016
20	10-B	Hyp	5	9	0.9	0.210	0.023
21	11-A	nonHyp	6	9	0.9	0.217	0.024
22	11-B	Hyp	6	9	0.9	0.203	0.023
23	12-A	nonHyp	6	8	0.8	0.159	0.020
24	12-B	Hyp	6	2	0.2	0.065	0.033
25	Ha_C1	Control	1	9		0.389	0.043
26	Ha_C2	Control	2	6		0.271	0.045
27	Ha_C3	Control	3	4		0.108	0.027
28	Ha_C4	Control	4	10		0.420	0.042
29	Ha_C5	Control	5	8		0.326	0.041
30	Ha_A	Initial	1	10		0.135	0.014
31	Ha_B	Initial	2	9		0.137	0.015
32	Ha_C	Initial	3	10		0.132	0.013
33	Ha_D	Initial	4	10		0.124	0.012
34	Ha_E	Initial	5	10		0.135	0.014

Appendix L. Chapter 3 porewater chemistry for initial and aged experiments, day 0 to day 91, including: Zn, Mn, Fe, Fe^{2+}, pH, dissolved oxygen (DO), temperature (Temp).

Exp	Flume	Day	Hyporheic	Sedi-ment	Zn (µg/L)	Fe (mg/L)	Mn (µg/L)	Fe2+ (mg/L)	pH	Temp (ºC)	DO (mg/L)
F3	1	0	non-Up	Zn	1224.564	0.339	915.929		7.04		
F3	1	0	Up	Zn	896.143	0.468	813.606		7.04		
F3	2	0	non-Up	Ref	6.087	2.849	753.500		7.44		
F3	2	0	Up	Ref	4.595	4.130	757.096		7.44		
F3	3	0	non-Up	Ref	8.890	10.149	1279.424		7.35		
F3	3	0	Up	Ref	61.828	4.164	739.747		7.35		
F3	4	0	non-Up	Zn	2249.248	1.394	1956.019		7.15		
F3	4	0	Up	Zn	1804.264	1.256	1510.190		7.15		
F3	5	0	non-Up	Ref	1.945	7.222	822.960		7.32		
F3	5	0	Up	Ref	7.361	7.570	1286.145		7.32		
F3	6	0	non-Up	Zn	2098.372	0.835	1683.828		6.97		
F3	6	0	Up	Zn	2267.074	2.397	1837.332		6.97		
F3	7	0	non-Up	Zn	2065.597	1.729	1821.950		7.01		
F3	7	0	Up	Zn	2881.329	1.663	2156.837		7.01		
F3	8	0	non-Up	Ref	1.379	3.908	757.188		7.11		
F3	8	0	Up	Ref	13.008	9.856	590.969		7.11		
F3	9	0	non-Up	Zn	1855.654	0.094	1510.653				
F3	9	0	Up	Zn	1811.137	0.151	1615.306				
F3	10	0	non-Up	Ref	3.775	7.842	961.265				
F3	10	0	Up	Ref	17.434	5.314	938.910				
F3	11	0	non-Up	Ref	7.249	1.600	696.315				
F3	11	0	Up	Ref	2.639	3.080	623.476				
F3	12	0	non-Up	Zn	3224.821	0.764	2460.536				
F3	12	0	Up	Zn	3381.801	0.462	2500.422				
F3	1	1	non-Up	Zn	2027.668	1.832	1606.418	1.501	6.91	22.0	3.92
F3	1	1	Up	Zn	521.885	0.171	253.748	0.000	7.39	22.0	5.51
F3	2	1	non-Up	Ref	24.718	8.445	701.656	4.434	7.24	21.7	3.81
F3	2	1	Up	Ref	7.625	2.998	289.494	0.585	7.40	22.0	4.43
F3	3	1	non-Up	Ref	3.452	12.769	1221.451	15.406	7.28	22.4	2.15
F3	3	1	Up	Ref	1.008	0.390	49.588	0.312	7.14	22.3	4.56
F3	4	1	non-Up	Zn	2680.783	5.266	2367.595	2.951	7.20	22.1	3.93
F3	4	1	Up	Zn	691.785	0.289	482.855	0.000	7.46	22.5	4.55
F3	5	1	non-Up	Ref	0.002	8.291	689.410	8.241	7.43	22.7	4.27
F3	5	1	Up	Ref	17.790	3.239	340.133	1.806	7.37	22.2	4.41
F3	6	1	non-Up	Zn	1911.101	1.367	1710.175	2.297	7.18	21.8	2.33
F3	6	1	Up	Zn	227.847	0.019	75.940	0.000	7.57	21.9	5.53
F3	7	1	non-Up	Zn	942.493	1.177	912.201	4.031	7.17	22.1	2.16
F3	7	1	Up	Zn	760.201	0.616	487.476	0.000	7.56	22.2	4.93
F3	8	1	non-Up	Ref	2.719	12.071	1401.849	5.525	7.33	22.2	3.67

F3	8	1	Up	Ref	0.000	0.000	5.872	2.471	7.34	22.2	2.80
F3	9	1	non-Up	Zn	1979.965	1.527	1790.301	0.497	7.13	21.7	2.80
F3	9	1	Up	Zn	288.189	0.032	124.387	0.000	7.45	21.8	4.56
F3	10	1	non-Up	Ref	2.117	8.730	732.379	12.854	7.35	21.8	1.89
F3	10	1	Up	Ref	1.289	1.788	184.454	1.435	7.39	21.7	4.64
F3	11	1	non-Up	Ref	15.480	7.767	838.541	5.536	7.27	21.6	3.24
F3	11	1	Up	Ref	1.760	0.168	56.176	0.454	7.28	22.1	3.57
F3	12	1	non-Up	Zn	2327.990	1.796	1771.745	2.428	7.08	22.1	2.85
F3	12	1	Up	Zn	706.040	0.057	557.056	0.000	7.36	21.8	4.00
F3	1	3	non-Up	Zn	1037.092	1.346	936.742	1.264	7.04	21.6	3.98
F3	1	3	Up	Zn	175.887	0.080	20.992	0.000	7.46	21.6	4.88
F3	2	3	non-Up	Ref	9.825	5.478	427.958	7.857	7.29	21.3	3.42
F3	2	3	Up	Ref	8.256	0.000	2.131	0.000	7.44	21.3	3.37
F3	3	3	non-Up	Ref	5.814	11.398	973.273	17.615	7.35	21.0	3.51
F3	3	3	Up	Ref	10.347	0.111	9.469	0.000	7.39	21.2	4.17
F3	4	3	non-Up	Zn	1087.056	1.443	1146.997	4.404	7.21	21.4	2.82
F3	4	3	Up	Zn	532.182	0.200	253.559	0.000	7.58	21.4	4.50
F3	5	3	non-Up	Ref	8.330	8.090	641.433	11.467	7.34	21.1	2.16
F3	5	3	Up	Ref	14.313	0.085	11.037	0.152	7.44	21.6	4.50
F3	6	3	non-Up	Zn	1344.505	1.496	1302.216	2.311	7.25	21.3	2.49
F3	6	3	Up	Zn	101.024	0.000	3.992	0.000	7.63	21.4	5.40
F3	7	3	non-Up	Zn	619.905	1.105	643.983	3.619	7.22	21.7	2.28
F3	7	3	Up	Zn	543.916	0.419	271.900	0.000	7.73	21.5	5.98
F3	8	3	non-Up	Ref	12.106	5.732	604.431	6.627	7.39	21.3	3.75
F3	8	3	Up	Ref	6.829	0.000	0.000	0.000	7.77	21.6	6.12
F3	9	3	non-Up	Zn	1220.895	1.407	1275.367	0.741	7.24	21.9	3.44
F3	9	3	Up	Zn	115.301	0.097	5.740	0.000	7.54	22.0	4.62
F3	10	3	non-Up	Ref	6.525	9.902	813.754	15.261	7.36	21.8	2.62
F3	10	3	Up	Ref	7.315	0.852	88.926	0.009	7.50	22.1	4.56
F3	11	3	non-Up	Ref	18.458	6.133	585.833	9.113	7.32	21.7	4.54
F3	11	3	Up	Ref	9.452	0.000	0.000	0.000	7.51	22.1	5.25
F3	12	3	non-Up	Zn	1260.045	1.390	1018.698	2.442	7.20	21.5	3.00
F3	12	3	Up	Zn	508.615	0.116	348.176	0.000	7.67	21.9	5.28
F3	1	5	non-Up	Zn	837.898	1.195	816.778	0.775	7.16	21.8	2.60
F3	1	5	Up	Zn	314.361	0.000	29.284	0.000	7.29	21.4	2.67
F3	2	5	non-Up	Ref	5.826	4.319	287.934	4.997	7.23	21.3	2.35
F3	2	5	Up	Ref	5.132	0.000	0.000	0.000	7.35	21.6	4.32
F3	3	5	non-Up	Ref	5.279	9.898	800.843	12.481	7.37	21.4	2.40
F3	3	5	Up	Ref	6.492	0.000	0.000	0.000	7.36	21.7	4.06
F3	4	5	non-Up	Zn	962.823	2.276	974.424	1.447	7.43	21.5	3.08
F3	4	5	Up	Zn	470.808	0.120	202.683	0.000	7.56	21.7	4.38
F3	5	5	non-Up	Ref	4.667	7.855	539.574	8.259	7.43	21.8	3.06
F3	5	5	Up	Ref	10.710	0.000	3.846	0.000	7.43	21.8	4.73

F3	6	5	non-Up	Zn	953.020	1.231	891.208	1.447	7.37	21.6	2.92
F3	6	5	Up	Zn	86.706	0.000	2.421	0.000	7.73	21.5	5.15
F3	7	5	non-Up	Zn	473.678	0.871	488.262	2.310	7.25	21.5	3.42
F3	7	5	Up	Zn	382.226	0.115	126.403	0.000	7.74	21.6	5.73
F3	8	5	non-Up	Ref	6.893	4.830	474.733	4.997	7.43	21.8	4.11
F3	8	5	Up	Ref	3.533	0.000	0.000	0.000	7.79	21.8	6.34
F3	9	5	non-Up	Zn	918.192	1.141	962.775	0.775	7.25	22.0	4.04
F3	9	5	Up	Zn	106.460	0.093	1.800	0.000	7.58	21.7	5.17
F3	10	5	non-Up	Ref	4.774	9.569	721.101	12.865	7.38	21.9	2.69
F3	10	5	Up	Ref	4.046	0.273	28.094	0.190	7.43	21.8	5.11
F3	11	5	non-Up	Ref	6.179	5.624	477.445	14.112	7.22	22.0	4.06
F3	11	5	Up	Ref	6.660	0.000	0.000	0.000	7.50	22.0	4.99
F3	12	5	non-Up	Zn	924.777	1.131	736.817	1.639	7.32	21.9	3.45
F3	12	5	Up	Zn	341.858	0.116	172.421	0.000	7.77	21.5	5.31
F3	1	7	non-Up	Zn	712.732	1.267	762.201	1.253	7.41	21.5	2.72
F3	1	7	Up	Zn	388.435	0.141	108.061	0.000	7.49	21.5	2.80
F3	2	7	non-Up	Ref	17.560	4.177	308.428	7.110	7.58	21.4	2.82
F3	2	7	Up	Ref	14.411	0.113	28.649	0.000	7.49	21.7	3.00
F3	3	7	non-Up	Ref	11.787	11.488	918.067	13.225	7.50	21.8	3.08
F3	3	7	Up	Ref	13.896	0.179	83.116	0.738	7.39	21.6	3.25
F3	4	7	non-Up	Zn	849.586	2.227	939.583	2.068	7.41	21.9	4.24
F3	4	7	Up	Zn				0.000	7.59	21.6	3.28
F3	5	7	non-Up	Ref	11.739	8.422	658.901	9.363	7.39	21.7	2.88
F3	5	7	Up	Ref	19.597	0.149	63.879	0.545	7.43	21.8	2.48
F3	6	7	non-Up	Zn	1004.981	1.395	942.705	1.854	7.38	21.6	3.54
F3	6	7	Up	Zn	194.474	0.108	182.937	0.000	7.74	21.5	2.38
F3	7	7	non-Up	Zn	462.731	0.930	498.225	2.605	7.55	21.9	2.55
F3	7	7	Up	Zn	262.852	0.136	76.425	0.000	7.80	21.9	5.27
F3	8	7	non-Up	Ref	17.927	6.086	541.239	6.467	7.94	22.2	2.72
F3	8	7	Up	Ref	12.808	1.256	21.795	0.000	7.54	21.8	6.04
F3	9	7	non-Up	Zn	919.260	1.291	1030.631	0.888	7.46	22.0	4.27
F3	9	7	Up	Zn	200.814	0.143	24.207	0.000	7.66	21.8	4.00
F3	10	7	non-Up	Ref	16.260	10.194	763.685	13.654	7.43	22.0	1.78
F3	10	7	Up	Ref	16.025	0.538	62.526	0.545	7.41	22.0	4.05
F3	11	7	non-Up	Ref	9.580	7.078	596.619	12.796	7.33	21.9	2.23
F3	11	7	Up	Ref	16.815	0.109	13.737	0.000	7.48	21.6	4.99
F3	12	7	non-Up	Zn	865.391	1.188	705.403	1.961	7.30	21.6	2.70
F3	12	7	Up	Zn	260.807	0.139	61.391	0.000	7.65	21.6	4.96
F3	1	10	non-Up	Zn	777.983	1.905	986.708	2.280	7.51	21.7	4.61
F3	1	10	Up	Zn	463.658	0.300	168.993	0.141	7.65	21.7	3.54
F3	2	10	non-Up	Ref	16.661	4.406	271.707	8.429	7.58	21.3	4.19
F3	2	10	Up	Ref	169.841	0.105	15.423	0.000	7.85	21.6	4.24
F3	3	10	non-Up	Ref	27.399	12.520	855.712	18.035	7.70	21.5	4.09

F3	3	10	Up	Ref	127.073	0.133	16.019	0.000	7.66	21.4	4.56
F3	4	10	non-Up	Zn	1005.311	2.491	858.861	2.665	7.75	22.3	5.04
F3	4	10	Up	Zn	417.913	0.214	198.543	0.000	7.96	21.5	5.14
F3	5	10	non-Up	Ref	60.791	8.276	599.979	12.912	7.68	21.4	4.35
F3	5	10	Up	Ref	74.762	0.186	25.521	0.000	7.78	21.4	4.27
F3	6	10	non-Up	Zn	969.226	1.520	821.820	3.689	7.60	21.6	3.82
F3	6	10	Up	Zn	337.489	0.104	31.393	0.000	7.98	21.5	5.24
F3	7	10	non-Up	Zn	421.688	0.959	430.948	4.970	7.65	21.3	3.23
F3	7	10	Up	Zn	252.477	0.120	26.338	1.512	8.09	21.6	4.80
F3	8	10	non-Up	Ref	54.456	5.996	451.510	6.635	7.74	21.9	3.25
F3	8	10	Up	Ref	13.313	0.222	12.177	0.000	7.89	21.9	4.89
F3	9	10	non-Up	Zn	862.153	1.325	869.299	1.768	7.47	22.1	4.12
F3	9	10	Up	Zn	165.355	0.130	15.607	0.000	7.88	22.2	5.09
F3	10	10	non-Up	Ref	17.182	11.521	767.403	17.267	7.62	22.0	2.84
F3	10	10	Up	Ref	39.336	0.734	35.094	0.794	7.64	21.6	4.34
F3	11	10	non-Up	Ref	26.302	7.817	576.662	16.498	7.67	21.3	2.87
F3	11	10	Up	Ref	14.262	0.115	11.712	0.090	7.85	22.2	3.92
F3	12	10	non-Up	Zn	776.375	1.196	641.776	2.408	7.59	21.9	4.91
F3	12	10	Up	Zn	181.006	0.134	33.050	0.000	7.98	21.8	5.81
F5	1	82	non-Up	Zn	150.169	5.849	1507.646	8.171	7.25	21.5	3.28
F5	1	82	Up	Zn	214.404	3.160	92.205	4.779	7.09	21.1	2.36
F5	2	82	non-Up	Ref	0.000	4.126	267.624	4.308	7.30	20.5	2.66
F5	2	82	Up	Ref	0.000	0.141	6.291	0.000	7.13	21.2	4.84
F5	3	82	non-Up	Ref	0.000	8.764	658.993	11.092	7.37	20.8	2.73
F5	3	82	Up	Ref	0.000	0.131	13.399	0.000	7.08	20.7	4.38
F5	4	82	non-Up	Zn	159.539	5.380	880.325	6.192	7.32	21.3	2.57
F5	4	82	Up	Zn	243.953	0.302	56.429	0.000	7.54	21.0	5.34
F5	5	82	non-Up	Ref	0.000	7.930	468.311	7.983	7.40	20.7	2.47
F5	5	82	Up	Ref	0.000	0.280	10.351	0.000	7.34	20.6	4.67
F5	6	82	non-Up	Zn	121.778	8.132	538.772	4.779	7.19	21.1	2.76
F5	6	82	Up	Zn	45.586	0.332	9.439	0.444	7.34	20.9	3.98
F5	7	82	non-Up	Zn	101.913	3.744	539.615	5.344	7.28	21.1	2.68
F5	7	82	Up	Zn	25.089	1.156	12.647	0.162	7.57	20.9	5.48
F5	8	82	non-Up	Ref	0.000	4.758	357.614	6.475	7.33	20.8	2.41
F5	8	82	Up	Ref	0.000	0.105	5.104	0.000	7.56	21.2	6.04
F5	9	82	non-Up	Zn	190.459	4.360	770.805	6.004	7.28	21.0	2.81
F5	9	82	Up	Zn	138.270	0.192	16.549	0.539	7.09	20.8	4.37
F5	10	82	non-Up	Ref	0.000	7.258	372.288	11.846	7.37	21.2	2.15
F5	10	82	Up	Ref	0.000	0.551	56.532	0.256	7.03	21.0	3.25
F5	11	82	non-Up	Ref	0.000	8.020	589.672	11.375	7.28	21.0	2.67
F5	11	82	Up	Ref	0.000	0.160	5.319	0.000	7.42	20.8	5.31
F5	12	82	non-Up	Zn	180.843	2.712	367.573	6.381	7.20	21.4	2.70
F5	12	82	Up	Zn	50.011	0.765	13.390	2.517	7.27	21.0	4.97

F5	1	84	non-Up	Zn	141.611	5.198	1341.970		7.25	23.5	2.23
F5	1	84	Up	Zn	240.223	3.071	70.005	4.939	7.08	22.4	2.79
F5	2	84	non-Up	Ref	10.834	4.220	257.511	4.234	7.17	22.7	2.20
F5	2	84	Up	Ref	13.063	0.119	3.988	0.000	7.13	22.7	5.02
F5	3	84	non-Up	Ref	12.555	7.393	590.428	11.689	7.45	22.5	2.60
F5	3	84	Up	Ref	10.222	0.032	25.025	0.000	7.03	22.4	4.43
F5	4	84	non-Up	Zn	149.247	4.900	782.404	6.551	7.27	22.9	2.69
F5	4	84	Up	Zn	238.706	0.216	45.030	0.003	7.29	22.8	3.57
F5	5	84	non-Up	Ref	12.666	6.584	366.382	8.263	7.34	22.8	2.24
F5	5	84	Up	Ref	12.301	0.026	2.911	0.000	7.10	22.6	4.85
F5	6	84	non-Up	Zn	112.271	7.593	517.699	5.141	7.11	22.8	2.80
F5	6	84	Up	Zn	103.731	0.209	7.348	0.507	7.18	22.8	4.33
F5	7	84	non-Up	Zn	98.072	2.815	420.826	5.241	7.18	22.8	2.46
F5	7	84	Up	Zn	59.001	0.791	11.504	0.507	7.38	22.6	4.88
F5	8	84	non-Up	Ref	9.599	4.403	321.574	5.846	7.35	22.6	2.63
F5	8	84	Up	Ref	11.671	0.054	2.125	0.000	7.41	22.7	5.36
F5	9	84	non-Up	Zn	166.601	3.727	676.196	5.241	7.25	23.1	2.72
F5	9	84	Up	Zn	169.886	0.092	8.582	0.507	7.11	22.9	5.21
F5	10	84	non-Up	Ref	11.923	7.074	527.099	11.991	7.40	22.9	2.05
F5	10	84	Up	Ref	10.945	0.131	26.532	0.104	7.01	22.6	3.60
F5	11	84	non-Up	Ref	12.933	6.309	331.984	11.084	7.40	22.5	2.05
F5	11	84	Up	Ref	11.364	0.077	2.199	0.000	7.22	22.5	4.70
F5	12	84	non-Up	Zn	161.425	2.109	323.246	5.544	7.16	23.3	2.48
F5	12	84	Up	Zn	86.219	0.652	11.344	2.421	7.19	22.4	4.55
F5	1	87	non-Up	Zn	130.118	4.797	1277.460	8.149	7.18	23.3	2.46
F5	1	87	Up	Zn	223.055	3.489	73.840	5.928	7.00	22.9	2.47
F5	2	87	non-Up	Ref	0.000	4.306	242.186	4.514	7.03	22.5	2.10
F5	2	87	Up	Ref	0.000	0.114	4.314	0.071	7.06	22.9	5.20
F5	3	87	non-Up	Ref	0.000	6.756	522.478	12.289	7.27	22.7	2.10
F5	3	87	Up	Ref	0.000	0.104	4.211	0.071	7.07	22.7	4.67
F5	4	87	non-Up	Zn	156.553	4.882	750.347	5.423	7.24	22.8	2.72
F5	4	87	Up	Zn	301.435	0.264	37.073	0.071	7.17	22.9	5.04
F5	5	87	non-Up	Ref	0.000	6.463	343.931	7.846	7.30	22.6	2.34
F5	5	87	Up	Ref	0.000	0.077	3.332	0.071	7.16	22.7	5.37
F5	6	87	non-Up	Zn	100.160	6.936	472.943	5.120	7.11	22.9	2.51
F5	6	87	Up	Zn	38.648	0.141	4.711	0.273	7.19	22.9	5.20
F5	7	87	non-Up	Zn	95.528	2.425	334.749	5.221	7.21	22.8	2.95
F5	7	87	Up	Zn	67.963	0.428	6.842	0.475	7.35	22.6	5.46
F5	8	87	non-Up	Ref	0.000	4.347	322.533	6.130	7.33	22.9	2.66
F5	8	87	Up	Ref	0.000	0.185	3.800	0.172	7.46	22.8	5.91
F5	9	87	non-Up	Zn	133.768	3.302	511.168	4.615	7.24	22.9	2.84
F5	9	87	Up	Zn	69.089	0.159	3.978	0.273	7.30	22.7	5.71
F5	10	87	non-Up	Ref	0.000	5.575	431.278	10.977	7.40	22.7	2.65

F5	10	87	Up	Ref	0.000	0.204	7.215	0.172	7.22	22.7	5.42
F5	11	87	non-Up	Ref	0.000	6.479	323.139	11.482	7.40	22.6	2.37
F5	11	87	Up	Ref	0.000	0.082	3.038	0.000	7.34	22.8	5.74
F5	12	87	non-Up	Zn	154.618	2.149	327.663	7.846	7.16	22.7	3.05
F5	12	87	Up	Zn	66.613	0.752	11.492	2.191	7.21	22.5	4.91
F5	1	91	non-Up	Zn	133.211	4.931	1282.422	7.693	6.79	23.3	2.15
F5	1	91	Up	Zn	238.788	3.961	98.928	6.016	6.53	22.8	2.14
F5	2	91	non-Up	Ref	5.444	4.200	247.789	3.748	6.65	22.5	2.14
F5	2	91	Up	Ref	5.403	0.032	3.745	0.000	6.65	22.8	4.60
F5	3	91	non-Up	Ref	0.000	6.633	487.845	10.652	6.95	22.8	2.44
F5	3	91	Up	Ref	0.000	0.000	4.044	0.000	6.70	22.8	4.10
F5	4	91	non-Up	Zn	183.743	5.280	761.369	4.734	6.90	23.2	2.41
F5	4	91	Up	Zn	268.757	0.116	28.112	0.000	6.94	22.7	5.13
F5	5	91	non-Up	Ref	7.297	6.278	310.868	6.707	7.00	22.9	2.58
F5	5	91	Up	Ref	5.024	0.020	2.883	0.000	6.77	22.7	4.76
F5	6	91	non-Up	Zn	95.877	6.677	436.789	4.439	6.85	22.9	2.65
F5	6	91	Up	Zn	35.903	0.050	4.687	0.109	6.91	22.7	4.49
F5	7	91	non-Up	Zn	98.813	2.143	286.185	4.340	6.86	23.2	2.45
F5	7	91	Up	Zn	60.575	0.278	4.459	0.247	7.13	22.6	5.10
F5	8	91	non-Up	Ref	0.000	4.504	315.467	6.312	7.01	22.7	2.41
F5	8	91	Up	Ref	5.641	0.025	3.140	0.000	7.18	22.7	5.84
F5	9	91	non-Up	Zn	128.326	2.680	430.327	3.354	6.90	22.8	2.67
F5	9	91	Up	Zn	68.128	0.016	2.862	0.089	7.04	22.4	5.20
F5	10	91	non-Up	Ref	5.795	5.268	394.387	8.088	7.14	23.9	2.43
F5	10	91	Up	Ref	0.000	0.061	3.818	0.060	6.82	22.1	3.48
F5	11	91	non-Up	Ref	5.545	6.661	314.722	12.033	7.20	22.2	1.91
F5	11	91	Up	Ref	11.508	0.000	2.054	0.000	7.22	22.6	5.38
F5	12	91	non-Up	Zn	281.369	4.801	522.342	7.397	7.00	23.3	2.56
F5	12	91	Up	Zn	75.132	0.470	7.404	1.263	7.06	22.3	4.79

Appendix M. Chapter 3 sediment chemistry for initial and aged experiments (total Zn, Fe, Mn, dw/ww, S^{2-}, AVS, SEM-Zn, fOC).

						Total Metals					(SEM-AVS)/fOC			
Exp	Flume-Basket	Day	Sedi-ment	Hypor-heic	fOC^	Fe (g/kg)	Mn (mg/kg)	Zn (mg/kg)	dw/ww*	S^{2-} (µmol)	AVS dw (µmol/g)	SEM Zn_{dw} (ug/g)	SEM Zn_{dw} (µmol/g)	(SEM-AVS)/fOC
initial		0	Ref		0.0068	5.398	42.121	7.575	0.758	2.429	1.042	6.313	0.097	-0.308
initial		0	Ref		0.0043	3.842	37.726	0.000	0.762	0.648	0.282	9.088	0.139	-0.048
initial		0	Zn		0.0057	3.880	36.650	425.871	0.760	1.891	0.801	615.991	9.420	2.774
F3	F1-A	10	Zn	non-Hyp	0.0034	3.780	34.665	363.096	0.884	1.448	0.538	294.872	4.509	1.304
F3	F1-B	10	Zn	Hyp	0.0039	4.170	26.918	376.551	0.772	0.478	0.194	305.343	4.670	1.403
F3	F2-A	10	Ref	non-Hyp	0.0050	4.248	36.209	5.666	0.773	0.618	0.265	9.765	0.149	-0.038
F3	F2-B	10	Ref	Hyp	0.0074	7.201	45.491	9.804	0.782	0.034	0.014	5.637	0.086	0.023
F3	F3-A	10	Ref	non-Hyp	0.0064	4.670	35.711	5.355	0.756	2.338	0.950	6.595	0.101	-0.261
F3	F3-B	10	Ref	Hyp	0.0054	5.031	30.998	11.333	0.753	0.993	0.428	1.889	0.029	-0.130
F3	F4-A	10	Zn	non-Hyp	0.0045	4.471	36.373	434.873	0.774	0.909	0.366	376.116	5.752	1.679
F3	F4-B	10	Zn	Hyp	0.0041	4.362	28.388	369.189	0.774	1.194	0.507	328.487	5.024	1.484
F3	F5-A	10	Ref	non-Hyp	0.0450	5.676	43.248	6.448	0.666	1.413	0.685	7.308	0.112	-0.185
F3	F5-B	10	Ref	Hyp	0.0067	5.891	36.595	8.209	0.757	0.834	0.351	5.819	0.089	-0.084
F3	F6-A	10	Zn	non-Hyp	0.0043	4.009	35.623	425.417	0.815	1.800	0.719	457.212	6.992	2.041
F3	F6-B	10	Zn	Hyp	0.0021	4.402	34.014	459.371	0.823	1.251	0.493	310.317	4.746	1.381
F3	F7-A	10	Zn	non-Hyp	0.0097	4.280	37.876	435.096	0.798	1.266	0.518	375.386	5.741	1.707
F3	F7-B	10	Zn	Hyp	0.0035	5.057	30.744	356.158	0.787	0.629	0.261	278.121	4.253	1.304
F3	F8-A	10	Ref	non-Hyp	0.0051	4.353	31.175	9.765	0.768	4.635	1.954	9.120	0.139	-0.587
F3	F8-B	10	Ref	Hyp	0.0064	5.538	36.806	7.563	0.769	0.315	0.135	7.077	0.108	-0.009
F3	F9-A	10	Zn	non-Hyp	0.0047	4.401	37.493	441.698	0.808	0.830	0.340	413.073	6.317	1.977
F3	F9-B	10	Zn	Hyp	0.0047	4.205	25.623	377.304	0.805	1.205	0.494	398.665	6.097	1.848
F3	F10-A	10	Ref	non-Hyp	0.0087	6.483	48.984	7.770	0.645	0.966	0.499	6.337	0.097	-0.134
F3	F10-B	10	Ref	Hyp	0.0072	4.353	29.133	5.863	0.769	0.887	0.378	5.498	0.084	-0.097
F3	F11-A	10	Ref	non-Hyp	0.0063	5.259	43.561	7.300	0.752	0.803	0.346	7.317	0.112	-0.076
F3	F11-B	10	Ref	Hyp	0.0096	4.642	31.493	6.176	0.757	1.656	0.712	1.991	0.030	-0.222
F3	F12-A	10	Zn	non-Hyp	0.0048	3.938	36.138	423.860	0.815	2.145	0.879	488.072	7.464	2.201

F3	F12-B	10	Zn	Hyp	0.0035	3.464	23.516	333.183	0.796	0.447	0.187	256.552	3.923	1.243
F5	F1-A	80	Zn	non-Hyp	0.0022	3.113	25.408	272.376	0.820	0.441	0.186	257.956	3.945	1.298
F5	F1-B	80	Zn	Hyp	0.0020	2.989	20.527	244.075	0.801	0.247	0.147	227.349	3.477	1.586
F5	F2-A	80	Ref	non-Hyp	0.0040	4.340	32.882	13.303	0.784	0.374	0.185	4.322	0.066	-0.046
F5	F2-B	80	Ref	Hyp	0.0044	4.693	26.451	10.615	0.821	-0.010	-0.006	1.870	0.029	0.017
F5	F3-A	80	Ref	non-Hyp	0.0069	7.129	43.113	16.034	0.756	3.307	1.687	1.998	0.031	-0.639
F5	F3-B	80	Ref	Hyp	0.0058	4.494	32.065	12.141	0.750	0.035	0.018	2.421	0.037	0.007
F5	F4-A	80	Zn	non-Hyp	0.0038	4.299	32.722	437.229	0.773	0.974	0.481	399.557	6.110	2.150
F5	F4-B	80	Zn	Hyp	0.0030	4.221	23.861	339.791	0.775	0.385	0.197	392.838	6.008	2.299
F5	F5-A	80	Ref	non-Hyp	0.0036	4.334	32.739	12.434	0.787	4.079	1.943	3.945	0.060	-0.706
F5	F5-B	80	Ref	Hyp	0.0145	12.178	71.243	23.889	0.702	0.985	0.641	10.892	0.167	-0.217
F5	F6-A	80	Zn	non-Hyp	0.0032	3.666	29.724	351.971	0.812	0.750	0.368	364.020	5.567	2.072
F5	F6-B	80	Zn	Hyp	0.0047	4.975	29.129	441.585	0.825	0.758	0.360	373.634	5.714	2.097
F5	F7-A	80	Zn	non-Hyp	0.0043	3.229	29.460	270.166	0.837	0.769	0.366	388.137	5.936	2.219
F5	F7-B	80	Zn	Hyp	0.0052	3.796	35.682	440.173	0.835	0.937	0.437	374.544	5.728	2.062
F5	F8-A	80	Ref	non-Hyp	0.0106	10.931	72.377	21.956	0.722	4.250	2.338	4.999	0.076	-0.898
F5	F8-B	80	Ref	Hyp	0.0065	7.085	45.971	15.964	0.761	-0.006	-0.003	4.235	0.065	0.027
F5	F9-A	80	Zn	non-Hyp	0.0127	4.082	38.944	355.887	0.842					
F5	F9-B	80	Zn	Hyp	0.0042	4.786	32.591	436.794	0.835					
F5	F10-A	80	Ref	non-Hyp	0.0098	9.353	63.701	20.355	0.729					
F5	F10-B	80	Ref	Hyp	0.0062	8.251	56.095	17.542	0.728					
F5	F11-A	80	Ref	non-Hyp	0.0053	4.935	33.877	12.589	0.776					
F5	F11-B	80	Ref	Hyp	0.0142	9.721	63.397	19.030	0.732					
F5	F12-A	80	Zn	non-Hyp	0.0040	3.951	34.856	353.738	0.777					
F5	F12-B	80	Zn	Hyp	0.0032	4.218	25.202	328.381	0.821					
F5	F1-A	91	Zn	non-Hyp	0.0031	3.635	29.892	346.665	0.772	0.735	0.369	318.874	4.876	1.746
F5	F1-B	91	Zn	Hyp	0.0040	4.519	31.953	418.159	0.773	1.633	0.841	517.376	7.912	2.815
F5	F2-A	91	Ref	non-Hyp	0.0052	4.788	53.335	11.560	0.759	0.467	0.238	1.724	0.026	-0.082
F5	F2-B	91	Ref	Hyp	0.0064	5.566	36.395	12.536	0.804	-0.006	-0.003	1.723	0.026	0.012
F5	F3-A	91	Ref	non-Hyp	0.0086	7.508	56.913	17.247	0.755	1.100	0.579	3.336	0.051	-0.210
F5	F3-B	91	Ref	Hyp	0.0085	7.291	54.081	14.060	0.747	0.720	0.376	3.745	0.057	-0.124

F5	F4-A	91	Zn	non-Hyp	0.0037	3.885	32.933	370.851	0.813	0.989	0.483	386.409	5.909	2.157
F5	F4-B	91	Zn	Hyp	0.0030	3.408	21.560	326.240	0.805	0.653	0.320	422.478	6.461	2.418
F5	F5-A	91	Ref	non-Hyp	0.0057	5.051	41.284	12.943	0.776	0.337	0.170	5.530	0.085	-0.034
F5	F5-B	91	Ref	Hyp	0.0121	11.358	64.018	20.324	0.732	-0.006	-0.001	2.310	0.035	0.007
F5	F6-A	91	Zn	non-Hyp	0.0053	6.289	49.406	550.353	0.779	1.577	0.363	195.123	2.984	0.470
F5	F6-B	91	Zn	Hyp	0.0039	4.686	28.442	454.717	0.780	0.326	0.167	295.769	4.523	1.740
F5	F7-A	91	Zn	non-Hyp	0.0039	4.192	26.772	359.580	0.790	1.022	0.500	301.724	4.614	1.590
F5	F7-B	91	Zn	Hyp	0.0038	4.748	41.041	463.094	0.817	0.881	0.430	353.954	5.413	1.987
F5	F8-A	91	Ref	non-Hyp	0.0070	6.631	68.548	19.527	0.403	0.784	0.774	11.868	0.181	-0.236
F5	F8-B	91	Ref	Hyp	0.0261	8.672	54.803	19.738	0.385	-0.006	-0.006	7.753	0.119	0.048
F5	F9-A	91	Zn	non-Hyp	0.0040	4.470	33.163	407.946	0.799					
F5	F9-B	91	Zn	Hyp	0.0038	4.718	28.956	436.522	0.792					
F5	F10-A	91	Ref	non-Hyp	0.0075	6.939	52.629	16.620	0.766					
F5	F10-B	91	Ref	Hyp	0.0044	4.219	34.251	12.684	0.781					
F5	F11-A	91	Ref	non-Hyp	0.0066	6.334	48.799	14.569	0.740					
F5	F11-B	91	Ref	Hyp	0.0087	5.661	33.150	13.386	0.795					
F5	F12-A	91	Zn	non-Hyp	0.0115	4.050	33.612	399.980	0.763					
F5	F12-B	91	Zn	Hyp	0.0039	3.795	22.717	334.666	0.776					

^fOC – fraction of organic carbon in sediment

*dw, ww – dry weight and wet weight, respectively

Appendix N. Chapter 4 biofilm data, including: depth of sediment burial (Depth) Net Primary Productivity (NPP) and Chlorophyll (Chl a).

Site	Sediment	Hyporheic	Drying	Rep	Depth (cm)	NPP (mg $O_2m^{-2}h^{-1}$)	Chl a (mg/m²)	Biomass (g)
EB	nat	cl	dry	1	0.1	-3.44	11.904	0.0154
EB	nat	cl	dry	2	0.1	12.29	19.557	0.0422
EB	nat	cl	dry	3	1.0	22.61	45.067	0.0000
EB	nat	cl	dry	4	0.5	-7.13	19.557	0.0658
EB	nat	cl	dry	5	0.8	-23.29	18.707	0.0674
EB	nat	cl	sat	1	0.3	16.27	63.774	0.1005
EB	nat	cl	sat	2	0.1	18.74	27.210	0.0858
EB	nat	cl	sat	3	0.3	-6.23	21.258	0.0802
EB	nat	cl	sat	4	1.4	-2.00	5.102	0.0467
EB	nat	cl	sat	5	2.0	-7.96	8.503	0.0000
EB	nat	op	dry	1	0.1	40.30	50.169	0.0674
EB	nat	op	dry	2	0.2	54.06	79.080	0.0484
EB	nat	op	dry	3	0.1	12.78	23.809	0.1181
EB	nat	op	dry	4	0.5	0.70	14.455	0.1048
EB	nat	op	dry	5	0.8	-9.04	16.156	0.0981
EB	nat	op	sat	1	0.1	38.47	66.325	0.0875
EB	nat	op	sat	2	0.5	2.80	15.306	0.0647
EB	nat	op	sat	3	0.2	2.78	13.605	0.0943
EB	nat	op	sat	4	1.5	-9.46	4.252	0.0000
EB	nat	op	sat	5	1.0	3.36	1.701	0.0058
EB	ref	cl	dry	1	1.5	-8.55	5.952	0.0000
EB	ref	cl	dry	2	1.5	0.00	5.102	0.0000
EB	ref	cl	dry	3	0.5	-4.82	19.557	0.0575
EB	ref	cl	sat	1	0.5	2.96	30.611	0.0302
EB	ref	cl	sat	2	1.3	0.66	5.102	0.0231
EB	ref	op	dry	1	1.5	0.00	5.102	0.0119
EB	ref	op	dry	2	0.9	-5.49	16.156	0.0451
EB	ref	op	dry	3	0.5	-6.82	11.904	0.0253
EB	ref	op	sat	1	1.0	2.46	22.959	0.0287
EB	ref	op	sat	2	0.5	-4.65	4.252	0.0000
LBC	nat	cl	dry	1	0.05	62.37	5.102	0.0351
LBC	nat	cl	dry	2	0.05	-3.19	7.653	0.0250
LBC	nat	cl	dry	3	0	38.52	12.755	0.0378
LBC	nat	cl	dry	4	0.05	-3.13	11.904	0.0210
LBC	nat	cl	dry	5	0	-22.66	11.054	0.0201
LBC	nat	cl	sat	1	0.6	36.53	1.701	0.0137
LBC	nat	cl	sat	2	0.2	20.52	2.551	0.0092

LBC	nat	cl	sat	3	0.3	20.42	6.803	0.0000
LBC	nat	cl	sat	4	0.1	0.00	3.401	0.0240
LBC	nat	op	dry	1	0.1	3.97	2.551	0.0087
LBC	nat	op	dry	2	0.1	22.72	2.551	0.0171
LBC	nat	op	dry	3	0.05	17.22	29.761	0.0265
LBC	nat	op	dry	4	0	-1.56	15.306	0.0145
LBC	nat	op	dry	5	0.1	15.62	11.054	0.0181
LBC	nat	op	sat	1	0.5	40.52	3.401	0.0000
LBC	nat	op	sat	2	0.6	6.27	0.850	0.0000
LBC	nat	op	sat	3	0.7	36.44	0.850	0.0351
LBC	nat	op	sat	4	x	31.68	0.850	0.0399
LBC	ref	cl	dry	1	0	77.68	65.475	0.0288
LBC	ref	cl	dry	2	0	34.80	7.653	0.0000
LBC	ref	cl	dry	3	0.05	23.12	4.252	0.0000
LBC	ref	cl	dry	4	0.05	-6.91	15.306	0.0005
LBC	ref	cl	dry	5	0.1	9.20	4.252	0.0000
LBC	ref	cl	sat	1	0	15.02	16.156	0.0000
LBC	ref	cl	sat	2	0.05	-18.11	1.701	0.0000
LBC	ref	cl	sat	3	0	31.88	74.828	0.0186
LBC	ref	op	dry	1	0	-3.99	27.210	0.0427
LBC	ref	op	dry	2	0	6.36	5.102	0.0030
LBC	ref	op	dry	3	0.3	24.75	5.102	0.0064
LBC	ref	op	dry	4	1	17.78	1.701	0.0157
LBC	ref	op	dry	5	0.05	27.05	4.252	0.0258
LBC	ref	op	sat	1	0.3	11.95	1.701	0.0000
LBC	ref	op	sat	2	0	0.78	10.204	0.0022
LBC	ref	op	sat	3	0	44.37	26.360	0.0000
QC	nat	cl	dry	1	0.0	28.64	9.354	
QC	nat	cl	dry	2	0.1	28.48	17.857	
QC	nat	cl	dry	3	0.0	23.07	6.803	
QC	nat	cl	dry	4	0.4	22.28	3.401	
QC	nat	cl	dry	5	0.1	13.52	4.252	
QC	nat	cl	sat	1	0.1	44.36	3.401	
QC	nat	cl	sat	2	0.9	17.28	3.401	
QC	nat	cl	sat	3	0.3	17.11	1.701	
QC	nat	op	dry	1	0.0	23.74	16.156	
QC	nat	op	dry	2	0.0	41.37	4.252	
QC	nat	op	dry	3	0.2	42.73	39.965	
QC	nat	op	dry	4	0.3	30.40	21.258	
QC	nat	op	dry	5	0.0	26.40	8.503	
QC	nat	op	sat	1	1.5	50.78	2.551	

QC	nat	op	sat	2	2.0	37.11	2.551
QC	nat	op	sat	3	1.5	45.05	2.551
QC	ref	cl	dry	1	0.0	60.80	35.713
QC	ref	cl	dry	2	0.0	59.02	31.462
QC	ref	cl	dry	3	0.0	40.70	12.755
QC	ref	cl	sat	1	0.0	63.61	22.959
QC	ref	cl	sat	2	0.0	23.20	3.401
QC	ref	cl	sat	3	0.5	40.37	19.557
QC	ref	op	dry	1	0.0	43.20	28.911
QC	ref	op	dry	2	0.0	58.87	62.924
QC	ref	op	dry	3	0.0	21.36	2.551
QC	ref	op	sat	1	0.0	32.47	3.401
QC	ref	op	sat	2	0.2	39.65	5.102
QC	ref	op	sat	3	0.5	56.79	7.653

Site location: QC = Quanicassee (Bay City), EB = East Bay (Traverse City), LBC = Little Black Creek (Muskegon)

Sediment type: nat = site sediment, ref = from Raisin River

Hyporheic conditions: op = open to hyporheic flow, cl = closed to hyporheic flow

Drying: dry = sediments in dry conditions for 30 days, sat = sediments continuously saturated

Appendix O. Chapter 4 benthic macroinvertebrate community composition summary data for each sediment basket, organized by site, sediment, hyporheic connectivity (Hyp) and drying treatment (Drying).

Site	Sedi-ment	Hyp	Drying	Rep	Abun-dance	Dominant Taxa	Relative Abund	Chiron Abund	EPT Abund	Richness	Gini-Simp Diversity	Shannon Diversity	Eveness
EB	nat	cl	dry	1	9	Oligochaeta	0.444	1	0	5	0.716	1.427	0.887
EB	nat	cl	dry	2	8	Chironomidae	0.375	3	0	3	0.594	0.974	0.887
EB	nat	cl	dry	3	43	Oligochaeta	0.581	5	1	5	0.582	1.089	0.677
EB	nat	cl	dry	4	35	Oligochaeta	0.886	3	0	3	0.207	0.420	0.382
EB	nat	cl	sat	1	22	Gammaridae	0.364	2	0	5	0.744	1.468	0.912
EB	nat	cl	sat	2	9	Oligochaeta	0.778	0	0	3	0.370	0.684	0.622
EB	nat	cl	sat	3	22	Oligochaeta	0.636	0	0	5	0.562	1.160	0.720
EB	nat	op	dry	2	48	Oligochaeta	0.417	13	3	10	0.727	1.616	0.702
EB	nat	op	dry	3	13	Oligochaeta	0.462	4	1	5	0.675	1.311	0.815
EB	nat	op	dry	4	14	Oligochaeta	0.786	1	0	3	0.357	0.656	0.597
EB	nat	op	sat	1	17	Chironomidae	0.294	5	1	6	0.775	1.611	0.899
EB	nat	op	sat	2	31	Oligochaeta	0.710	0	0	4	0.460	0.874	0.631
EB	nat	op	sat	3	11	Oligochaeta	0.818	1	0	3	0.314	0.600	0.546
EB	ref	cl	dry	1	12	Chironomidae	0.500	6	0	4	0.625	1.127	0.813
EB	ref	cl	dry	2	36	Oligochaeta	0.833	1	1	4	0.292	0.595	0.429
EB	ref	cl	dry	3	1	Hirudinea	1.000	0	0	1	0.000	0.000	
EB	ref	cl	sat	1	5	Hirudinea	0.600	1	0	3	0.560	0.950	0.865
EB	ref	cl	sat	2	10	Oligochaeta	0.800	0	0	3	0.340	0.639	0.582
EB	ref	op	dry	1	78	Oligochaeta	0.628	9	0	7	0.572	1.228	0.631
EB	ref	op	dry	2	35	Oligochaeta	0.714	0	0	4	0.456	0.868	0.626
EB	ref	op	dry	3	27	Oligochaeta	0.296	0	2	8	0.785	1.736	0.835
EB	ref	op	sat	1	4	Oligochaeta	0.500	2	0	2	0.500	0.693	1.000
EB	ref	op	sat	2	26	Oligochaeta	0.808	1	0	5	0.337	0.746	0.463
LBC	nat	cl	dry	1	12	Oligochaeta	0.583	4	0	3	0.542	0.888	0.808
LBC	nat	cl	dry	2	17	Oligochaeta	0.647	1	0	4	0.519	0.955	0.689
LBC	nat	cl	dry	3	70	Gammaridae	0.257	7	0	8	0.627	1.289	0.620
LBC	nat	cl	dry	4	10	Oligochaeta	0.400	0	0	4	0.700	1.280	0.923

149

LBC	nat	cl	sat	1	19	Chironomidae	0.421	8	0	5	0.715	1.399	0.869
LBC	nat	cl	sat	2	66	Asellidae	0.273	13	1	10	0.805	1.815	0.788
LBC	nat	cl	sat	3	11	Gammaridae	0.545	3	0	3	0.595	0.995	0.906
LBC	nat	cl	sat	4	6	Gammaridae	0.333	2	0	4	0.722	1.330	0.959
LBC	nat	op	dry	1	12	Chironomidae	0.333	4	0	5	0.764	1.517	0.943
LBC	nat	op	dry	2	62	Asellidae	0.661	4	0	6	0.518	1.048	0.585
LBC	nat	op	dry	3	89	Asellidae	0.461	4	0	6	0.611	1.146	0.640
LBC	nat	op	dry	4	82	Asellidae	0.720	1	0	7	0.453	0.958	0.493
LBC	nat	op	sat	1	19	Oligochaeta	0.474	5	0	6	0.687	1.407	0.785
LBC	nat	op	sat	2	14	Oligochaeta	0.286	4	0	5	0.745	1.451	0.901
LBC	nat	op	sat	3	13	Chironomidae	0.462	6	0	3	0.568	0.911	0.829
LBC	nat	op	sat	4	8	Gammaridae	0.375	3	0	3	0.656	1.082	0.985
LBC	ref	cl	dry	1	33	Asellidae	0.667	0	0	5	0.520	1.050	0.652
LBC	ref	cl	dry	2	33	Asellidae	0.879	1	0	4	0.222	0.495	0.357
LBC	ref	cl	dry	3	84	Chironomidae	0.250	21	0	11	0.826	1.915	0.799
LBC	ref	cl	dry	4	23	Asellidae	0.652	3	0	4	0.526	0.985	0.711
LBC	ref	cl	sat	1	38	Gammaridae	0.447	3	0	7	0.716	1.515	0.778
LBC	ref	cl	sat	2	9	Asellidae	0.333	0	0	4	0.716	1.311	0.946
LBC	ref	cl	sat	3	36	Asellidae	0.639	3	0	4	0.522	0.939	0.678
LBC	ref	op	dry	1	116	Asellidae	0.836	3	0	9	0.295	0.746	0.340
LBC	ref	op	dry	2	372	Asellidae	0.702	3	0	12	0.731	1.592	0.641
LBC	ref	op	dry	3	39	Asellidae	0.282	9	0	6	0.763	1.528	0.853
LBC	ref	op	dry	4	16	Asellidae	0.563	1	0	5	0.609	1.190	0.739
LBC	ref	op	sat	1	15	Sphaeriidae	0.333	3	0	6	0.791	1.675	0.935
LBC	ref	op	sat	2	123	Asellidae	0.683	5	0	6	0.476	0.900	0.502
LBC	ref	op	sat	3	132	Asellidae	0.750	5	0	6	0.411	0.850	0.474
QC	nat	cl	dry	3	30	Chironomidae	0.767	23	0	3	0.371	0.639	0.582
QC	nat	cl	sat	2	1	Chironomidae	1.000	1	0	1	0.000	0.000	
QC	nat	op	dry	1	4	Chironomidae	0.750	3	1	2	0.375	0.562	0.811
QC	nat	op	dry	3	12	Chironomidae	0.500	6	0	4	0.653	1.199	0.865
QC	nat	op	sat	2	4	Chironomidae	1.000	4	0	2	0.375	0.562	0.811

QC	nat	op	sat	3	4	Chironomidae	0.500	2	0	3	0.625	1.040	0.946
QC	ref	cl	dry	3	25	Chironomidae	0.680	17	0	3	0.458	0.747	0.680
QC	ref	cl	sat	1	36	Oligochaeta	0.361	6	0	6	0.722	1.439	0.803
QC	ref	op	dry	3	24	Chironomidae	0.292	7	0	5	0.757	1.477	0.917
QC	ref	op	sat	3	22	Chironomidae	0.864	19	0	3	0.244	0.485	0.442

Site location: QC = Quanicassee (Bay City), EB = East Bay (Traverse City), LBC = Little Black Creek (Muskegon)
Sediment type: nat = site sediment, ref = from Raisin River
Hyporheic conditions: op = open to hyporheic flow, cl = closed to hyporheic flow
Drying: dry = sediments in dry conditions for 30 days, sat = sediments continuously saturated

Appendix P. Chapter 4 porewater chemistry, including: Fe, Mn, Zn, dissolved oxygen (DO), Eh, pH, Fe^{2+} and hardness.

Site	Day	Hyp	Drying	Sediment	Rep	Fe (mg/L)	Mn (mg/L)	Zn (µg/L)	DO (mg/L)	Eh (mV)	pH	Fe^{2+} (mg/L)	Hardness (mg/L CO_3)
EB	d9	op	dry	nat	1	40.22	0.99	17.77	1.28	-139.9	6.83	2.194	1178.2
EB	d9	op	dry	nat	2	21.28	0.96	18.06	2.01	-101.3	6.83	0.000	899.6
EB	d9	op	dry	nat	3	45.02	0.99	10.66	1.80	-122.6	6.71	5.001	1243.5
EB	d9	cl	dry	nat	1	27.39	0.73	10.96	1.14	-130.6	6.91	2.364	1181.1
EB	d9	cl	dry	nat	2	19.87	0.89	10.05	2.09	-120.0	6.96	0.752	1160.2
EB	d9	cl	dry	nat	3	23.74	0.92	10.98	1.79	-130.8	6.95	0.273	1270.2
EB	d9	op	sat	nat	1	26.46	0.70	9.84	2.05	-103.6	6.76	4.151	663.5
EB	d9	op	sat	nat	2	19.92	0.73	16.78	3.12	-84.1	6.73	4.151	678.5
EB	d9	op	sat	nat	3	14.10	0.50	5.55	3.41	-73.8	7.03	2.613	541.3
EB	d9	cl	sat	nat	1	19.38	0.63	6.55	2.81	-98.0	6.87	3.921	495.0
EB	d9	cl	sat	nat	2	23.45	0.90	10.22	2.49	-105.9	6.78	3.118	694.1
EB	d9	cl	sat	nat	3	9.99	0.48	5.57	3.38	-83.8	6.88	0.892	486.7
EB	d9	op	dry	ref	1	3.12	12.64	5.86	3.03	-102.4	7.15	0.098	1016.0
EB	d9	op	dry	ref	2	7.31	11.37	5.70				0.344	926.7
EB	d9	op	dry	ref	3	3.73	12.40	9.27				0.209	894.2
EB	d9	cl	dry	ref	1	5.44	21.10	11.34	3.11	-93.1	7.05	0.360	1499.5
EB	d9	cl	dry	ref	2	5.46	18.82	9.67				0.750	1428.2
EB	d9	cl	dry	ref	3	6.15	21.40	8.60				0.521	2359.0
EB	d9	op	sat	ref	1	42.56	10.27	8.75	1.10	-139.2	6.85	1.498	1043.6
EB	d9	op	sat	ref	2	41.03	10.28	5.69				12.505	951.9
EB	d9	op	sat	ref	3	43.88	11.61	11.10				12.826	1212.1
EB	d9	cl	sat	ref	1	14.74	2.44	7.78	2.73	-96.9	7.21	2.429	1044.4
EB	d9	cl	sat	ref	2	16.60	3.06	9.79				1.076	1229.7
EB	d9	cl	sat	ref	3	17.13	3.01	7.40				0.830	1245.2
EB	d1	op	dry	nat	1	0.17	0.17	21.93	4.18	-18.7	7.30	0.020	154.7
EB	d1	op	dry	nat	2	0.59	0.69	25.20	5.17	-19.8	7.30	0.057	173.7
EB	d1	op	dry	nat	3	6.91	1.26	11.31	3.44	-93.4	7.01	0.057	227.6
EB	d1	cl	dry	nat	1	2.12	1.18	19.75	3.04	-71.7	6.97	0.283	310.3

EB	d1	cl	dry	nat	2	0.42	0.76	25.93	3.85	-44.3	6.91	0.232	269.6
EB	d1	cl	dry	nat	3	1.42	1.45	23.72	4.77	-64.3	6.83	0.389	353.5
EB	d1	op	sat	nat	1	26.95	0.74	8.88	3.07	-94.6	6.85	6.789	209.6
EB	d1	op	sat	nat	2	24.04	0.82	12.28	2.28	-92.3	6.81	4.454	213.5
EB	d1	op	sat	nat	3	20.19	0.67	7.29	3.05	-101.7	6.88	2.367	151.4
EB	d1	cl	sat	nat	1	27.90	0.92	14.95	2.36	-109.2	6.72	4.930	203.5
EB	d1	cl	sat	nat	2	28.09	1.14	13.65	2.30	-109.7	6.71	4.842	266.9
EB	d1	cl	sat	nat	3	13.48	0.57	6.61	3.93	-88.3	6.87		167.5
EB	d1	op	dry	ref	1	0.20	0.12	15.11	4.03	-52.1	6.98	0.004	172.8
EB	d1	op	dry	ref	2	0.06	0.14	20.36				0.000	158.4
EB	d1	op	dry	ref	3	0.36	0.28	14.10				0.004	160.0
EB	d1	cl	dry	ref	1	0.07	0.12	7.02	3.55	-31.1	6.90	0.004	369.4
EB	d1	cl	dry	ref	2	0.07	0.27	8.48				0.000	352.7
EB	d1	cl	dry	ref	3	0.67	0.20	6.15				0.033	410.3
EB	d1	op	sat	ref	1	36.23	11.23	9.31	1.79	-147.6	6.85	10.484	215.9
EB	d1	op	sat	ref	2	39.68	6.39	7.60				10.374	273.3
EB	d1	op	sat	ref	3	43.91	6.32	6.10				10.042	216.2
EB	d1	cl	sat	ref	1	16.35	2.86	7.93	1.98	-125.8	7.07	4.997	211.3
EB	d1	cl	sat	ref	2	20.83	8.17	7.36				2.518	269.5
EB	d1	cl	sat	ref	3	19.96	8.43	6.50				2.430	247.8
EB	d6	op	dry	nat	1	28.42	0.97	8.97	1.96	-118.0	6.90	1.331	285.5
EB	d6	op	dry	nat	2	23.93	1.21	8.83	2.77	-103.4	6.87	1.703	299.4
EB	d6	op	dry	nat	3	45.67	1.03	6.09	1.73	-123.0	6.73	5.169	349.9
EB	d6	cl	dry	nat	1	18.30	0.68	6.89	2.64	-115.8	7.02	0.868	317.3
EB	d6	cl	dry	nat	2	16.15	1.04	9.36	2.78	-117.9	7.03	1.049	345.5
EB	d6	cl	dry	nat	3	19.89	1.07	7.95	2.23	-113.3	6.94	2.542	385.9
EB	d6	op	sat	nat	1	25.63	0.72	8.27	2.46	-95.1	6.70	7.263	221.6
EB	d6	op	sat	nat	2	16.80	0.65	54.31	3.76	-85.1	6.72	5.756	182.3
EB	d6	op	sat	nat	3	16.51	0.57	5.21	3.45	-80.7	6.64	1.730	181.0
EB	d6	cl	sat	nat	1	19.66	0.67	4.18	3.07	-92.3	6.79	6.486	158.1
EB	d6	cl	sat	nat	2	25.22	1.03	5.09	3.45	-97.9	6.76	5.803	248.9

EB	d6	cl	sat	nat	3	9.33	0.44	3.31	2.92	-72.9	6.46	1.141	151.5
EB	d6	op	dry	ref	1	1.69	8.84	3.05	3.52	-98.0	7.19	0.095	333.2
EB	d6	op	dry	ref	2	1.48	10.15	9.98				0.161	349.5
EB	d6	op	dry	ref	3	5.18	9.12	4.59				0.512	317.0
EB	d6	cl	dry	ref	1	4.53	17.02	7.51	3.05	-89.6	7.07	0.872	480.9
EB	d6	cl	dry	ref	2	3.95	17.36	9.27				0.882	499.3
EB	d6	cl	dry	ref	3	3.82	13.94	6.70				1.263	508.1
EB	d6	op	sat	ref	1	39.09	11.12	5.96	1.61	-127.6	6.86	6.557	245.8
EB	d6	op	sat	ref	2	39.05	11.09	6.21				8.040	246.2
EB	d6	op	sat	ref	3	42.96	12.34	3.39				7.899	302.9
EB	d6	cl	sat	ref	1	15.10	2.61	4.58	3.32	-100.4	7.07	1.612	240.3
EB	d6	cl	sat	ref	2	18.48	7.20	6.94				2.224	332.9
EB	d6	cl	sat	ref	3	17.70	3.23	5.70				1.636	287.8
EB	d30	op	dry	nat	1	38.12	0.89	12.96					848.5
EB	d30	op	dry	nat	2	21.20	0.64	14.79					703.7
EB	d30	op	dry	nat	3	27.35	0.66	16.50					1016.1
EB	d30	cl	dry	nat	1	21.06	0.56	15.02					948.1
EB	d30	cl	dry	nat	2	30.24	0.93	14.87					1536.2
EB	d30	cl	dry	nat	3	35.51	0.86	18.93					1593.7
EB	d30	op	sat	nat	1	28.92	0.71	18.35					889.7
EB	d30	op	sat	nat	2	21.03	0.67	14.61					826.9
EB	d30	op	sat	nat	3	22.65	0.75	12.94					1076.2
EB	d30	cl	sat	nat	1	16.36	0.58	17.29					720.2
EB	d30	cl	sat	nat	2	23.90	0.96	14.84					1061.4
EB	d30	cl	sat	nat	3	9.00	0.42	9.19					664.3
EB	d30	op	dry	ref	1	14.83	8.52	42.47					750.3
EB	d30	cl	dry	ref	1	14.03	10.50	49.75					2286.0
EB	d30	op	sat	ref	1	71.24	8.16	14.58					1288.5
EB	d30	cl	sat	ref	1	17.58	2.68	12.46					1021.7
QC	d1	op	dry	nat	1	8.76	0.82	39.96	4.44	-44.6	6.35		1141.7
QC	d1	op	dry	nat	2	5.63	0.56	11.23	3.98	-63.4	6.41		970.4

QC	d1	op	dry	nat	3	6.82	0.66	7.94	3.15	-70.3	6.27		1023.5
QC	d1	cl	dry	nat	1	23.89	1.45	27.64	2.40	-98.5	6.42		1154.3
QC	d1	cl	dry	nat	2	29.03	1.70	1.45	2.28	-90.3	6.29		1344.9
QC	d1	cl	dry	nat	3	17.06	1.28	3.99	2.44	-103.4	6.48		976.2
QC	d1	op	sat	nat	1	16.34	1.16	8.04	3.81	-94.4	6.68		1370.1
QC	d1	op	sat	nat	2	18.42	1.38	5.17	3.34	-89.6	6.56		1575.3
QC	d1	op	sat	nat	3	23.17	1.69	35.95	5.41	-80.1	6.66		1553.8
QC	d1	cl	sat	nat	1	18.17	1.12	10.91	3.68	-75.3	6.31		1409.9
QC	d1	cl	sat	nat	2	14.24	1.00	12.95	2.92	-81.0	6.40		1399.4
QC	d1	cl	sat	nat	3	11.00	0.76	0.00	3.20	-85.4	6.39		1264.1
QC	d1	op	dry	ref	1	23.04	3.08	6.59	2.92	-129.4	6.61		1282.2
QC	d1	op	dry	ref	2	28.89	2.77	15.38					1176.6
QC	d1	op	dry	ref	3	22.60	4.01	4.05					1382.8
QC	d1	cl	dry	ref	1	6.23	5.88	11.69	2.93	-108.4	6.57		1637.1
QC	d1	cl	dry	ref	2	3.38	3.15	47.46					1510.6
QC	d1	cl	dry	ref	3	2.34	3.55	3.58					1518.2
QC	d1	op	sat	ref	1	49.18	3.89	26.68	2.64	-128.4	6.53		1355.4
QC	d1	op	sat	ref	2								1738.1
QC	d1	op	sat	ref	3	58.85	5.97	15.64					1589.6
QC	d1	cl	sat	ref	1	29.79	3.66	0.00	2.65	-143.1	6.62		1700.1
QC	d1	cl	sat	ref	2	27.42	3.70	5.81					1789.9
QC	d1	cl	sat	ref	3	32.48	4.35	1.11					1632.7
QC	d5	op	dry	nat	1	14.12	1.04	21.22	3.38	-70.0	6.54	0.989	1244.9
QC	d5	op	dry	nat	2	9.31	0.77	11.60	4.34	-65.5	6.54	1.257	1177.0
QC	d5	op	dry	nat	3	11.66	0.91	6.79	5.47	-78.4	6.70	2.058	1197.9
QC	d5	cl	dry	nat	1	25.76	1.49	13.40	2.77	-84.4	6.44	5.341	1086.9
QC	d5	cl	dry	nat	2	29.33	1.65	5.21	2.61	-82.1	6.47	7.366	1136.7
QC	d5	cl	dry	nat	3	19.82	1.32	133.29	2.75	-95.1	6.59	5.582	956.9
QC	d5	op	sat	nat	1	16.64	1.19	4.12	3.97	-58.7	6.41	9.610	1266.4
QC	d5	op	sat	nat	2	16.34	1.21	24.03	3.75	-66.7	6.49		1323.6
QC	d5	op	sat	nat	3	20.70	1.53	7.07	4.50	-55.3	6.30	2.963	1306.7

QC	d5	cl	sat	nat	1	16.90	1.08	10.74	3.93	-73.5	6.57	5.054	1277.7
QC	d5	cl	sat	nat	2	15.44	1.01	8.44	4.39	-71.3	6.58	5.887	1220.3
QC	d5	cl	sat	nat	3	10.82	0.76	2.62	3.87	-77.5	6.56	4.108	1109.6
QC	d5	op	dry	ref	1	37.61	4.65	5.83	2.70	-130.1	6.71	1.817	1434.6
QC	d5	op	dry	ref	2	39.16	3.90	7.87					1438.4
QC	d5	op	dry	ref	3	38.80	5.35	22.13				2.290	
QC	d5	cl	dry	ref	1	20.98	7.21	19.52	3.36	-122.5	6.89	0.300	1490.2
QC	d5	cl	dry	ref	2	12.00	5.92	13.70					1641.4
QC	d5	cl	dry	ref	3	11.35	6.17	16.21				0.043	1887.4
QC	d5	op	sat	ref	1	59.83	4.25	9.85	1.38	-147.6	6.77	0.917	1884.4
QC	d5	op	sat	ref	2	62.85	5.90	25.02					1808.5
QC	d5	op	sat	ref	3	76.01	7.27	0.00				1.416	
QC	d5	cl	sat	ref	1	32.25	3.64	13.75	2.40	-132.9	6.91	0.214	1479.1
QC	d5	cl	sat	ref	2	33.83	4.59	8.92					1835.2
QC	d5	cl	sat	ref	3	24.55	3.02	9.99				0.223	1411.9
QC	d9	op	dry	nat	1	17.00	1.12	12.38	2.62	-85.6	NA	0.398	1602.4
QC	d9	op	dry	nat	2	11.05	0.84	9.58	2.58	-87.0	NA	0.316	1476.5
QC	d9	op	dry	nat	3	15.52	1.07	15.80	2.63	-97.5	NA	0.486	1629.1
QC	d9	cl	dry	nat	1	26.44	1.50	10.23	2.40	-104.2	NA	1.692	1299.1
QC	d9	cl	dry	nat	2	30.29	1.66	9.68	2.36	-91.7	NA	2.258	1312.2
QC	d9	cl	dry	nat	3	16.54	1.03	19.51	2.38	-104.5	NA	1.635	1200.7
QC	d9	op	sat	nat	1	16.13	1.11	16.00	3.84	-83.9	NA	0.786	1380.1
QC	d9	op	sat	nat	2	18.88	1.35	18.70	3.06	-92.9	NA	1.154	1568.8
QC	d9	op	sat	nat	3	19.80	1.35	15.34	2.45	-77.5	NA	1.380	1309.0
QC	d9	cl	sat	nat	1	18.70	1.11	19.27	2.71	-100.6	NA	1.720	1494.4
QC	d9	cl	sat	nat	2	13.42	0.95	12.13	3.27	-81.7	NA	4.096	1386.7
QC	d9	cl	sat	nat	3	10.84	0.73	13.72	2.58	-83.6	NA	2.503	1260.5
QC	d9	op	dry	ref	1	26.91	6.65	12.02	2.55	-122.9	NA	3.510	1872.1
QC	d9	op	dry	ref	2	18.84	5.79	11.68				3.587	1930.7
QC	d9	op	dry	ref	3	17.15	6.14	18.01				4.012	2025.2
QC	d9	cl	dry	ref	1	51.21	5.53	16.33	0.65	-135.3	NA	15.894	1885.4

QC	d9	cl	dry	ref	2	61.81	7.28	9.58				5.964	1879.4
QC	d9	cl	dry	ref	3	59.38	5.25	11.65				20.392	1833.6
QC	d9	op	sat	ref	1	71.00	4.10	17.51	0.82	-157.3	NA	25.768	1807.4
QC	d9	op	sat	ref	2	92.72	7.98	20.68				29.870	2575.3
QC	d9	op	sat	ref	3	67.14	5.82	25.39				15.555	1788.6
QC	d9	cl	sat	ref	1	28.70	2.98	11.13	1.10	-131.6	NA	3.276	1363.5
QC	d9	cl	sat	ref	2	26.09	2.95	16.25				0.749	1469.0
QC	d9	cl	sat	ref	3	30.70	4.25	20.55				0.865	1881.7
QC	d30	op	dry	nat	1	12.90	0.96	33.30					1384.7
QC	d30	op	dry	nat	2	10.41	0.86	36.78					1525.3
QC	d30	op	dry	nat	3	12.92	0.91	38.40					1351.8
QC	d30	cl	dry	nat	1	21.94	1.36	29.92					1305.8
QC	d30	cl	dry	nat	2	23.42	1.41	36.59					1324.0
QC	d30	cl	dry	nat	3	19.68	1.35	21.07					1281.9
QC	d30	op	sat	nat	1	13.47	0.94	11.69					1282.4
QC	d30	op	sat	nat	2	18.85	1.35	15.11					1555.5
QC	d30	op	sat	nat	3	8.64	0.66	24.71					1107.4
QC	d30	cl	sat	nat	1	18.61	1.18	19.33					1477.9
QC	d30	cl	sat	nat	2	14.04	0.96	20.46					1372.1
QC	d30	cl	sat	nat	3	10.04	0.75	24.29					1223.2
QC	d30	op	dry	ref	1	73.92	6.85	23.40					1737.6
QC	d30	cl	dry	ref	1	37.72	7.05	26.87					2028.3
QC	d30	op	sat	ref	1	69.19	2.65	27.01					1305.2
QC	d30	cl	sat	ref	1	19.59	2.34	8.74					1218.5
LBC	d1	op	dry	nat	1	57.94	4.49	29.01	2.78	-89.6	6.72	9.863	594.9
LBC	d1	op	dry	nat	2	46.63	3.21	38.82	2.51	-75.3	6.60	4.871	521.4
LBC	d1	op	dry	nat	3	38.92	4.08	29.47	2.26	-73.9	6.75	8.025	189.9
LBC	d1	cl	dry	nat	1	0.59	0.02	278.36	3.45	-51.6	6.76	0.000	2583.7
LBC	d1	cl	dry	nat	2	2.38	0.09	149.76	3.41	-38.1	6.74	0.000	1990.3
LBC	d1	cl	dry	nat	3	31.34	4.49	20.25	1.65	-146.4	7.04	0.939	1357.9
LBC	d1	op	sat	nat	1	59.30	5.72	21.06	2.14	-114.7	6.71	3.163	1356.4

157

LBC	d1	op	sat	nat	2	57.32	4.86	19.48	2.15	-94.8	6.60	13.343	837.7
LBC	d1	op	sat	nat	3	58.88	5.23	23.52	2.26	-116.8	6.78	12.435	1227.5
LBC	d1	cl	sat	nat	1	54.19	6.44	18.95	0.84	-147.5	6.88	14.187	1504.3
LBC	d1	cl	sat	nat	2	52.72	6.30	13.61	1.86	-132.5	6.87	8.911	1489.3
LBC	d1	cl	sat	nat	3	49.68	4.64	24.40	1.95	-134.5	6.87	5.214	1311.0
LBC	d1	op	dry	ref	1	81.64	8.57	28.47	2.24	-126.2	6.87	4.296	898.8
LBC	d1	op	dry	ref	2	70.68	8.84	25.85				24.154	620.9
LBC	d1	op	dry	ref	3	45.63	5.19	30.50				15.830	611.5
LBC	d1	cl	dry	ref	1	0.76	5.18	21.06	2.97	-33.8	7.29	0.018	1693.4
LBC	d1	cl	dry	ref	2	2.68	2.84	50.62					802.3
LBC	d1	cl	dry	ref	3	0.25	6.09	20.25					1956.3
LBC	d1	op	sat	ref	1	89.24	6.94	17.48	0.87	-165.3	6.84	5.864	1584.4
LBC	d1	op	sat	ref	2	84.62	6.19	18.30				19.397	1388.1
LBC	d1	op	sat	ref	3	79.69	6.52	21.83				27.505	1493.4
LBC	d1	cl	sat	ref	1	64.27	6.43	22.28	1.13	-148.3	6.93	10.684	1962.1
LBC	d1	cl	sat	ref	2	36.82	3.73	81.35					877.5
LBC	d1	cl	sat	ref	3	71.12	7.51	17.21					2178.6
LBC	d5	op	dry	nat	1	52.83	3.73	26.18	2.15	-114.3	6.69	3.183	587.7
LBC	d5	op	dry	nat	2	57.75	3.33	36.82	2.57	-72.6	6.64	3.546	532.7
LBC	d5	op	dry	nat	3	30.14	2.96	31.32	3.16	-84.1	6.74	2.884	323.9
LBC	d5	cl	dry	nat	1	0.46	2.79	313.52	4.64	-39.6	6.76	0.021	1849.9
LBC	d5	cl	dry	nat	2	1.51	4.29	171.78	3.43	-60.5	6.77	0.026	1645.6
LBC	d5	cl	dry	nat	3	34.46	4.49	16.64	2.13	-144.4	7.05	0.438	1110.4
LBC	d5	op	sat	nat	1	48.87	4.28	33.68	3.76	-107.0	6.47	9.465	820.1
LBC	d5	op	sat	nat	2	42.92	3.33	28.49	3.08	-100.1	6.55	14.758	528.5
LBC	d5	op	sat	nat	3	54.28	4.33	29.42	2.72	-108.8	6.67	8.599	823.5
LBC	d5	cl	sat	nat	1	56.14	6.30	16.37	2.28	-133.8	6.81	6.350	1163.0
LBC	d5	cl	sat	nat	2	53.67	6.05	23.26	2.34	-122.1	6.72	14.407	1076.7
LBC	d5	cl	sat	nat	3	42.31	3.87	36.20	2.29	-126.3	6.76	15.507	899.4
LBC	d5	op	dry	ref	1	96.73	7.97	24.43	1.11	-131.8	6.72	3.712	714.2
LBC	d5	op	dry	ref	2	86.30	8.38	26.56				6.069	613.8

LBC	d5	op	dry	ref	3	75.82	6.43	23.88				4.641	622.1
LBC	d5	cl	dry	ref	1	3.74	7.62	24.77	1.85	-97.3	7.08		1260.7
LBC	d5	cl	dry	ref	2	22.05	6.46	35.29				0.078	1223.7
LBC	d5	cl	dry	ref	3	2.00	9.04	23.80					1346.1
LBC	d5	op	sat	ref	1	62.02	4.74	36.89	1.73	-120.0	6.72	1.901	828.8
LBC	d5	op	sat	ref	2	67.77	4.72	34.28				2.182	804.4
LBC	d5	op	sat	ref	3	65.03	4.96	24.64				2.276	822.3
LBC	d5	cl	sat	ref	1	67.57	6.26	34.04	0.54	-178.9	6.76		1299.8
LBC	d5	cl	sat	ref	2	66.84	6.58	24.89				5.232	1192.8
LBC	d5	cl	sat	ref	3	68.16	6.86	18.56					1402.5
LBC	d9	op	dry	nat	1	75.52	5.43	8.47	1.69	-101.1	6.36	14.557	1142.1
LBC	d9	op	dry	nat	2	68.93	3.80	10.33	1.52	-96.5	6.73	15.222	867.4
LBC	d9	op	dry	nat	3	34.47	3.13	7.15	2.63	-93.0	6.59	3.816	518.7
LBC	d9	cl	dry	nat	1	3.87	6.03	249.24	3.29	-73.3	6.72	0.468	2707.3
LBC	d9	cl	dry	nat	2	6.23	5.05	99.46	4.05	-45.8	6.58	0.098	2266.4
LBC	d9	cl	dry	nat	3				2.08	-122.1	6.75	1.441	
LBC	d9	op	sat	nat	1	34.98	3.26	699.03	3.27	-103.4	6.54	10.960	913.4
LBC	d9	op	sat	nat	2	59.32	4.16	225.50	2.99	-101.1	6.58	13.202	1115.8
LBC	d9	op	sat	nat	3	66.86	4.98	8.31	3.50	450.0	0.62	20.789	1405.4
LBC	d9	cl	sat	nat	1	58.16	6.20	4.53	1.63	-125.7	6.78	9.975	1748.0
LBC	d9	cl	sat	nat	2	54.64	6.03	27.48	2.11	-119.4	6.30	10.197	1592.4
LBC	d9	cl	sat	nat	3	43.60	3.82	12.03	2.53	-106.6	6.67	9.236	1272.9
LBC	d9	op	dry	ref	1	95.18	7.57	23.71	1.10	-115.5	6.87	10.049	984.4
LBC	d9	op	dry	ref	2	99.91	8.81	16.50				12.389	961.8
LBC	d9	op	dry	ref	3	84.75	6.61	0.34				10.246	934.0
LBC	d9	cl	dry	ref	1	6.40	8.96	5.18	1.95	-69.6	6.94	0.029	2130.8
LBC	d9	cl	dry	ref	2	30.87	5.25	6.09					1501.0
LBC	d9	cl	dry	ref	3	3.73	10.09	24.52				0.015	2228.0
LBC	d9	op	sat	ref	1	71.84	5.17	16.84	1.90	-101.6	6.52	2.141	1440.8
LBC	d9	op	sat	ref	2	72.77	5.10	2.05				3.299	1452.6
LBC	d9	op	sat	ref	3	67.80	5.35	11.45				2.535	1365.5

LBC	d9	cl	sat	ref	1	44.96	5.75	64.43	1.84	-110.6	6.75	0.000	2193.4
LBC	d9	cl	sat	ref	2	68.66	6.41	23.11				7.117	1832.6
LBC	d9	cl	sat	ref	3	73.73	6.86	7.96				2.215	2136.3
LBC	d30	op	dry	nat	1	36.93	1.48	23.15					1266.2
LBC	d30	op	dry	nat	2	72.65	3.59	17.67					1152.2
LBC	d30	op	dry	nat	3	58.50	5.34	13.45					948.0
LBC	d30	cl	dry	nat	1	32.05	6.56	51.36					2623.8
LBC	d30	cl	dry	nat	2	23.29	5.06	7109.98					2061.0
LBC	d30	cl	dry	nat	3	40.34	4.01	2257.19					1368.3
LBC	d30	op	sat	nat	1	61.08	3.98	15.15					1542.3
LBC	d30	op	sat	nat	2	59.72	2.91	22.83					1263.4
LBC	d30	op	sat	nat	3	76.15	3.44	15.91					1540.0
LBC	d30	cl	sat	nat	1	60.55	5.67	17.33					1581.1
LBC	d30	cl	sat	nat	2	50.39	6.70	14.40					1883.4
LBC	d30	cl	sat	nat	3	39.37	3.35	6473.80					1132.0
LBC	d30	op	dry	ref	1	103.91	6.50	43.23					1102.2
LBC	d30	cl	dry	ref	1	14.25	9.10	27.32					2125.7
LBC	d30	op	sat	ref	1	62.41	2.93	24.76					1316.0
LBC	d30	cl	sat	ref	1	86.84	6.25	495.96					1976.5

Site location: QC = Quanicassee (Bay City), EB = East Bay (Traverse City), LBC = Little Black Creek (Muskegon)
Sediment type: nat = site sediment, ref = from Raisin River
Hyporheic conditions, op = open to hyporheic flow, cl = closed to hyporheic flow
Drying: dry = sediments in dry conditions for 30 days, sat = sediments continuously saturated
Hardness units: mg/L of $CaCO_3$ + $MgCO_3$

Appendix Q. Chapter 4 sediment chemistry (AVS, SEM, fOC, (SEM-AVS)/*f*OC, total Fe, Mn, Zn).

| Site | Day | Hyporheic | Drying | Sediment | AVS, S^{2-} (µmol/g) | (SEM-AVS)/*f*OC | | | Total Metals | | |
						SEM (µmol/g)	*f*OC	SEM-AVS /*f*OC	Fe (mg/kg)	Mn (mg/kg)	Zn (mg/kg)
QC	initial			nat	0.197	0.290	0.010	7.60			
EB	initial			nat	5.041	0.190	0.020	-203.25			
EB	initial			ref	0.133	0.090	0.010	-3.58			
QC	d0	op	dry	nat	0.038	0.110	0.010	5.79	1661.23	28.75	13.15
QC	d0	op	dry	nat	0.038	0.170	0.020	8.91	1881.61	27.34	14.63
QC	d0	op	dry	nat	-0.012	0.120	0.010	12.96	1730.12	25.41	9.39
QC	d0	cl	dry	nat	0.081	0.050	0.010	-2.13	1660.23	29.09	10.78
QC	d0	cl	dry	nat	0.029	0.120	0.020	5.71	1734.27	34.48	12.07
QC	d0	cl	dry	nat	0.003	0.280	0.020	17.99	1518.67	28.41	10.49
QC	d0	op	sat	nat	0.398	0.070	0.010	-25.48	1707.34	30.65	10.82
QC	d0	cl	sat	nat	0.689	0.030	0.020	-41.68	1867.46	26.05	11.10
QC	d0	op	dry	ref	0.149	0.130	0.010	-3.12	7381.40	206.03	16.91
QC	d0	op	sat	ref	0.514	0.070	0.020	-21.86	9201.10	256.08	26.60
QC	d0	cl	dry	ref	0.090	0.100	0.020	0.63	8349.09	243.64	20.82
QC	d0	cl	sat	ref	0.292	0.020	0.010	-23.41	7410.64	200.75	16.66
QC	d10	op	dry	nat	2.031	0.290	0.030	-55.10	2925.43	61.83	0.00
QC	d10	op	dry	nat	0.377	0.130	0.020	-11.30	1810.70	36.58	4.72
QC	d10	op	dry	nat	0.703	0.500	0.050	-4.25	3566.06	82.14	5.78
QC	d10	cl	dry	nat	0.354	0.040	0.030	-11.27	1367.39	27.82	3.85
QC	d10	cl	dry	nat	0.431	0.260	0.040	-3.85	1558.71	32.51	4.02
QC	d10	cl	dry	nat	1.067	0.220	0.040	-23.56	2095.37	43.74	2.20
QC	d10	op	sat	nat	0.706	0.240	0.030	-16.58	1795.08	43.88	3.49
QC	d10	cl	sat	nat	0.892	0.060	0.030	-25.00	1872.46	47.01	4.48
QC	d10	op	dry	ref	0.580	0.080	0.030	-18.07	5568.53	176.70	5.77
QC	d10	cl	dry	ref	2.175	0.080	0.030	-60.59	6319.57	201.11	3.51
QC	d10	op	sat	ref	1.241	0.120	0.040	-27.65	6844.66	236.32	0.00

QC	d10	cl	sat	ref	1.204	0.310	0.050	-18.82			
QC	d26	op	dry	nat	1.080	0.250	0.020	-35.24	2162.94	37.71	20.33
QC	d26	op	dry	nat	0.525	0.130	0.020	-21.15	1929.44	33.52	14.14
QC	d26	op	dry	nat	0.342	0.120	0.010	-16.39	1856.25	37.63	11.35
QC	d26	cl	dry	nat	0.299	0.040	0.010	-23.47	1412.87	21.59	12.49
QC	d26	cl	dry	nat	0.278	0.090	0.010	-13.83	1591.90	24.63	11.11
QC	d26	cl	dry	nat	0.327	0.090	0.010	-20.29	1722.79	26.91	13.32
QC	d26	op	sat	nat	1.250	0.120	0.020	-68.71	2195.52	41.53	12.25
QC	d26	op	sat	nat	0.219	0.000	0.010	-19.09	1495.73	26.88	23.64
QC	d26	cl	sat	nat	0.624	0.050	0.080	-7.42	1681.40	33.80	13.42
QC	d26	op	dry	ref	0.329	0.110	0.010	-16.64	6471.89	189.29	3.80
QC	d26	cl	dry	ref	1.551	0.080	0.040	-39.88	6600.47	188.64	18.08
QC	d26	op	sat	ref	0.556	0.080	0.020	-20.01	5009.06	155.18	16.69
QC	d26	cl	sat	ref	0.935	0.120	0.020	-41.87	13392.29	309.73	21.97
EB	d0	op	dry	nat	0.015	0.080	0.020	4.13	1417.93	33.16	0.00
EB	d0	op	dry	nat	0.005	0.330	0.020	16.53	1446.95	45.74	2.81
EB	d0	op	dry	nat	0.014	0.000	0.010	-1.64	1352.26	33.19	0.00
EB	d0	cl	dry	nat	-0.027	0.070	0.010	14.98	1290.63	33.27	0.00
EB	d0	cl	dry	nat	0.009	0.080	0.010	5.53	1380.31	35.23	0.00
EB	d0	cl	dry	nat	0.009	0.000	0.010	-1.16	1051.31	26.64	0.00
EB	d0	op	sat	nat	2.097	0.130	0.020	-108.56	1848.43	45.38	3.71
EB	d0	cl	sat	nat	2.596	0.110	0.030	-96.72	2113.17	59.86	0.00
EB	d0	op	dry	ref	0.058	0.150	0.020	4.28	6124.52	248.94	4.44
EB	d0	cl	dry	ref	0.138	0.130	0.010	-0.84	5368.67	223.27	4.77
EB	d0	op	sat	ref	1.239	0.120	0.030	-44.24	5713.37	214.75	5.67
EB	d0	cl	sat	ref	1.517	0.090	0.010	-111.69	5670.84	191.03	4.07
EB	d10	op	dry	nat	14.447	0.430	0.080	-175.33	4315.25	141.61	0.00
EB	d10	op	dry	nat	0.816	0.340	0.060	-8.11	3025.80	93.30	0.00
EB	d10	op	dry	nat	0.678	0.000	0.020	-31.93	1447.35	54.65	0.00
EB	d10	cl	dry	nat	4.340	0.200	0.070	-55.24	3683.69	97.88	0.00
EB	d10	cl	dry	nat	7.225	0.320	0.050	-139.86	3121.87	80.67	0.00

EB	d10	cl	dry	nat	8.206	0.040	0.090	-94.63	4328.12	107.91	0.00
EB	d10	op	sat	nat	10.440	13.720	0.030	96.01	2257.70	77.11	0.00
EB	d10	op	sat	nat	2.209	0.190	0.020	-89.18	1736.12	58.55	0.00
EB	d10	cl	sat	nat	4.431	0.180	0.010	-458.41	1512.91	45.24	0.00
EB	d10	op	dry	ref	15.654	0.560	0.100	-155.52	6970.29	209.89	0.00
EB	d10	cl	dry	ref	3.238	0.200	0.040	-74.92	6970.29	209.89	0.00
EB	d10	op	sat	ref	7.747	0.290	0.040	-202.94	6018.92	230.77	0.00
EB	d10	cl	sat	ref	0.715	0.170	0.010	-58.40	6554.32	222.73	0.00
EB	d30	op	dry	nat	1.572	0.100	0.010	-122.32	2723.08	62.68	0.00
EB	d30	op	dry	nat	1.228	0.030	0.030	-47.79	1808.43	58.06	0.00
EB	d30	op	dry	nat	2.354	0.000	0.030	-73.00	2326.79	59.68	0.00
EB	d30	cl	dry	nat	0.733	0.110	0.020	-36.00	2025.61	53.62	0.00
EB	d30	cl	dry	nat	4.141	0.000	0.040	-98.40	2609.96	78.91	0.00
EB	d30	cl	dry	nat	1.416	0.050	0.020	-68.99	1786.78	51.45	0.00
EB	d30	op	sat	nat	1.900	0.100	0.020	-87.06	2412.49	58.99	0.00
EB	d30	cl	sat	nat	0.911	0.070	0.010	-87.04	1918.88	61.15	0.00
EB	d30	cl	sat	nat	1.565	0.000	0.020	-67.87	1806.19	48.83	0.00
EB	d30	op	dry	ref	2.914	0.230	0.090	-31.39	7621.63	322.90	0.00
EB	d30	cl	dry	ref	17.509	0.230	0.050	-369.32	4792.27	164.78	0.00
EB	d30	op	sat	ref	1.602	0.130	0.020	-80.89	6137.87	230.20	0.00
EB	d30	cl	sat	ref	1.539	0.170	0.010	-118.85	5450.49	187.86	0.00
LBC	d0	op	dry	nat	0.483	1.310	0.040	23.50	2132.15	171.55	0.00
LBC	d0	op	dry	nat	0.313	1.440	0.050	24.49	3064.47	164.06	27.05
LBC	d0	op	dry	nat	1.357	1.060	0.020	-13.42	1564.76	103.80	0.00
LBC	d0	cl	dry	nat	0.101	1.350	0.040	30.44	2450.29	129.50	0.00
LBC	d0	cl	dry	nat	0.240	1.040	0.030	25.59	2141.43	166.36	0.00
LBC	d0	cl	dry	nat	0.473	1.390	0.040	21.17	3504.76	241.14	0.00
LBC	d0	op	sat	nat	6.348	2.010	0.030	-126.68	2220.16	142.43	0.00
LBC	d0	cl	sat	nat	1.259	1.120	0.030	-4.32	2010.82	124.50	0.00
LBC	d0	cl	sat	nat	4.343	2.450	0.030	-63.59	2115.42	163.40	1.99
LBC	d0	op	dry	ref	0.196	0.130	0.020	-3.61	7561.35	283.79	0.00

LBC	d0	cl	dry	ref	0.041	0.000	0.010	-3.30	4600.83	156.59	0.00
LBC	d0	op	sat	ref	0.523	0.170	0.010	-25.58			
LBC	d0	cl	sat	ref	0.251	0.530	0.010	19.08	4391.58	152.53	0.00
LBC	d9	op	dry	nat	2.053	1.610	0.030	-13.09	3165.98	183.49	110.32
LBC	d9	op	dry	nat	3.250	4.770	0.120	13.10	6253.92	263.28	302.29
LBC	d9	op	dry	nat	1.761	1.420	0.040	-9.49	2172.98	112.09	74.82
LBC	d9	cl	dry	nat	0.310	1.190	0.020	41.65	2104.70	142.77	0.00
LBC	d9	cl	dry	nat	0.822	1.130	0.020	17.10	3015.12	239.41	12.97
LBC	d9	cl	dry	nat	1.097	1.860	0.030	23.76	2323.82	97.55	2.40
LBC	d9	op	sat	nat	7.867	8.830	0.090	10.15	6509.37	307.94	372.45
LBC	d9	cl	sat	nat	1.342	1.410	0.020	3.49	2232.91	127.11	70.75
LBC	d9	cl	sat	nat	1.950	3.530	0.040	43.34	2535.28	161.61	104.49
LBC	d9	op	dry	ref	0.384	0.490	0.010	7.41	6019.84	175.69	0.00
LBC	d9	cl	dry	ref	0.156	0.220	0.010	4.52	4980.52	187.41	0.00
LBC	d9	op	sat	ref	0.706	1.820	0.020	54.41	6028.14	192.87	39.53
LBC	d9	cl	sat	ref	0.676	0.350	0.010	-23.18	6471.69	188.95	0.00
LBC	d30	op	dry	nat	2.550	2.080	0.020	-20.47	2587.57	187.61	81.37
LBC	d30	op	dry	nat	3.794	2.070	0.070	-24.32	4788.54	248.93	191.00
LBC	d30	op	dry	nat	2.200	1.530	0.030	-26.62	2634.96	150.47	63.88
LBC	d30	cl	dry	nat	1.239	1.420	0.030	6.72	1887.81	164.35	52.64
LBC	d30	cl	dry	nat	0.264	1.080	0.020	44.21	1781.95	151.23	59.61
LBC	d30	cl	dry	nat	0.502	1.360	0.020	45.55	2171.02	150.21	47.02
LBC	d30	op	sat	nat	2.803	2.730	0.450	-0.16	3920.53	206.63	157.26
LBC	d30	cl	sat	nat	4.168	3.630	0.060	-9.41	6164.03	288.43	214.80
LBC	d30	cl	sat	nat	4.632	4.870	0.080	3.18	3749.73	153.82	154.89
LBC	d30	op	dry	ref	6.861	5.410	0.060	-22.70	6407.62	260.32	148.29
LBC	d30	cl	dry	ref	0.037	0.260	0.010	21.16	4310.33	154.91	0.00
LBC	d30	op	sat	ref	0.227	0.210	0.010	-1.65	5801.43	206.63	35.53
LBC	d30	cl	sat	ref	1.463	0.270	0.010	-92.85	6297.95	215.44	0.00

Site location: QC = Quanicassee (Bay City), EB = East Bay (Traverse City), LBC = Little Black Creek (Muskegon)
Sediment type: nat = site sediment, ref = from Raisin River

Hyporheic conditions, op = open to hyporheic flow, cl = closed to hyporheic flow
Drying: dry = sediments in dry conditions for 30 days, sat = sediments continuously saturated

Appendix R. Chapter 4 hyporheic data from minipiezometers, including: porewater metals (Fe, Mn, Zn), vertical hydraulic gradient (VHG), and reduced iron (Fe^{2+}).

Site	Depth	Mini-piezometer	Day	Fe (mg/L)	Mn (µg/L)	Zn (µg/L)	VHG	Fe^{2+} (mg/L)
EB	5	A	1	0.511	444.36	31.69		0.013
EB	10	A	1	0.153	326.46	57.98		0.002
EB	15	A	1	0.093	235.48	69.94		0.000
EB	20	A	1	0.086	179.45	63.22	0	0.000
EB	5	B	1	4.124	574.54	65.31		0.174
EB	10	B	1	2.530	365.11	438.60	0.1	0.099
EB	15	B	1	1.984	250.71	628.11		0.081
EB	20	B	1	2.628	201.02	671.82	0.155	0.104
EB	5	C	1	2.896	533.69	0.00		0.152
EB	10	C	1	0.442	262.37	20.61	0.06	0.013
EB	15	C	1	0.251	199.72	0.00		0.002
EB	20	C	1	0.396	167.20	71.43	0.02	0.020
EB	5	A	9	5.195	357.19	20.54		
EB	10	A	9	3.987	271.22	19.55	0.2	
EB	15	A	9	4.355	229.56	92.18		
EB	20	A	9	2.093	150.77	0.00	0.155	
EB	5	B	9	4.713	309.70	22.47		
EB	10	B	9	3.514	224.85	19.76	0.28	
EB	15	B	9	2.836	197.29	0.00		
EB	20	B	9	2.207	181.30	0.00	0.17	
EB	5	C	9	8.041	502.26	28.47		
EB	10	C	9	4.975	317.98	79.19	0.07	
EB	15	C	9	3.472	224.63	232.28		
EB	20	C	9	2.568	180.02	253.56	0.09	
LBC	5	A	1	1.461	1008.41	47.50		0.098
LBC	10	A	1	0.814	692.74	42.77	0.19	0.044
LBC	15	A	1	1.099	636.82	119.80		0.091
LBC	20	A	1	0.201	558.12	282.51	0.11	0.000
LBC	5	B	1	10.699	4878.13	23.65		1.871
LBC	10	B	1	20.102	2999.75	29.61	0.15	3.933
LBC	15	B	1	15.162	1733.71	27.39		2.922
LBC	20	B	1	18.396	2135.17	89.06	0.15	3.636
LBC	5	C	1	1.032	1138.18	38.66		0.052
LBC	10	C	1	1.404	1080.36	129.39	0.11	0.000
LBC	15	C	1	0.783	962.59	266.45		0.050
LBC	20	C	1	1.030	679.11	281.09	0.005	0.087
LBC	5	A	9	19.688	1158.65	171.61		4.101
LBC	10	A	9	14.979	620.92	77.35	0.2	3.252
LBC	15	A	9	4.690	515.89	58.29		0.717

LBC	20	A	9	5.506	529.73	45.73	0.105	0.731
LBC	5	B	9	46.109	3485.29	63.48		10.172
LBC	10	B	9	22.852	2185.49	27.10	0.28	5.294
LBC	15	B	9	36.459	1822.79	44.01		8.669
LBC	20	B	9	19.137	1634.09	51.97	0.16	4.605
LBC	5	C	9	19.343	1338.67	334.47		4.569
LBC	10	C	9	15.843	1126.63	812.54	0.2	3.956
LBC	15	C	9	13.004	973.28	844.98		0.347
LBC	20	C	9	8.064	757.84	483.83	0.055	0.175
LBC	0	A	9	0.189	200.24	89.03		
LBC	0	B	9	0.099	62.72	57.26		
LBC	0	C	9	0.098	189.62	24.98		
QC	5	A	5	4.434	1610.35	292.79	0.6	
QC	10	A	5	2.640	1402.46	44.88		
QC	15	A	5	2.288	1402.57	84.90		
QC	20	A	5	6.590	1349.64	333.45	0.125	
QC	5	B	5	15.871	783.67	26.91		
QC	10	B	5	24.252	1086.39	144.25	0.01	
QC	15	B	5	21.257	1079.28	176.39	0.04	
QC	5	C	5	40.997	3296.65	33.17		
QC	10	C	5	35.563	2087.58	102.89	0.22	
QC	15	C	5	44.983	2058.21	58.28		
QC	20	C	5	50.612	2520.94	25.42	0.08	
QC	5	A	9	3.060	2876.36	75.17		0.124
QC	10	A	9	10.638	2214.94	19.39		1.799
QC	15	A	9	9.632	2012.61	0.00		1.665
QC	20	A	9	9.223	1931.91	25.14		1.732
QC	5	B	9	2.627	799.00			0.124
QC	10	B	9	2.162	945.88	56.04		0.000
QC	15	B	9	7.713	1087.88	60.22		1.419
QC	20	B	9	5.959	1307.80	45.27		0.861
QC	5	C	9	7.573	1124.31	41.68		1.218
QC	10	C	9	13.460	1390.01	25.21		2.893
QC	15	C	9	11.667	1432.84	27.82		2.312
QC	20	C	9	9.295	1281.93	124.57		1.598

Bibliography

Allen, H. E., G. Fu, W. S. Boothman, D. M. DiToro, and J. D. Mahony. 1991. Determination of acid volatile sulfide and selected simultaneously extractable metals in sediment. EPA 821/R-91/100. U.S. Environmental Protection Agency, Washington, D.C.

Ancion, P. Y., G. Lear, A. Dopheide, and G. D. Lewis. 2013. Metal concentrations in stream biofilm and sediments and their potential to explain biofilm microbial community structure. Environmental Pollution 173:117–124.

Ancion, P. Y., G. Lear, and G. D. Lewis. 2010a. Three common metal contaminants of urban runoff (Zn, Cu & Pb) accumulate in freshwater biofilm and modify embedded bacterial communities. Environmental Pollution 158:2738–2745.

Ancion, P. Y., G. Lear, and G. D. Lewis. 2010b. Three common metal contaminants of urban runoff (Zn, Cu & Pb) accumulate in freshwater biofilm and modify embedded bacterial communities. Environmental Pollution 158:2738–2745.

ATSDR. 2005. Toxicological Profile for Zinc.

Barbour, M. T., J. Gerritsen, B. D. Snyder, and J. B. Stribling. 1999. Rapid bioassessment protocols for use in wadeable streams and Rivers: Periphyton, Benthic Macroinvertebrates, and Fish. Second Edition. EPA 841-B-99-002. Washington, D.C.

Barlocher, F., and J. H. Murdoch. 1989. Hyporheic biofilms--a potential food source for interstitial animals. Hydrobiologia 184:61–68.

Benner, S. G., E. W. Smart, and J. N. Moore. 1995. Metal behavior during surface-groundwater interaction, Silver Bow Creek, Montana. Environmental Science & Technology 29:789–1795.

Borgmann, U., and W. P. Norwood. 1995. Kinetics of excess background copper and zinc in Hyalella azteca and their relationship to chronic toxicity. Canadian Journal of Fisheries and Aquatic Sciences 52:864–874.

Borgmann, U., and W. P. Norwood. 1997. Toxicity and accumulation of zinc and copper in Hyalella azteca exposed to metal-spiked sediments. Canadian Journal of Fisheries and Aquatic Sciences 54:1046–1054.

Boulton, A. J. 1993. Stream Ecology and Surface-Hyporheic Hydrologic Exchange: Implications, Techniques and Limitations.

Boulton, A. J., T. Datry, T. Kasahara, M. Mutz, and J. a. Stanford. 2010. Ecology and management of the hyporheic zone: stream–groundwater interactions of running waters and their floodplains. Journal of the North American Benthological Society 29:26–40.

Boulton, A. J., S. Findlay, P. Marmonier, E. H. Stanley, and H. M. Valett. 1998. the Functional Significance of the Hyporheic Zone in Streams and Rivers. Annual Review of Ecology and Systematics 29:59–81.

Brinkman, S. F., and W. D. Johnston. 2008. Acute toxicity of aqueous copper, cadmium, and zinc to the mayfly Rhithrogena hageni. Archives of Environmental Contamination and Toxicology 54:466–472.

Brunke, M., and T. Gonser. 1997. The ecological significance of exchange processes between rivers and groundwater. Freshwater Biology 37:1–33.

Buchman, M. F. 2008. NOAA Screening Quick Reference Tables.

Burton, G. A. 2010. Metal Bioavailability and Toxicity in Sediments. Critical Reviews in Environmental Science and Technology 40:852–907.

Burton, G. A. 2013. Assessing sediment toxicity: past, present, and future. Environmental toxicology and chemistry / SETAC 32:1438–40.

Burton, G. A., L. T. H. Nguyen, C. Janssen, R. Baudo, R. McWilliam, B. Bossuyt, M. Beltrami, and A. Green. 2005. Field validation of sediment zinc toxicity. Environmental toxicology and chemistry / SETAC 24:541–553.

Burton, G. A., and R. E. Pitt. 2002. The stormwater handbook. Lewis Publishers.

Calmano, W., J. Hong, and U. Forstner. 1993. Binding and mobilization of heavy metals in contaminated sediments affected by pH and redox potential. Water Science TechnologySci. Tech 28:223–235.

Cela, S., and M. E. Sumner. 2002. Soil zinc fractions determine inhibition of nitrification. Water, Air, and Soil Pollution 141:91–104.

Chapman, P. M., F. Wang, C. Janssen, G. Persoone, and H. E. Allen. 1998. Ecotoxicology of metals in aquatic sediments: binding and release, bioavailability, risk assessment, and remediation. Canadian Journal of Fisheries and Aquatic Sciences 55:2221–2243.

Clements, W. H., J. H. Van Hassel, D. S. Cherry, and J. Cairns. 1989. Colonization , variability , and the use of substratum-filled trays for biomonitoring benthic communities:45–53.

Clements, W. H., C. W. Hickey, and K. A. Kidd. 2012. How do aquatic communities respond to contaminants? It depends on the ecological context. Environmental toxicology and chemistry / SETAC 31:1932–40.

Cooper, M. J., R. R. Rediske, D. G. Uzarski, and T. M. Burton. 2001. Sediment contamination and faunal communities in two subwatersheds of Mona Lake, Michigan. Journal of environmental quality 38:1255–1265.

Costello, D. M., and G. A. Burton. 2014. Response of stream ecosystem function and structure to sediment metal : Context- dependency and variation among endpoints. Elementa:1–13.

Costello, D. M., G. A. Burton, C. R. Hammerschmidt, E. C. Rogevich, and C. E. Schlekat. 2011. Nickel phase partitioning and toxicity in field-deployed sediments. Environmental science & technology 45:5798–805.

Costello, D. M., C. R. Hammerschmidt, and G. A. Burton. 2015. Copper Sediment Toxicity and Partitioning during Oxidation in a Flow-Through Flume. ENVIRONMENTAL SCIENCE

& TECHNOLOGY 49:6926–6933.

Costello, D. M., E. J. Rosi-Marshall, L. E. Shaw, M. R. Grace, and J. J. Kelly. 2016. A novel method to assess effects of chemical stressors on natural biofilm structure and function. Freshwater Biology:1–12.

Crouch, C. M., D. M. Mcknight, and A. S. Todd. 2013. Quantifying sources of increasing zinc from acid rock drainage in an alpine catchment under a changing hydrologic regime. Hydrological Processes 27:721–733.

Danner, K. M., C. R. Hammerschmidt, D. M. Costello, and G. A. Burton. 2015. Copper and nickel partitioning with nanoscale goethite under variable aquatic conditions. Environmental Toxicology and Chemistry 34:1705–1710.

Datry, T. 2012. Benthic and hyporheic invertebrate assemblages along a flow intermittence gradient: effects of duration of dry events. Freshwater Biology 57:563–574.

Davy-Bowker, J., W. Sweeting, N. Wright, R. T. Clarke, and S. Arnott. 2006. The distribution of benthic and hyporheic macroinvertebrates from the heads and tails of riffles. Hydrobiologia 563:109–123.

Delucchi, C. M. 1989. Movement patterns of invertebrates in temporary and permanent streams. Oecologia 78:199–207.

Dole-Olivier, M.-J., P. Marmonier, and J.-L. Beffy. 1997. Response of invertebrates to lotic disturbance: is the hyporheic zone a patchy refugium? Freshwater Biology 37:257–276.

Farag, A. M., D. F. Woodard, J. N. Goldstein, W. Brumbaugh, and J. S. Meyer. 1998. Concentrations of metals associated with mining waste in sediments, biofilm, benthic macroinvertebrates, and fish from the Coeur d'Alene River Basin, Idaho. Archives 34:119–127.

Feris, K. P., P. W. Ramsey, S. M. Gibbons, C. Frazar, M. C. Rillig, J. N. Moore, J. E. Gannon, and W. E. Holben. 2009. Hyporheic microbial community development is a sensitive indicator of metal contamination. Environmental science & technology 43:6158–6163.

Feris, K., P. Ramsey, C. Frazar, J. N. Moore, J. E. Gannon, and W. E. Holben. 2003. Differences in Hyporheic-Zone Microbial Community Structure along a Heavy-Metal Contamination Gradient. Applied and environmental microbiology 69:5563–5573.

Fetters, K. J., D. M. Costello, C. R. Hammerschmidt, and G. A. Burton. 2016. Toxicological effects of short-term resuspension of metal-contaminated freshwater and marine sediments. Environmental Toxicology and Chemistry in press:676–686.

Findlay, S., and W. V. Sobczak. 2000. Microbial communities in hyporheic sediments. Pages 287–306 in J. B. Jones and P. J. Mulholland, editors.Streams and Groundwaters. Academic Press, San Diego, CA.

Franken, R. J. M., R. G. Storey, and D. D. Williams. 2001. Biological, chemical and physiucal characteristics of downwelling and upwelling zones in the hyporheic zone of a north-temperature stream. Hydrobiologia 444:183–195.

Fuller, C. C., and J. W. Harvey. 2000. Reactive uptake of trace metals in the hyporheic zone of a mining-contaminated stream , Pinal Creek , Arizona 34:1150–1155.

Gandy, C. J., J. W. N. Smith, and A. P. Jarvis. 2007. Attenuation of mining-derived pollutants in the hyporheic zone : A review. Science of the Total Environment 373:435–446.

Genter, R. B., D. S. Cherry, E. P. Smith, and J. Cairns. 1987. Algal-periphyton population and community changes from zinc stress in stream mesocosms. Hydrobiologia 153:261–275.

Gerhardt, A. 1992. Effects of subacute doses of iron (Fe) on Leptophlebia marginata (Insecta: Ephemeroptera). Freshwater Biology 27:79–84.

Gibert, J., S. Plénet, P. Marmonier, and V. Vanek. 1995. Hydrological exchange and sediment characteristics in a riverbank: relationship between heavy metals and invertebrate community structure. Canadian Journal of Fisheries and Aquatic Sciences 52:2084–2097.

Gilbert, F., R. C. Aller, and S. Hulth. 2003. The influence of macrofaunal burrow spacing and diffusive scaling on sedimentary nitrification and denitrification: An experimental simulation and model approach. Journal of Marine Research 61:101–125.

Gilbert, J., J. A. Standord, M.-J. Dole-Olivier, and J. V. Ward. 1994. Basic attributes of groundwater ecosystems and prospects for research. Pages 7–40*in* J. Gibert, D. L. Danielopol, and J. A. Stanford, editors.Groundwater Ecology. Academic Press, San Diego.

Greenberg, M. S., G. A. Burton, and C. D. Rowland. 2002. Optimizing interpretation of in situ effects of riverine pollutants: impact of upwelling and downwelling. Environmental toxicology and chemistry / SETAC 21:289–97.

Harvey, J. W., and C. C. Fuller. 1998. Effect of enhanced manganese oxidation in the hyporheic zone on basin-scale geochemical mass balance. Water Resources Research 34:623.

Hatch, C. E., A. T. Fisher, J. S. Revenaugh, J. Constantz, and C. Ruehl. 2006. Quantifying surface water-groundwater interactions using time series analysis of streambed thermal records: Method development. Water Resources Research 42:n/a-n/a.

Hendricks, S. P., S. Journal, N. American, B. Society, and N. Mar. 1993. Microbial Ecology of the Hyporheic Zone : A Perspective Integrating Hydrology and Biology Microbial ecology of the hyporheic zone : a perspective integrating hydrology and biology. Journal of the North American Benthological Society 12:70–78.

Hendricks, S. P., and D. S. White. 1991. Physicochemical Patterns within a Hyporheic Zone of a Northern Michigan River, with Comments on Surface Water patterns'. Canadian Journal of Fisheries and Aquatic Sciences 48:1645–1654.

Hendricks, S. P., and D. S. White. 2000. Stream and Groundwater Influences on Phosphorous Biogeochemistry. Pages 221–235Streams and Groundwaters.

Hutchins, C. M., P. R. Teasdale, S. Y. Lee, S. L. Simpson, C. M. Hutchins, P. R. Teasdale, S. Y. Lee, S. L. Simpson, S. Y. I. P. Lee, and S. L. Simpson. 2009. The Effect of Sediment Type and pH-Adjustment on the Porewater Chemistry of Copper- and Zinc-Spiked Sediments. Soil and Sediment Contamination 18:55–73.

Jones, I., I. Growns, A. Arnold, S. McCall, and M. Bowes. 2015. The effects of increased flow and fine sediment on hyporheic invertebrates and nutrients in stream mesocosms. Freshwater Biology 60:813–826.

Kashian, D. R., B. A. Prusha, and W. H. Clements. 2004. Influence of total organic carbon and

UV-B radiation on zinc toxicity and bioaccumulation in aquatic communities. Environmental Science and Technology 38:6371–6376.

Kaufman, M. H., M. B. Cardenas, J. Buttles, A. J. Kessler, and P. L. M. Cook. 2017. Hyporheic hot moments: Dissolved oxygen dynamics in the hyporheic zone in response to surface flow perturbations. Water Resources Research:6642–6662.

Kayhanian, M., C. Stransky, S. Bay, S. L. Lau, and M. K. Stenstrom. 2008. Toxicity of urban highway runoff with respect to storm duration. Science of the Total Environment 389:386–406.

Keery, J., A. Binley, N. Crook, and J. W. N. Smith. 2007. Temporal and spatial variability of groundwater-surface water fluxes: Development and application of an analytical method using temperature time series. Journal of Hydrology 336:1–16.

Kim, K. S., D. H. Funk, and D. B. Buchwalter. 2012. Dietary (periphyton) and aqueous Zn bioaccumulation dynamics in the mayfly Centroptilum triangulifer. Ecotoxicology 21:2288–2296.

Kostka, J. E., and G. W. Luther. 1994. Partitioning and speciation of solid phase iron in saltmarsh sediments. Geochimica et Cosmochimica Acta 58:1701–1710.

Kostka, J. E., and G. W. Luther III. 1994. Partitioning and speciation of solid phase iron in saltmarsh sediments. Geochimica et Cosmochimica Acta 58:1701–1710.

Kreiling, R. M., N. R. De Jager, W. Swanson, E. A. Strauss, and M. Thomsen. 2015. Effects of Flooding on Ion Exchange Rates in an Upper Mississippi River Floodplain Forest Impacted by Herbivory, Invasion, and Restoration. Wetlands 35:1005–1012.

Lawrence, J. E., M. E. Skold, F. a. Hussain, D. R. Silverman, V. H. Resh, D. L. Sedlak, R. G. Luthy, and J. E. McCray. 2013. Hyporheic Zone in Urban Streams: A Review and Opportunities for Enhancing Water Quality and Improving Aquatic Habitat by Active Management. Environmental Engineering Science 30:480–501.

MacDonald, D. D., C. G. Ingersoll, and T. a. Berger. 2000. Development and evaluation of consensus-based sediment quality guidelines for freshwater ecosystems. Archives of Environmental Contamination and Toxicology 39:20–31.

Malcolm, I. a., C. Soulsby, a. F. Youngson, and D. M. Hannah. 2005. Catchment-scale controls on groundwater-surface water interactions in the hyporheic zone: Implications for salmon embryo survival. River Research and Applications 21:977–989.

Marchant, R. 1988. Vertical distribution of benthic invertebrates in the bed of the thomson river, Victoria. Marine and Freshwater Research 39:775–784.

Mathers, K. L., J. Millett, A. L. Robertson, R. Stubbington, and P. J. Wood. 2014. Faunal response to benthic and hyporheic sedimentation varies with direction of vertical hydrological exchange. Freshwater Biology 59:2278–2289.

Meylan, S., R. Behra, and L. Sigg. 2003. Accumulation of Copper and Zinc in Periphyton in Response to Dynamic Variations of Metal Speciation in Freshwater Accumulation of Copper and Zinc in Periphyton in Response to Dynamic Variations of Metal Speciation in Freshwater. Environmental Science & Technology 37:5204–5212.

Moldovan, O. T., E. Levei, C. Marin, M. Banciu, H. L. Banciu, C. Pavelescu, T. Brad, M. Cîmpean, I. Meleg, S. Iepure, and I. Povară. 2011. Spatial distribution patterns of the hyporheic invertebrate communities in a polluted river in Romania. Hydrobiologia 669:63–82.

Navel, S., F. Mermillod-Blondin, B. Montuelle, E. Chauvet, L. Simon, and P. Marmonier. 2011. Water-sediment exchanges control microbial processes associated with leaf litter degradation in the hyporheic zone: a microcosm study. Microbial ecology 61:968–79.

Nedrich, S. M., and G. A. Burton. 2017a. Sediment Zn-release during post-drought re-flooding: Assessing environmental risk to Hyalella azteca and Daphnia magna. Environmental Pollution 230:1116–1124.

Nedrich, S. M., and G. A. Burton. 2017b. Indirect effects of climate change on zinc cycling in sediments: The role of changing water levels. Environmental Toxicology and Chemistry 36:2456–2464.

Nelson, S. M., and R. a. Roline. 1999. Relationships between metals and hyporheic invertebrate community structure in a river recovering from metals contamination. Hydrobiologia 397:211–226.

Ng, G. H. C., A. R. Yourd, N. W. Johnson, and A. E. Myrbo. 2017. Modeling hydrologic controls on sulfur processes in sulfate-impacted wetland and stream sediments. Journal of Geophysical Research: Biogeosciences 122:2435–2457.

Nguyen, L. T. H., G. A. Burton, C. E. Schlekat, and C. R. Janssen. 2011. Field measurement of nickel sediment toxicity: Role of acid volatile sulfide. Environmental Toxicology and Chemistry 30:162–172.

Nimick, D. a., T. E. Cleasby, and R. B. McCleskey. 2005. Seasonality of diel cycles of dissolved trace-metal concentrations in a Rocky Mountain stream. Environmental Geology 47:603–614.

Olsen, D. A., and C. R. Townsend. 2003. Hyporheic community composition in a gravel-bedstream: influence of vertical hydrological exchange,sediment structure and physicochemistry. Freshwater Biology 48:1363–1378.

Packman, A. I., and K. E. Bencala. 2000. Modeling Surface-Subsurface Hydrological Interactions. Pages 51–53*in* J. B. Jones and P. J. Mulholland, editors.Streams and Groundwaters. Academic Press., San Diego.

Palmer, M. A. 1993. Experimentation in the hyporheic zone: Challenges and prospectus. Journal of the North American Benthological Society 12:84–93.

Pepin, D. M., and F. R. Hauer. 2002. Benthic responses to groundwater – surface water exchange in 2 alluvial rivers in northwestern Montana. Journal of the North American Benthological Society 21:370–383.

Rehg, K. J., A. I. Packman, and J. Ren. 2005. Effects of suspended sediment characteristics and bed sediment transport on streambed clogging. Hydrological Processes 19:413–427.

Ren, J., and A. I. Packman. 2005. Coupled stream-subsurface exchange of colloidal hematite and dissolved zinc, copper, and phosphate. Environmental Science and Technology 39:6387–6394.

Rhea, D. T., D. D. Harper, A. M. Farag, and W. G. Brumbaugh. 2006. Biomonitoring in the Boulder River watershed, Montana, USA: Metal concentrations in biofilm and macroinvertebrates, and relations with macroinvertebrate assemblage. Environmental Monitoring and Assessment 115:381–393.

Rivett, M. O., P. a. Ellis, R. B. Greswell, R. S. Ward, R. S. Roche, M. G. Cleverly, C. Walker, D. Conran, P. J. Fitzgerald, T. Willcox, and J. Dowle. 2008. Cost-effective mini drive-point piezometers and multilevel samplers for monitoring the hyporheic zone. Quarterly Journal of Engineering Geology and Hydrogeology 41:49–60.

Sarriquet, P. E., P. Bordenave, and P. Marmonier. 2007. Effects of bottom sediment restoration on interstitial habitat characteristics and benthic macroinvertebrate assemblages in a headwater stream. River Research and Applications2 23:815–828.

Simpson, S. L., B. M. Angel, and D. F. Jolley. 2004. Metal equilibration in laboratory-contaminated (spiked) sediments used for the development of whole-sediment toxicity tests. Chemosphere 54:597–609.

Stampfli, N. C., S. Knillmann, M. Liess, Y. a Noskov, R. B. Schäfer, and M. a Beketov. 2013. Two stressors and a community: effects of hydrological disturbance and a toxicant on freshwater zooplankton. Aquatic toxicology (Amsterdam, Netherlands) 127:9–20.

Steinman, A. D., G. A. Lamberti, and P. R. Leavitt. 2007. Biomass and Pigments of Benthic Algae. Pages 357–380*in* F. R. Hauer and G. A. Lamberti, editors.Methods in Stream Ecology. Second Edi. Academic Press, Burlington, MA.

Steinman, A., R. Rediske, R. Denning, and L. Nemeth. 2003. Preliminary watershed assessment: Mona Lake Watershed.

Stookey, L. L. 1970. Ferrozine---a new spectrophotometric reagent for iron. Analytical Chemistry 42:779–781.

Stubbington, R. 2012. The hyporheic zone as an invertebrate refuge: a review of variability in space, time, taxa and behaviour. Marine and Freshwater Research 63:293.

Tercier-Waeber, M. Lou, T. Hezard, M. Masson, and J. Schäfer. 2009. In situ monitoring of the diurnal cycling of dynamic metal species in a stream under contrasting photobenthic biofilm activity and hydrological conditions. Environmental Science and Technology 43:7237–7244.

Tiegs, S. D., J. E. Clapcott, N. A. Griffiths, and A. J. Boulton. 2013. A standardized cotton-strip assay for measuring organic-matter decomposition in streams. Ecological Indicators 32:131–139.

U.S. EPA. 2000. Methods for Measuring the Toxicity and Bioaccumulation of Sediment-associated Contaminants with Freshwater Invertebrates. Page EPA 600/R-99/064.

U.S. EPA. 2005. Procedures for the Derivation of Equilibrium Partitioning Sediment Benchmarks (ESBs) for the Protection of Benthic Organisms: Metal Mixtures (Cadmium, Copper, Lead, Nickel, Silver, Zinc). EPA/600/R-02/011. Washington, D.C. 20460.

U.S. EPA. 2008. Evaluating Ground-Water/Surface-Water Transition Zones in Ecological Risk Assessment. EPA-540-R06-072. Washington, D.C.

US EPA. 1996. Method 3050B - Acid digestion of sediments, sludges, and soils. Revision 2.

Vadher, A. N., R. Stubbington, and P. J. Wood. 2015. Fine sediment reduces vertical migrations of Gammarus pulex (Crustacea: Amphipoda) in response to surface water loss. Hydrobiologia 753:61–71.

Vuori, K.-M. 1995. Direct and indirect effects of iron on river ecosystems. Annales Zoologici Fennici 32:317–329.

Williams, D. D., and H. B. N. Hynes. 1974. The occurence of benthos deep in the substratum of a stream. Freshwater Biology 4:233–256.

Winter, T. C., J. T. LaBaugh, and D. O. Roseberry. 1988. The design and use of a hydraulic potentiomanometer for direct measurement of differences in hydraulic head between groundwater and surface water. Limnology and Oceanography 33:1209–1214.

Wood, P. J., A. J. Boulton, S. Little, and R. Stubbington. 2010. Is the hyporheic zone a refugium for aquatic macroinvertebrates during severe low flow conditions ? Fundamental and Applied Limnology, Arch. Hydrobiol. 176:377–390.

Wuycheck, J. 2003. TMDL for biota for Little Black Creek.

Zaramella, M., A. Marion, and A. I. Packman. 2006. Applicability of the Transient Storage Model to the hyporheic exchange of metals. Journal of Contaminant Hydrology 84:21–35.